CR-172026

CSDL-T-926

PREDICTIVE MOMENTUM MANAGEMENT FOR A SPACE STATION MEASUREMENT AND COMPUTATION REQUIREMENTS

by

John Carl Adams

August 1986

The Charles Stark Draper Laboratory, Inc.
555 Technology Square
Cambridge, Massachusetts 02139

Predictive Momentum Management for a Space Station

Measurement and Computation Requirements

by

John Carl Adams

B.S., Massachusetts Institute of Technology, 1984

Submitted in Partial Fulfillment
of the Requirements for the
Degree of

MASTER OF SCIENCE
in
AERONAUTICS AND ASTRONAUTICS

at the

MASSACHUSETTS INSTITUTE OF TECHNOLOGY

August 1986

Signature of Author.....John Carl Adams.....
Department of Aeronautics and Astronautics
August, 1986

Approved by.....Michael Paluszek.....
Michael A. Paluszek
Technical Supervisor, CSDL

Certified by.....Walter M. Hollister.....
Prof. Walter M. Hollister
Thesis Supervisor

Accepted by.....Harold Y. Wachman.....
Prof. Harold Y. Wachman
Chairman, Departmental Graduate Committee

The Charles Stark Draper Laboratory, Inc.
Cambridge, Massachusetts 02139

ABSTRACT

Predictive Momentum Management for a Space Station
Measurement and Computation Requirements

Submitted to the Massachusetts Institute of Technology
in Partial Fulfillment of the Requirements of
Master's of Science
August 1986
by John Carl Adams

An analysis is made of the effects of errors and uncertainties in the predicting of disturbance torques on the peak momentum buildup on a space station.

Models of the disturbance torques acting on a space station in low earth orbit are presented, to estimate how accurately they can be predicted. An analysis of the torque and momentum buildup about the pitch axis of the Dual Keel space station configuration is formulated, and a derivation of the Average Torque Equilibrium Attitude (ATEA) is presented, for the case of no MRMS (Mobile Remote Manipulation System) motion, Y vehicle axis MRMS motion, and Z vehicle axis MRMS motion.

Results showed the peak momentum buildup to be approximately 20000 N-m-s and to be relatively insensitive to errors in the predicting torque models, for Z axis motion of the MRMS. The peak disturbance momentum for no motion and Y axis motion of the MRMS was found to vary significantly with model errors, but not exceed a value of approximately 15000 N-m-s for the Y axis MRMS motion with 1 deg attitude hold error.

Minimum peak disturbance momentum was found not to occur at the ATEA angle, but at a slightly smaller angle. However, this minimum peak momentum attitude was found to produce significant disturbance momentum at the end of the predicting time interval.

Thesis Supervisor: Prof. Walter M. Hollister
Professor of Aeronautical and Astronautical Engineering

Technical Supervisor: Michael A. Paluszek
Technical Staff, Charles Stark Draper Laboratory

ACKNOWLEDGEMENTS

I'd like to salute the understanding and infinite patience of Mike Palusek and my advisor Prof. Walter Hollister, as well as a host of family and friends, without whom I'd never have gotten through this.

This report was prepared at The Charles Stark Draper Laboratory, Inc., under contract number NAS 9-16023 with the National Aeronautics and Space Administration.

Publication of this report does not constitute approval by the Draper Laboratory or NASA of the findings or conclusions contained herein. It is published solely for the exchange and stimulation of ideas.

TABLE OF CONTENTS

LIST OF ILLUSTRATIONS

LIST OF TABLES

1.0 INTRODUCTION

NASA's plans for a permanently orbiting space station have raised many interesting questions in the area of attitude control, and particularly in the area of momentum management. Over a long operational lifetime, even the relatively small torques of the environment in low earth orbit can provide significant momentum buildup that must be dealt with in some manner; either through the use of magnetic torquers, CMG's (Control Moment Gyros), or thrusters.

There are many sources of unwanted momentum on the space station. The two most significant result from the aerodynamic torques and gravity gradient torques acting on the spacecraft. But there are many other sources, such as, crew motion, docking, and MRMS (Mobile Remote Manipulation System) movement.

The usual method for dealing with this unwanted momentum would be to allow the momentum to increase to a certain point and then dump it using the RCS jets, magnetic torquers, or just tilting the spacecraft and using the gravity gradient torques to counteract this momentum. It has been shown [5] though, that the disturbance torques expected on the

space station will require a large momentum storage if momentum exchange devices are to be used to neutralize these disturbances.

Because of this, it has been proposed that a new system for controlling the buildup of unwanted momentum be implemented, namely one which predicts in advance the disturbance torques on the space station, rather than dealing with their effects after-the-fact. Such a predictive momentum management system would allow a more optimal placement of the attitude of the space station so that disturbance torques might cancel each other. This, in general, reduces the momentum storage requirements placed upon the momentum exchange devices.

One example of such a predictive momentum management scheme is to fly the space station at an "average torque equilibrium attitude". It is desired that the space stations attitude remain constant, but for a given period of time what should this attitude be? The average torque equilibrium attitude is such that if we can predict the disturbance torques on the space station for a time T in the future, then at the end of that time the integral of all the disturbance torques, and thus the net momentum, will be zero. Flying the space station at such an attitude has been shown to reduce the momentum storage requirements for attitude control by a factor of 4 (see fig. 1).

The goal is to find an attitude in which to orient the spacecraft such that, for a given time, the peak momentum storage requirement on the attitude control system is minimized.

The problem with a predictive system is that accurate knowledge of the torques expected on the spacecraft must be had in advance in order to choose an attitude such that the unwanted momentum is zero after a given period of time.

Here is a list of possible sources of disturbance torques;

1. Gravity Gradient forces
2. Aerodynamic drag
3. Docking
4. MRMS motion
5. Crew motion
6. Venting
7. Solar radiation pressure
8. Radiation pressure from re-radiated and scattered radiation from earth
9. Frictional torques between rotating and non-rotating components
10. Changes in inertia due fuel consumption, solar panel motion, crew motion, MRMS motion, etc.

The prediction of these torques requires accurate modeling or measurement of many of the characteristics of the space station and its

environment. Some of the more important quantities that need to be specified are;

1.Vehicle Inertia Matrix- An accurate model which includes the changes due to mass shifts involved with MRMS motion, solar panel rotation, docking, crew motion, venting and fuel consumption.

2.Vehicle Drag Coefficient- A model which includes changes due to orientation, solar panel motion, shadowing, changes in atmospheric conditions(i.e. composition, density), and configuration changes(i.e. MRMS position, docked vehicles)

3.Vehicle Center of Mass and Center of Pressure- Again, a model which accounts for changes in configuration due to docking, MRMS activity, etc.

4.Vehicle Environment- Atmospheric density and composition, Gravitational anamolies, Earth's radiation and re-radiation, solar radiation and its fluctuations.

5.Vehicle Position, Velocity, and Attitude

2.0 DISTURBANCE TORQUE MODELS

This chapter gives an assessment of the sources of disturbance momentum on the space station. It presents for each disturbance torque the mechanics of the disturbing phenomena, the mathematical models involved with prediction of these torques, and the assumptions and simplifications that have gone into each model. It also provides the intended sources for each of the parameters in the models, be it direct measurement or estimation, and an application of these torque predicting models to an example configuration of the space station; the dual keel configuration.

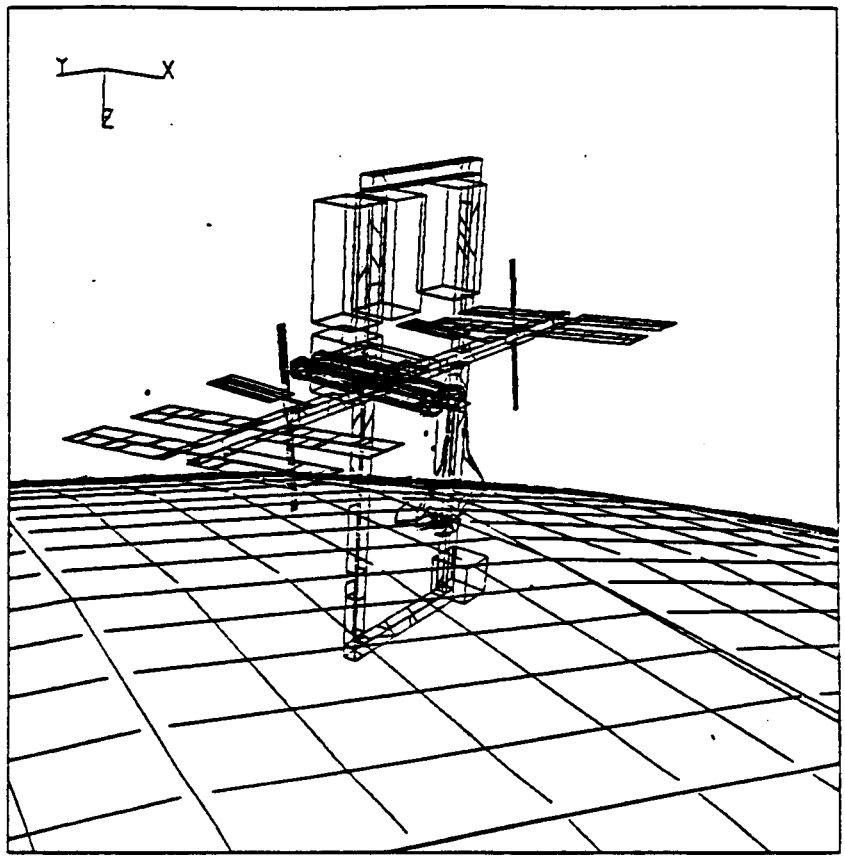

Figure 1. Space Station, Dual Keel configuration

There are many different disturbance torques that act on the space station, some of which can be characterized as forces acting at a certain moment arm from the center of mass of the station (r X F), and others which are more easily characterized as a change in the space station's angular momentum (dH/dt). In table 1, the disturbance torques that will be dealt with in this paper are separated into these two catagories and into two sub catagories. Those torques characterized as forces acting at moment arms are separated into those that act as body forces and those that act as surface, contact forces. And of the torques that are characterized as a change in momentum, some are the result of changes in the space station's inertia, and some are due to changes in the angular velocity of the station's orbit.

Table 1. Disturbance Torques

r X F		dH/dt	
Body Forces	Contact Forces	dI/dt	dw/dt
Gravity Gradient	Aerodynamic Torques	Docking	Non-circular orbits
Magnetic	Solar Radiation Pressure	MRMS motion	
	Earth Radiation Pressure	Solar Panel Motion	
	Venting Torques	Crew Motion	
	Docking Torques	Radiator Motion	
	Friction Torques	Consumable Depletion	
	Crew motion	Antennae Motion	
		Station Growth	
		Station Reconfig-uration	

The torque, and corresponding angular momentum, disturbance associated with each of these phenomena are to be expressed in a coordinate frame fixed in the vehicle. Altogether, there are five coordinate frames that are of importance to the dynamics of the space station. Their definition and the transformation matrices between them allow for the characterization and resolution of the forces and torques that act upon the space station. These frames are;

Inertial

Sun-fixed

Local Vertical/Local Horizontal

Vehicle C.O.M.

Component C.O.M.

The inertial frame is important because the radiators are to be fixed inertially, so to determine the inertia change due to their motion, a transformation is needed from inertial coordinates to vehicle coordinates.

The same reasoning applies to the solar panels, which are to remain sun-fixed. A transformation between vehicle frame and a sun-fixed frame is needed to specify their motion.

The basic approach of this analysis is that the space station is assumed to be a combination of several components, each of which can be characterized by its own mass, inertias, and body-fixed coordinate frame. In general, a torque or force can be defined in the components frame more easily than in the vehicle frame. So in the final analysis these component torques must be combined and transformed into the total vehicle frame.

2.1 GRAVITY GRADIENT TORQUE

One of the most significant torques on the space station will come from the "gravity gradient" forces, which arise due to the fact that only the center of mass of an object in orbit is in force equilibrium (see Figure 2 on page 21). The net force on any other incremental mass is;

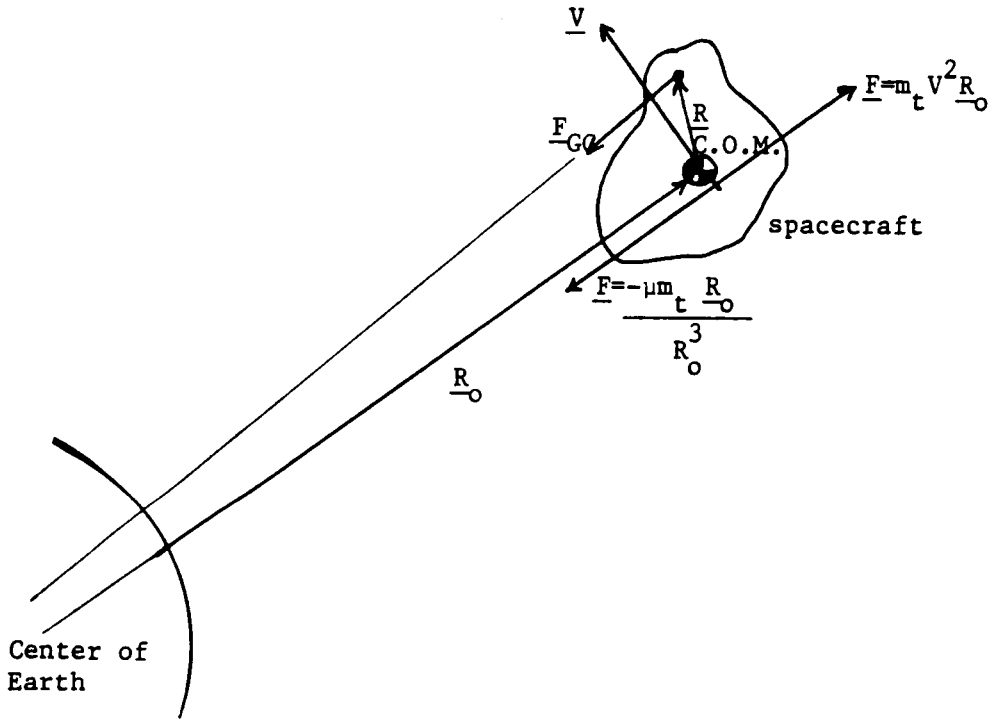

Figure 2. Net Force on an Object in Orbit

$$F_{GG} = \frac{-\mu (R_o+R)\, dm}{|R_o+R|^3} \qquad (1)$$

$$M_{GG} = \int_b R \times \frac{[-\mu(R_o + R)\,dm]}{|R_o+R|^3} \tag{2}$$

where;

R_o = Radius from the center of the earth to space station center of mass (C.O.M.)

R = Radius from space station C.O.M. to incremental mass dm

μ = earth's gravitational constant (GM_e)

M_{GG} = Gravity Gradient moment about C.O.M. of station

$$\frac{1}{|R_o+R|^3} = \frac{1}{(R_o^2+2(R_o \cdot R)+R^2)^{3/2}} \tag{3}$$

(from Law of Cosines)

$$= \frac{1}{R_o^3\,(1+2(R_o \cdot R)/R_o^2 + R^2/R_o^2)^{3/2}} \tag{4}$$

$$\approx 1/R_o^3[1-3(R_o \cdot R)/R_o^2 + \ldots.\,] \tag{5}$$

(from Binomial Theorem)

$$M_{GG} = \int_b R \times [-\mu/R_o^3\,(1-3(R_o \cdot R)/R_o^2)\,(R_o+R)]\,dm \tag{6}$$

and since $R \times (R_o+R) = R \times R_o$

$$M_{GG} = \int_b \frac{-\mu}{R_o^3}[1-3(R_o \cdot R)/_o^2]\,(R \times R_o)\,dm \tag{7}$$

$$= \int_b -\mu/R_o^3\ (R \times R_o)\,dm \tag{8}$$

($\rightarrow 0$, since $\int R dm = 0$ about the C.O.M.)

$$+ \int_b 3\mu/R_o^5\ (R \cdot R_o)\,(R \times R_o)\,dm \tag{9}$$

$$\therefore M_{GG} = 3n^2/R_o^2 \int_b (R \cdot R_o)(R \times R_o)\, dm \qquad (10)$$

where; $n = \sqrt{\mu/R_o^3}$

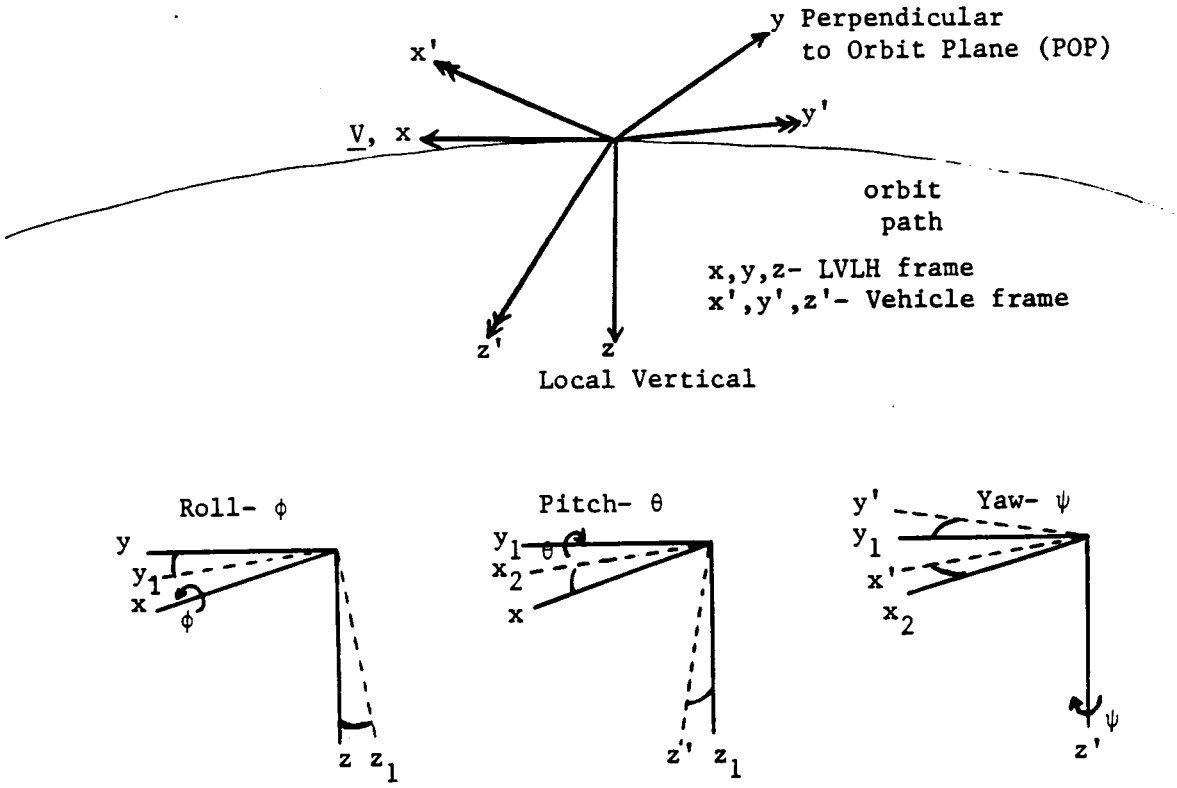

Figure 3. Transformation from body frame to LVLH frame

In order to obtain the gravity gradient torque in the body coordinates it is necessary to transform the earth radius vector into body coordinates. Assuming roll(ϕ), pitch(θ), and yaw(Ψ) as the three euler angles, the transformation matrix from the LVLH frame to the body center of mass frame is;

$$T_{LVLH\text{-}b} = \begin{bmatrix} \cos\psi\cos\theta & \sin\theta\sin\phi\cos\psi + \sin\psi\cos\phi & -\sin\theta\cos\phi\cos\psi + \sin\phi\sin\psi \\ -\sin\psi\cos\theta & -\sin\theta\sin\phi\sin\psi + \cos\psi\cos\phi & \sin\theta\cos\phi\sin\psi + \sin\phi\cos\psi \\ \sin\theta & -\sin\phi\cos\theta & \cos\theta\cos\phi \end{bmatrix} \tag{11}$$

and using the small angles approximation; $\cos\theta \approx 1$, $\sin\theta \approx \theta$, $\theta^2 \approx 0$

$$\therefore T_{LVLH\text{-}b} \approx \begin{bmatrix} 1 & \theta\phi + \psi & -\theta + \phi\psi \\ -\psi & -\theta\phi\psi + 1 & \theta\psi + \phi \\ \theta & -\phi & 1 \end{bmatrix} \tag{12}$$

$$T_{LVLH\text{-}b} \approx \begin{bmatrix} 1 & \psi & -\theta \\ -\psi & 1 & \phi \\ \theta & -\phi & 1 \end{bmatrix} \tag{13}$$

$$R_{oLVLH} = \begin{bmatrix} 0 \\ 0 \\ R_o \end{bmatrix} \qquad R_{ob} = [T_{LVLH\text{-}b}]\, R_{oLVLH} \qquad \therefore R_{ob} = R_o \begin{bmatrix} -\theta \\ \phi \\ 1 \end{bmatrix} \tag{14}$$

$$R = \begin{bmatrix} x \\ y \\ z \end{bmatrix} \tag{15}$$

$$\therefore R \cdot R_o = (-\theta x + \phi y + z) R_o \tag{16}$$

$$R \times R_o = R_o \begin{bmatrix} y - \phi z \\ -x - \theta z \\ \phi x + \theta y \end{bmatrix} \tag{17}$$

$$(R \cdot R_o)(R \times R_o) = \begin{bmatrix} -\theta xy+\phi y^2+yz+\theta\phi xz-\phi^2 yz-\phi z^2 \\ \theta x^2-\phi xy-xz+\theta^2 xz-\theta\phi yz-\theta z^2 \\ -\theta\phi x^2+\phi^2 xy+\phi xz-\theta^2 xy+\theta\phi y^2+\theta yz \end{bmatrix} R_o^2 \tag{18}$$

$$\approx \begin{bmatrix} -\theta xy + yz + \phi(y^2-z^2) \\ -\phi xy - xz + \theta(x^2-z^2) \\ \phi xz + \theta yz \end{bmatrix} R_o^2 \, dm \tag{19}$$

and with the definitions for moments and products of inertia;

$$\begin{aligned} I_x &= \int_b (y^2+z^2)\,dm & I_{xy} &= \int_b (xy)\,dm \\ I_y &= \int_b (x^2+z^2)\,dm & I_{xz} &= \int_b (xz)\,dm \\ I_z &= \int_b (x^2+y^2)\,dm & I_{yz} &= \int_b (yz)\,dm \end{aligned} \tag{20}$$

So the linearized gravity gradient torque in body coordinates becomes;

$$M_{GG} = 3n^2 \begin{bmatrix} -\theta I_{xy} + I_{yz} + \phi(I_z-I_y) \\ -\phi I_{xy} - I_{xz} + \theta(I_z-I_x) \\ \phi I_{xz} + \theta I_{yz} \end{bmatrix} \tag{21}$$

2.2 AERODYNAMIC TORQUES

The density of the atmosphere falls off exponentially with altitude, but even at the space station's nominal altitude of 250 nautical miles (450 km) the effects of atmospheric drag can be felt, especially for large spacecraft over extended periods of time. However, in this region of the atmosphere, the exosphere, the density is so low that the principles of contimuum aerodynamics no longer apply. Since the mean free path of the molecules at this altitude is greater than the characteristic length of the vehicle, each particle interaction with the surface of the spacecraft must be considered as independent and uninfluenced by another molecule's interaction. Another assumption that can be made is that the velocity of the vehicle is much greater than the thermal velocity of the molecules. Because of this, the atmosphere can be modeled as a molecular beam, with all incoming particle velocities parallel.

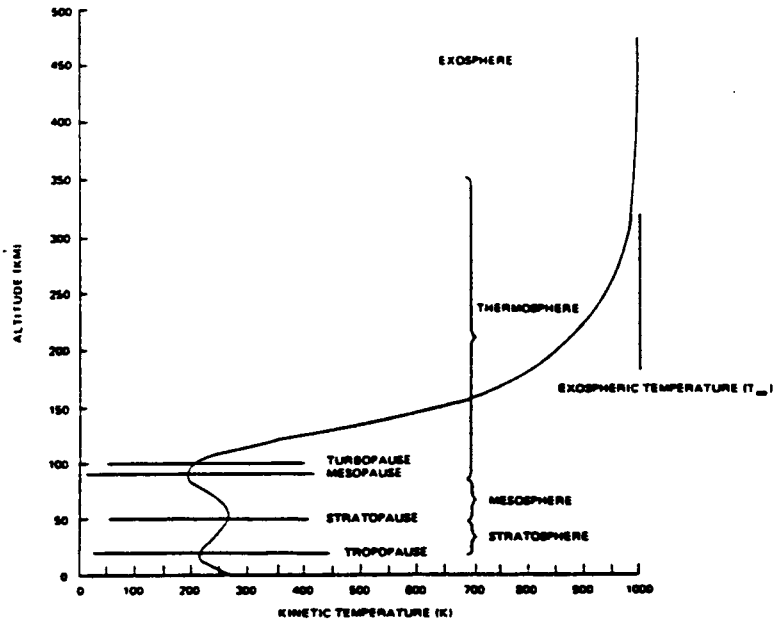

Mean Atmospheric Temperature as a Function of Altitude

Figure 4. Structure of Upper Atmosphere

When a particle collides with a surface, the resulting interaction can range from a totally inelastic collision where the particle is absorbed by the surface, to a totally elastic collision where the normal momentum of the particle with respect to the surface is reversed and its tangential momentum is left unchanged. (see Figure 5)

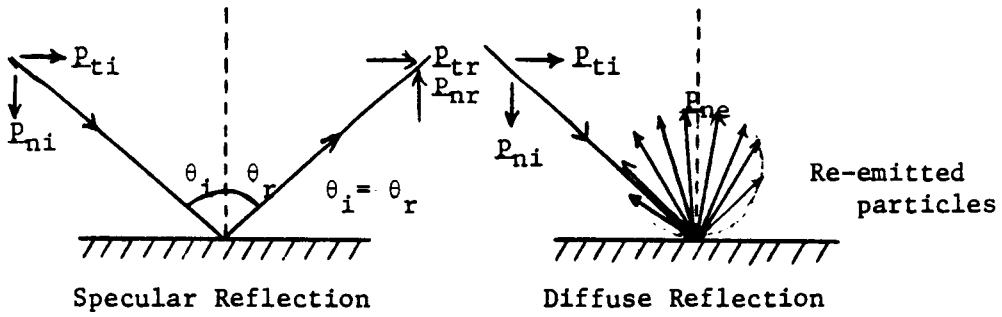

Figure 5. Specular and Diffuse reflection

To characterize this range of interactions for a given surface of a given material it is customary to define two 'momentum accommodation

coefficients', one for the tangential momentum and one for the normal momentum.

$$\sigma = \text{Tangential momentum accommodation coefficient} = \frac{p_{Ti} - p_{Tr}}{p_{Ti}} \quad (22)$$

$$\sigma' = \text{Normal momentum accommodation coefficient} = \frac{p_{Ni} - p_{Nr}}{p_{Ni} - p_{Ne}} \quad (23)$$

where;

p_{Ti} = Tangential momentum incoming particles
p_{Tr} = Tangential momentum reflected particles
p_{Ni} = Normal momentum incoming particles
p_{Nr} = Normal momentum reflected particles
p_{Ne} = Normal momentum re-emitted particles

When both of these coefficients are equal to 1, then the particle interactions are completely inelastic, which is diffuse reflection. When both of the coefficients are 0, then the particle interactions are completely elastic, which is specular reflection. In reality they will be somewhere in between, with specular reflection generally increasing for an increasing angle of incidence between incoming particles and the normal to the surface. Some experimental values for σ and σ' are shown in Figure 6. [1]

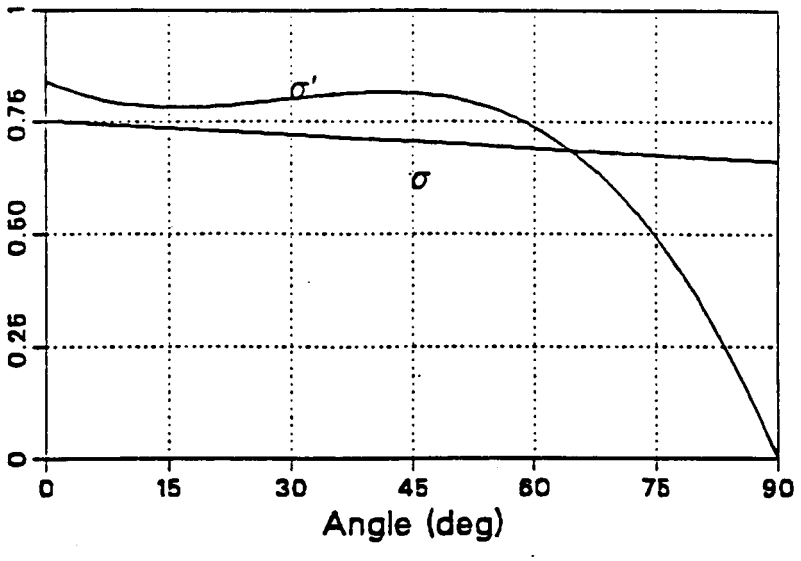

Figure 6. Some Experimentally Determined Values for σ and σ'

The collision process is a complex physical and chemical interaction, and the behavior of absorbed and reflected particles varies for each specific surface composition and the type of incoming particles. However, a simplifying assumption can be made due to the fact that in the steady state, the space craft surfaces will not be 'clean', but will be contaminated by a layer of atmospheric particles both stuck and chemically bonded to the surface. The most notable of these contaminants is monatomic oxygen. This layer of contaminants produces a more homogeneous surface condition on the overall spacecraft, and makes the definition of the momentum accommodation coefficients easier.

In general, a layer of surface contaminants greatly raises the tangential momentum accommodation coefficient, to about the .85 to .90 region, for all types of surface materials, except at very high angles of incidence ('grazing' angles). The normal momentum accommodation

coefficient is less affected by surface contamination but this coefficient tends to vary less from material to material.

Once the net momentum transfer from particle to surface is characterized by these momentum accommodation coefficients, then a drag coefficient equivalent to that for continuum flows can be formulated as a function of these coefficients and the surface's attitude with respect to the incoming flow. [2]

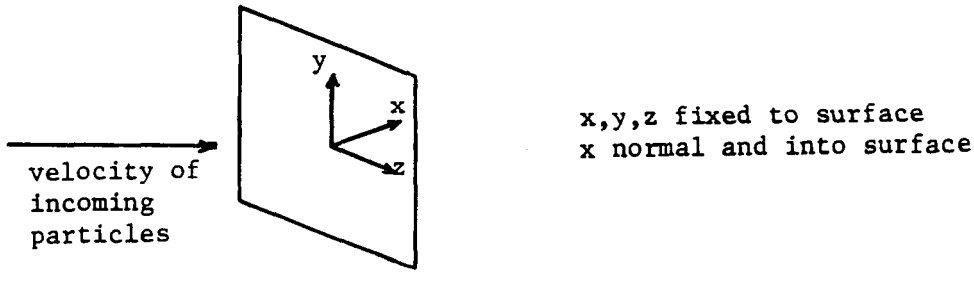

Figure 7. Frame of reference for surface

The drag coefficients for each direction in the surface are;

$$C_{Fx} = [((2-\sigma')\,Su_x/\sqrt{\pi} + (\sigma'/2)\sqrt{T_w/T})\,e^{-(Su_x)^2}$$

$$+ (2-\sigma')\,(1/2+(Su_x)^2) + ((\sigma/2)\sqrt{T_w\pi/T})\,(1+\mathrm{erf}\,(Su_x))]/S^2$$

$$C_{Fy} = (\sigma u_y/S^2)\,[S\sqrt{\pi}e^{-(Su_x)^2} + u_x S^2\,(1+\mathrm{erf}\,(Su_x))]$$

$$C_{Fz} = (\sigma u_z/S^2)\,[S\sqrt{\pi}e^{-(Su_x)^2} + u_x S^2\,(1+\mathrm{erf}\,(Su_x))] \qquad (24)$$

where $u = \begin{bmatrix} u_x \\ u_y \\ u_z \end{bmatrix}$

= unit velocity vector in surface frame

S = ratio of vehicle speed to average molecular speed (≈ 10)

T_w/T = ratio of wall temp. to ambiant temp. ($\approx .25$)

Once these drag coefficients have been calculated for a surface, then the forces exerted on that surface follow as;

$$F_x = 1/2\ \rho V^2 A C_{Fx}$$
$$F_y = 1/2\ \rho V^2 A C_{Fy}$$
$$F_z = 1/2\ \rho V^2 A C_{Fz} \qquad (25)$$

where,

ρ = atmospheric density
A = area of surface normal to flow
V = magnitude of velocity

And the torque about the center of mass due to the aerodynamic force on each surface is simply;

$$M_{Ai} = r_i \times F_i \qquad (26)$$

To find the total aerodynamic moment it is necessary to sum the moments from all the individual surfaces. What complicates this is the fact that for different orientations of the vehicle, some parts of the spacecraft may be partially or totally shielded from the flow by other parts of the spacecraft. This is known as 'shadowing'. Realizing this, the total aerodynamic moment about the center of mass is;

$$M_A = \Sigma_i \; r_i \times F_i \tag{27}$$

where i = space station surfaces exposed to the flow

It may be more convenient, however, to define the moment in terms of two other quantities, r_{cp}, and C_F, where,

r_{cp} = radius vector from center of mass to center of pressure

$$= \Sigma_i \; r_i A_i / \Sigma_i \; A_i \tag{28}$$

C_F = total space station drag coeff.

$$= \Sigma_i \; C_{F_i} \tag{29}$$

where, again, i = spacecraft surfaces not shadowed

Using these definitions, equation (27) can be rearranged to form,

$$M_A = r_{cp} \times 1/2 \; \rho V^2 A_T C_F \tag{30}$$

There are three limiting factors in the degree of accuracy with which the aerodynamic moment M_A can be predicted. The first limitation is in the ability to determine C_F, the total drag coefficient of the space station. This is accomplished computationally by simplifying complex spacecraft geometries into more basic surfaces such as flat plates, spheres, rectangular solids, cylinders, etc., and then predicting which surfaces will be shadowed and to what extent by using the geometry of the space station's configuration and attitude.

Also, the values for the momentum accommodation coefficients are derived experimentally, and the conditions of the space station's external surfaces in the space environment will not be an exact match for those in an experimental environment. Simplifications in the space station's geometry and the experimental nature of the accommodation coefficients both limit the accuracy of the total vehicle coefficient of drag.

One way of improving tha accuracy of the momentum accommodation is to perform the measurements similar to those done in laboratory molecular beam experiments on board the space station itself [34], using the incoming atmospheric particles as the molecular beam. This would avoid the problem of simulating the surface contamination the spacecraft would encounter in orbit, in the laboratory.

Another limiting factor is the determination of the spacecraft's velocity. This is essentially a navigation problem and it doesn't appear that there will be any problem achieving the desired accuracy. Using the Global Positioning System, at the proposed altitude of the space station, accuracies 45 to 60 feet in position and .2 feet/sec in velocity have been shown to be feasible. [37]

The strongest limitation on the ability to determine the aerodynamic torque is in the prediction of the atmospheric density. At the space station's altitude the density is extremely variable. In general, density decreases exponentially with altitude, but it has also been shown to be dependent on the incoming flux of solar radiation, (see Figure 8) particularly at the 10.7 cm wavelength, and is also dependent on the variations in the earth's magnetic field.(see Figure 8) It can change by up to three orders of magnitude over the entire solar cycle.[13] Some of the variations are random in nature while others appear regularly. Some of the regular variations are;

1. An 11 year solar activity cycle variation
2. An annual variation
3. A semi-annual variation
4. A 27 day solar rotation variation
5. A diurnal variation due to earth's rotation
6. Magnetic disturbance variations

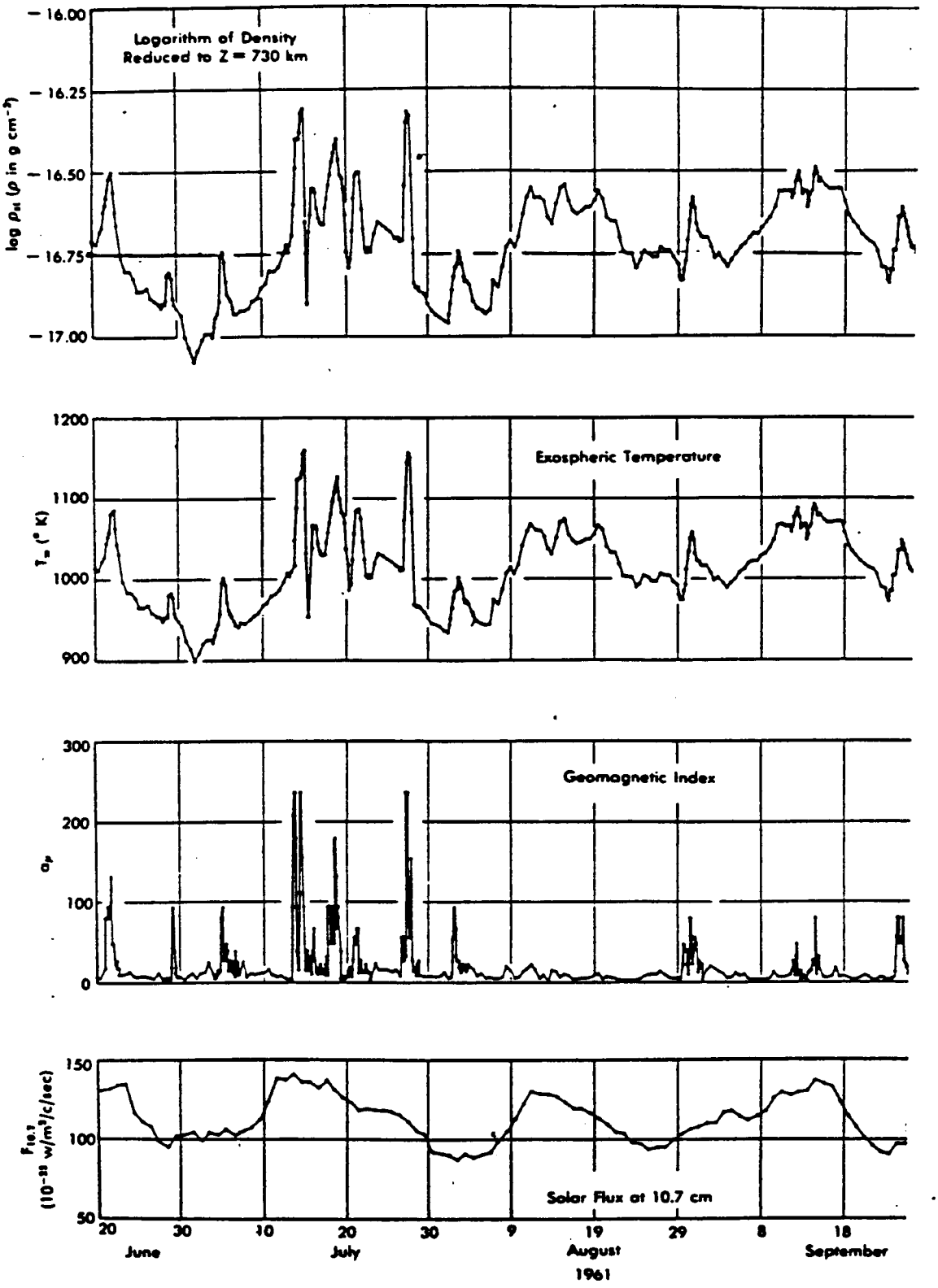

Figure 8. Correlation between density and solar flux and geomagnetic activity

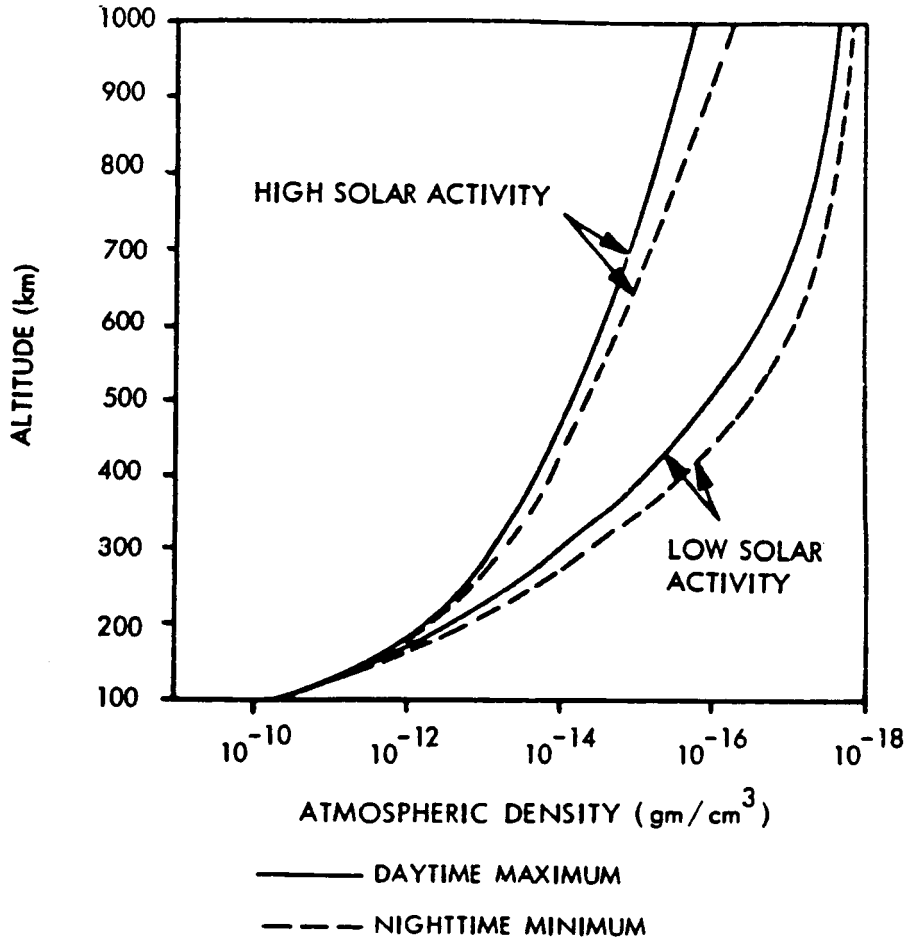

Figure 9. Density vs. Altitude for maximum and minimum solar activity and diurnal variation

The annual variation in atmospheric density is due to the changing composition of the constituent gasses of the upper atmosphere with latitude and season.

The semi-annual variation is a product of the interaction of the earth's magnetic field with the solar wind. This effect reaches its minimum in July, its maximum in October or November, and a secondary minimum and maximum in January and April, respectively.

The variation with the highest frequency is the diurnal variation. The diurnal density 'bulge' reaches its maximum at a point lagging the subsolar point by about 30°, or 2 hours. It varies roughly sinusoidally with longitude, about an average value;

$$\rho = \rho_{ave}(1 + .5 \cos(\lambda - 30°)) \tag{31}$$

where λ = the angular separation between the space station and the subsolar point.

2.3 SOLAR RADIATION TORQUE

The incoming solar radiation carries with it some incoming momentum. If the radiation is thought of as a stream of incoming particles, photons, each with a momentum proportional to its energy, then the situation is analogous to the aerodynamic drag case, where incoming

particles interact with the projected area of of the surfaces of the spacecraft resulting in a net exchange of momentum.

The analogy is carried further when the types of possible interactions are considered. As in the case of aerodynamic particle interactions, photons can be either absorbed, reflected diffusely, or reflected specularly. (see Figure 10 on page 37)

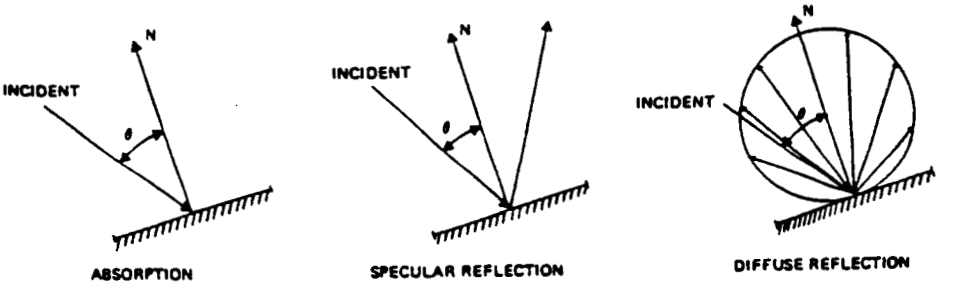

Figure 10. Possible photon interactions with space station surfaces

To characterize what portion of the incident radiation experiences each of the different interactions, three coefficients are defined;

σ_A = coefficient of absorption
σ_{RD} = coefficient of diffuse reflection
σ_{RS} = coefficient of specular reflection

where $0 < \sigma_A, \sigma_{RD}, \sigma_{RS} < 1$

and $\sigma_A + \sigma_{RD} + \sigma_{RS} = 1$

These coefficients represent the fraction of the incoming momentum that is either absorbed, reflected diffusely, or reflected specularly,

for a given surface of a given material, and like the momentum accommodation coefficients, they are determined experimentally. [26]

The total energy flux radiated from the sun is known as the 'solar constant', S, and is $\approx 1.35 \times 10^3$ J/m^2-sec at the radius of the earth's orbit. The solar constant varies annually by about 6% due to the eccentricity of earth's orbit around the sun. The momentum flux is;

$$p = S/c \tag{32}$$

p is in the outward radial direction from the sun and c is the speed of light, $\approx 3 \times 10^8$ m/sec.

If we define a coordinate frame that is fixed to the surface of the spacecraft; (see Figure 11 on page 38)

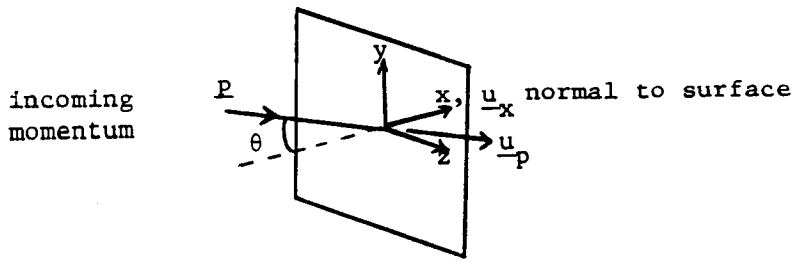

Figure 11. Surface coordinate frame, incoming momentum

with u_x being a unit normal into the surface, and with u_p being a unit vector in the incident momentum direction, then the force imparted to the i^{th} surface by each type of interaction is;

specular reflection- $$F_{RSi} = 2p\cos\theta\,(A\cos\theta)\,u_x$$
$$= 2S/c\,\cos^2\theta A u_x \qquad (33)$$

diffuse reflection- $$F_{RDi} = p\,(A\cos\theta)\,(u_p + (2/3)\,u_x)$$
$$= S/c\,\,(A\cos\theta)\,(u_p + 2/3\,u_x) \qquad (34)$$

absorption- $$F_{Ai} = p\,(A\cos\theta)\,u_p$$
$$= S/c\,\,(A\cos\theta)\,u_p \qquad (35)$$

Specular reflection is simply a reversal of the normal component of the incoming momentum, while diffuse reflection causes the net momentum transfer to be along the the direction $(u_p + 2/3\,u_x)$. Absorption causes a force along the direction of incoming momentum, u_p

The total force on this surface can now be expressed by incorporating the absorption and reflection coefficients;

F_{Ri} = Solar radiation pressure force

$$= \sigma_A F_{Ai} + \sigma_{RS} F_{RSi} + \sigma_{RD} F_{RDi}$$

$$= SA\cos\theta/c \; [(\sigma_A+\sigma_{RD})\, u_p + 2\,(\sigma_{RS}\cos\theta+\sigma_{RD}/3)\, u_x] \tag{36}$$

Expressing the force in a coordinate frame that is normal and tangential to the surface can be accomplished by replacing the vector u_p by $u_p = \cos\theta u_t + \sin\theta u_x$. The resulting expression is;

$$F_{Ri} = SA\cos\theta/c \; [(\sigma_A+\sigma_{RD})\cos\theta u_t + (\sigma_A\sin\theta+\sigma_{RD}(2/3 +\sin\theta)+2\sigma_{RS}\cos\theta)\, u_x] \tag{37}$$

The associated moment for that surface about the center of mass is,

$$M_{Ri} = r_i \times F_{Ri} \tag{38}$$

And summing across the entire vehicle gives the total moment due to radiation pressure;

$$M_R = \Sigma_i \; r_i \times F_{Ri} \tag{39}$$

where the summation is over those surfaces exposed to the sunlight, thus eliminating 'shadowing' effects.

2.4 EARTH EMITTED AND SCATTERED RADIATION TORQUES

The sun is not the only source of radiation which can place a torque on the space station. Another important source of radiation is the earth itself. The earth can radiate in two ways, first as a black body it emits in the infrared range, and second it scatters incoming solar radiation. On average, the earth scatters 34% of the incoming solar flux[9], and if we assume that the earth eventually re-radiates all of the energy that is incident upon it, the amount of radiation energy emitted in the IR range is 66% of the incoming solar energy flux. The corresponding momentum flux from this radiation is;

$$P_{SC} = \frac{p_s \pi R_e^2 (.34)}{2\pi R_o^2} \tag{40}$$

$$P_{IR} = \frac{p_s \pi R_e^2 (.66)}{4\pi R_o^2} \tag{41}$$

where; R_e = Radius of the earth
R_o = Radius from center of earth to space station
P_s = Incoming solar momentum flux

The incoming solar radiation is intercepted by the projected area the earth presents to the sun, πR_e^2. The next assumption is that both the scattered and emitted radiation are radial in direction with the IR radiation being emitted over the entire surface of the planet, and the scattered radiation only being emitted from the illuminated side of the planet. The amount of momentum reaching the spacecraft must therefore be divided by the surface area into which the radiation is being divided, which is $4\pi R_o^2$ and $2\pi R_o^2$ respectively. The assumption that the scattered momentum is radial becomes suspect near the division between day and night in the orbit.

The forces and torques due to this momentum flux from the earth can be found by using the same procedure as outlined for the solar radiation torque. The momentum flux defined above is simply substituted for that of the direct solar radiation. But already it can be seen that these torques will be much smaller than those from direct solar radiation, due to the division by the surface area of a sphere with the orbit's radius.

2.5 MAGNETIC TORQUES

When in orbit, there will be an interaction between the earth's magnetic field and the net magnetic dipole of the space station, arising from current loops or permanent magnetism. Although the spacecraft may be designed such that the net magnetic dipole is approximately zero, there will be some residual that will interact with the earth's field to produce a torque;

$$M_M = D \times B \tag{42}$$

where M_M = magnetic torque about c.o.m.
D = residual magnetic dipole of space station
B = earth's magnetic field (in LEO $\approx$.1 gauss)

To accurately determine this torque it is necessary to be able to accurately define both D and B The earth's magnetic field can be modeled as a magnetic dipole centered in the earth, with a dipole strength μ_M, with an axis that protrudes from the earth's surface at 78.5° N latitude, 69.0° W longitude. It varies with altitude as $1/R^3$ and is also time varying due to the bombardment of charged particles from the solar wind. The field is also latitude and longitude dependent, but still a complete model can be formulated.

The magnetic field potential is;

$$V(r,\theta,\phi) = a\sum_{n=1}^{k} (a/r)^{n+1} \sum_{M=0}^{n} (g_n^m \cos m\phi + h_n^m \sin m\phi) P_n^m(\theta) \qquad (43)$$

where;

a = equatorial radius of the earth
g_n^m, h_n^m = Gaussian coefficients (empirical)
r = geocentric distance
θ = colatitude
ϕ = east longitude
$P_n^m(\theta)$ = Legendre functions

The n=1 terms are called 'dipole', the n=2 'quadrupole', and so on.

It is easier and more accurate in view of the time variations due to "magnetic storms", to directly monitor the magnetic field vector with an on-board magnetometer.

Determining the magnetic dipole of the space station is not as simple a measurement. Dipoles arise from three sources;

1. Current loops and permanent magnetism
2. Eddy currents
3. Hysteresis effects

The first source is the dominant one, and also the one most easily accounted for in design, either in an attempt to null the dipole or use it to produce a control torque. What is needed is a value for the resi-

dual magnetic dipole for each component of the space station, so that a value for the total residual magnetic dipole can be obtained by adding the component values vectorially. Whether these dipoles can be measured in orbit or must be measured at the time of the components manufacture is unclear, as is the question whether they will vary significantly with time.

The average expected magnetic torque on the dual keel space station is on the order of .0001 N-m, while the maximum expected torque, assuming a failure which causes the main y axis truss to be the current loop, is on the order of .01 N-m.

2.6 INERTIA CHANGE TORQUES

The desired attitude for the space station is one which keeps the stations z axis aligned with local vertical. This will require that the station maintain a constant angular velocity equal to the spacecraft's orbital angular velocity(ω_o). The angular momentum of the space craft will be;

$$H = I\omega_o \tag{44}$$

Any change in the space stations mass or configuration will lead to a change in the total inertia matrix of the vehicle. Since the stations angular velocity is constrained to remain at orbit rate, the angular momentum must change, and thus a disturbance torque results on the spacecraft.

$$M_d = \omega_o \times \underline{I}'' \omega_o + (d\underline{I}''/dt)\omega_o + \underline{I}'' d\omega_o/dt \tag{45}$$

$$M_d = \frac{d}{dt}(I_b)\omega_o \tag{46}$$

There are several ways in which the space station's inertia can change. These are some, ranked according to how big an impact they have on the total inertia;

1. Station growth - module addition
2. Station reorganization - module movement
3. Docking - Shuttle orbiter or OTV
4. Motion of the Remote Manipulation System (RMS)
5. Solar panel motion
6. Radiator motion
7. Crew motion
8. Consumable depletion - fuel,water,air,food,garbage,etc.
9. Antenna, and other platform, motion
10. Motion due to structural flexibility

When the space station is considered as a combination of rigid body components, each of which can be characterized by its own inertia and mass, then any change in the total vehicle inertia can be described as some combination of these four sources;

1. Component Rotation
2. Component Translation
3. Change in Component Inertia
4. Change in Component Mass

The inertia of the entire space station can be found as a function of the component inertias, $\underline{I}''_c$, the component masses, m_c, and the radius vector from the overall vehicle center of mass to the component center of mass, R_c.

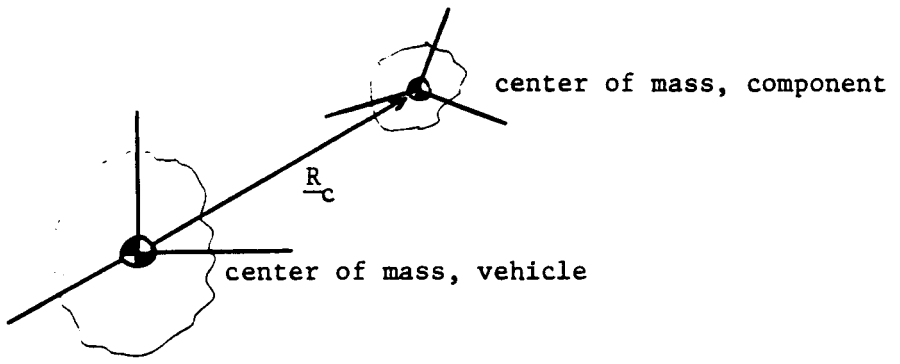

Figure 12. Relationship of C.O.M. Component and C.O.M. Station Frames

$$\underline{I}'_c = T_{c\text{-}b}\underline{I}''_c T^T_{c\text{-}b} \tag{47}$$

where I''_c = component inertia matrix in component frame

I'_c = component inertia rotated into vehicle frame

and T_{c-b} = rotation matrix from component frame to vehicle frame.

$$R_c = \begin{bmatrix} R_{cx} \\ R_{cy} \\ R_{cz} \end{bmatrix} \tag{48}$$

d_x = separation between x_b and x_c axes

$$= \sqrt{R^2_{cy} + R^2_{cz}}$$

$$d_y = \sqrt{R^2_{cx} + R^2_{cz}}$$

$$d_z = \sqrt{R^2_{cx} + R^2_{cy}} \tag{49}$$

The component moments of inertia translated into the vehicle axes are;

$$\begin{aligned} I_{cx} &= I'_{cx} + m_c d^2_x \\ I_{cy} &= I'_{cy} + m_c d^2_y \\ I_{cz} &= I'_{cz} + m_c d^2_z \end{aligned} \quad \text{(from Parallel Axis Theorem)} \tag{50}$$

And the component products of inertia translated into vehicle axes are;

$$\begin{aligned} I_{cxy} &= I'_{cxy} + m_c R_x R_y \\ I_{cxz} &= I'_{cxz} + m_c R_x R_z \\ I_{cyz} &= I'_{cyz} + m_c R_y R_z \end{aligned} \tag{51}$$

$$I_c = I_c' + m_c \begin{bmatrix} R^2_{cy} + R^2_{cz} & -R_{cx}R_{cy} & -R_{cx}R_{cz} \\ -R_{cx}R_{cy} & R^2_{cx} + R^2_{cz} & -R_{cy}R_{cz} \\ -R_{cx}R_{cz} & -R_{cy}R_{cz} & R^2_{cx} + R^2_{cy} \end{bmatrix} \tag{52}$$

which can be written more compactly as,

$$\underline{I}_c = \underline{I}'_c + m_c((R_c \cdot R_c)\underline{E} - R_c R_c^T) \tag{53}$$

where $\underline{E}$ is the identity matrix

$\therefore$ Total station inertia;

$$\underline{I} = \Sigma_c (T\underline{I}_c'' T^T + m_c((R_c \cdot R_c)\underline{E} - R_c R_c^T)) \tag{54}$$

In order to find the inertia change torques, this expression for the vehicle's inertia matrix must be differentiated with respect to time.

$$d\underline{I}/dt = \Sigma_c \left[d/dt(T\underline{I}_c T^T) + dm_c/dt((R_c \cdot R_c)\underline{E} - R_c R_c^T) + m_c d/dt((R_c \cdot R_c)\underline{E} - R_c R_c^T) \right] \tag{55}$$

$$= \Sigma_c \left[d/dt(T)\underline{I}T^T + Td/dt(\underline{I}_c)T^T + T\underline{I}_c d/dt(T^T) + dm_c/dt((R_c \cdot R_c)\underline{E} - R_c R_c^T) + m_c(d/dt(R_c \cdot R_c)\underline{E} - d/dt(R_c R_c^T)) \right] \tag{56}$$

For simplicity, $\underline{I}_c''$ has been shown simply as $\underline{I}_c$, and the transformation matrix, $T_{c\text{-}b}$, has been shown simply as T.

And since $$d/dt(R_c \cdot R_c) = 2(V_c \cdot R_c) \tag{57}$$

where V_c = velocity of component center of mass with respect to the center of mass of the vehicle.

And $$d/dt(R_c R_c^T) = V_c R_c^T + R_c V_c^T \tag{58}$$

The derivative of the inertia matrix in the vehicle frame becomes;

$$d\underline{I}/dt = \sum_c [d/dt(T)\underline{I}T^T + Td/dt(\underline{I}_c)T^T + T\underline{I}_c d/dt(T^T) \quad (59)$$
$$+ dm_c/dt((R_c \cdot R_c)\underline{E} - R_c R_c^T)$$
$$+ m_c((2V_c \cdot R_c)\underline{E} - V_c R_c^T - R_c V_c^T)$$

So there are eight parameters which need to be specified to determine rate of change of the inertia of the space station so that the torque due to these changes can be found. They are;

T_{c-b}, $d(T_{c-b})/dt$ (Component Rotation)

R_c, V_c (Component Translation)

$\underline{I}_c$, $d\underline{I}_c/dt$ (Change in component inertia)

m_c, dm_c/dt (Change in component mass)

2.6.1 Solar Panel Torques

As an example of the torques that can be produced on the space station due to a time varying moment of inertia, here is an analysis of the most predominant motion, the once per orbit rotation of the solar panels. The figure shows the coordinate frames and relative motion with respect to the rest of the space station for this motion.

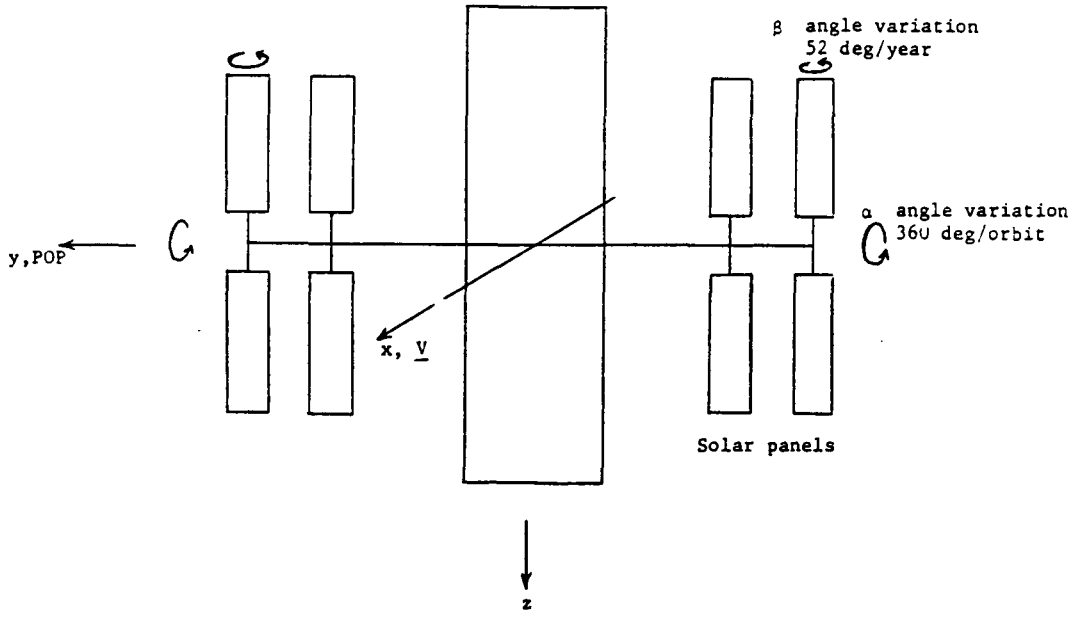

Figure 13. Relative motion of solar panels

As a component of the entire space station, the solar panels are constrained such that their center of mass does not translate with respect to the spacecraft. Their mass and inertia are constant, and so equation (59) reduces to

$$d\underline{I}''/dt = (dC/dt)JC^T + CJ(dC/dt)^T \tag{60}$$

The torque on the vehicle due to this changing inertia is;

$$M = \omega_o{}^x\underline{I}''\omega_o + (d\underline{I}''/dt)\omega_o \tag{61}$$

$$= \omega_o{}^x\underline{I}''\omega_o + [(dC/dt)JC^T + CJ(dC/dt)^T]\omega_o \tag{62}$$

$$dC/dt = \begin{bmatrix} -\sin\theta d\theta/dt & 0 & \cos\theta d\theta/dt \\ 0 & 0 & 0 \\ -\cos\theta d\theta/dt & 0 & -\sin\theta d\theta/dt \end{bmatrix} \tag{63}$$

where;

$$\theta = \Omega t$$
$$\therefore d\theta/dt = \Omega$$

$$dC/dt = -\Omega \begin{bmatrix} \sin\theta & 0 & -\cos\theta \\ 0 & 0 & 0 \\ \cos\theta & 0 & \sin\theta \end{bmatrix} \tag{64}$$

$$\therefore (dC/dt)^T = -\Omega \begin{bmatrix} \sin\theta & 0 & \cos\theta \\ 0 & 0 & 0 \\ -\cos\theta & 0 & \sin\theta \end{bmatrix} \tag{65}$$

The solar panel inertia matrix, J, is diagonal

$$J = \begin{bmatrix} J_1 & 0 & 0 \\ 0 & J_2 & 0 \\ 0 & 0 & J_3 \end{bmatrix} \tag{66}$$

So the torque becomes;

$$M = \omega_o{}^{\times} I'' \omega_o + -\Omega \begin{bmatrix} \cdots & 0 & \cdots \\ \cdots & 0 & \cdots \\ \cdots & 0 & \cdots \end{bmatrix} \begin{bmatrix} 0 \\ -n \\ 0 \end{bmatrix} \tag{67}$$

With the vehicle angular rate only about the y axis, the second term in the torque equation is zero and only the euler coupling term is left.

$$M = \begin{bmatrix} 0 & 0 & -n \\ 0 & 0 & 0 \\ n & 0 & 0 \end{bmatrix} \begin{bmatrix} I_{11}'' & I_{12}'' & I_{13}'' \\ I_{12}'' & I_{22}'' & I_{23}'' \\ I_{13}'' & I_{23}'' & I_{33}'' \end{bmatrix} \begin{bmatrix} 0 \\ -n \\ 0 \end{bmatrix} \tag{68}$$

$$M = \begin{bmatrix} n^2 I_{23}'' \\ 0 \\ -n^2 I_{12}'' \end{bmatrix} \tag{69}$$

The torque due to the solar panel rotation is the same as if they weren't rotating, that is simply the euler coupling torque from the vehicles rotation at orbit rate. This is because the cross terms I_{12}'' and I_{23}'' in the total vehicle inertia matrix are not dependent on the motion of the solar panels. It is also interesting to note that there is no pitch torque, about the y axis, due to the motion. If friction is included, there will be a pitch torque due to the solar panel motion.

2.6.2 Torque due to MRMS motion

Determining the inertia change due to MRMS motion requires a few assumptions. First, the MRMS itself is assumed to be a point mass with no rotational inertia. The mass of the MRMS is assumed to be constant, and its motion is constrained to the y-z plane in space station coordinates, along paths that are parallel to either the y or z axes.

The equation for the change in inertia of the vehicle (59) reduces to

$$d\underline{I}/dt = m_{MRMS}((2v_m \cdot \omega r_m)\underline{E} - v_m r_m^T - r_m v_m^T) \tag{70}$$

where r_m and v_m equal the MRMS position and velocity with respect to the core/solar panels center of mass. The possible MRMS velocities considering the constraints on the motion are;

$$v_m = \begin{bmatrix} 0 \\ v_{my} \\ 0 \end{bmatrix} \quad \text{(for y-motion)} \tag{71}$$

$$v_m = \begin{bmatrix} 0 \\ 0 \\ v_{mz} \end{bmatrix} \quad \text{(for z-motion)} \tag{72}$$

And the MRMS position is of the form;

$$r_m = \begin{bmatrix} 0 \\ r_{my} \\ r_{mz} \end{bmatrix} \tag{73}$$

The rate of change of the inertia matrix for motion of the MRMS parallel to the y and z axes becomes, respectively;

$$\dot{\underline{I}} = m_{MRMS} \begin{bmatrix} 2r_{my}v_{my} & 0 & 0 \\ 0 & 0 & -r_{mz}v_{my} \\ 0 & -r_{mz}v_{my} & 2r_{my}v_{my} \end{bmatrix} \tag{74}$$

$$\dot{\underline{I}} = m_{MRMS} \begin{bmatrix} 2r_{mz}v_{mz} & 0 & 0 \\ 0 & 2r_{mz}v_{mz} & -r_{my}v_{mz} \\ 0 & -r_{my}v_{mz} & 0 \end{bmatrix} \tag{75}$$

And the torques due to this MRMS motion are,

$$M_{MRMS} = \begin{bmatrix} 0 \\ 0 \\ -m_{MRMS} r_{mz} v_{my} n \end{bmatrix} \tag{76}$$

$$M_{MRMS} = \begin{bmatrix} 0 \\ 2m_{MRMS} r_{mz} v_{mz} n \\ -m_{MRMS} r_{my} v_{mz} n \end{bmatrix} \tag{77}$$

where;

$$\omega_o = \begin{bmatrix} 0 \\ n \\ 0 \end{bmatrix} \tag{78}$$

and

$$r_{my} = v_{my} t \tag{79}$$

$$r_{mz} = v_{mz} t \tag{80}$$

There is no pitch torque produced by the MRMS motion along the y axis, but there is a torque about the z axis. The motion along the z axis produces torques about both the y and z axes.

A plot of the pitch torque produced for an MRMS manuever when the space station is held stationary in LVLH is shown in Figure 14 The maneuver is motion along the z axis of the spacecraft from z=+20m to z=-20m with a speed of .5 m/s.

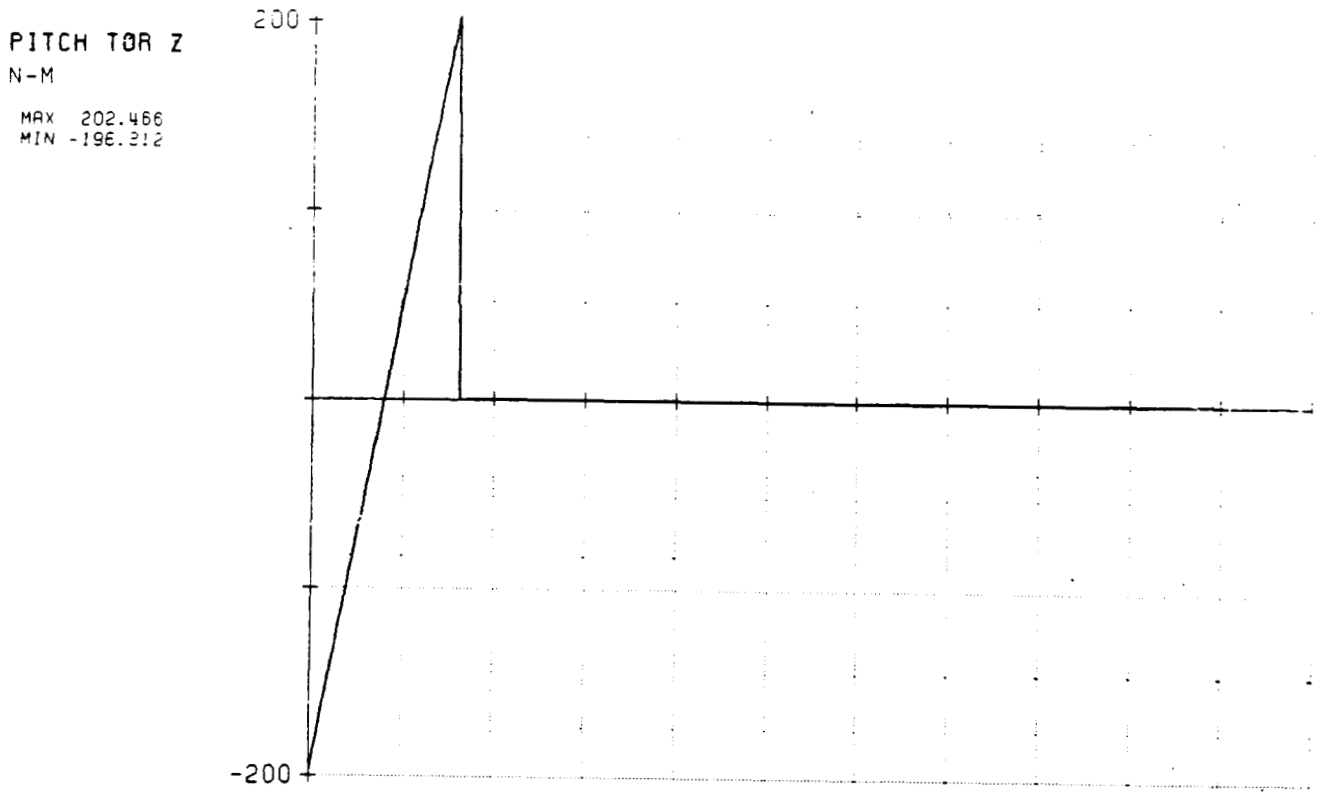

Figure 14. MRMS motion torques, z axis maneuver

2.7 FRICTIONAL TORQUES

Since the space station core is to remain nominally earth pointing, while the solar panels are sun pointing, there will have to be some kind of rotating hinge at the joint between the two. This interface will have to transmit the power that is being generated by the solar panels to the core and will necessarily involve some friction between the two. This friction will cause an internal torque on the space station that if correctly modeled could be useful in the decreasing unwanted disturbance momentum.

There are two types of power transmission that are likely to be used at solar panel/core interface. One is slip rings which transmit DC power and the other is rotary transformers which transmit AC power. In the case of slip rings, friction arises due to the carbon copper contact across which the current passes, while in the case of rotary transformers, the friction occurs in the bearings which support the rotating coils of the transformer.

In either case, a simple model of the frictional forces is that they are proportional to the normal force applied between the two contacting surfaces. The constant of proportionality is the coefficient of kinetic friction, μ_k, which is approximately constant for varying values of solar panel angular velocity.

$$F_F = \mu_k F_n \tag{81}$$

The torque associated with this frictional force is;

$$M_F = r \times F_F \tag{82}$$

where r is the moment arm at which the friction force is applied. It is necessary to know the geometry of the contact at the interface in order to determine this moment arm. It is also necessary to know the geometry of the contact in order to determine in what direction normal forces are

being applied. The net force on the hinge will be the net acceleration of the space station at that point, times some mass, as yet to be determined.

In order to determine the friction torque, it is necessary to know the coefficient of friction, the geometry of the contact, and the acceleration of the spacecraft at the hingepoint. The structure and size of the slip rings or rotary transformers are constrained by the amount of power they are meant to transfer. The total power production on the space station is on the order of 150 kw, which is divided between two hinges. The interfaces are sized for roughly 75 kw of power, and this will determine the diameter of the slip rings or transformers and thus the moment arm of the friction torque. The total torque will be the sum of the torques for each hinge.

A simplifying assumption can be made that the acceleration of the space station at the hingepoint will be small, so the normal forces will be small and can be assumed to be constant. The friction in these types of devices, as determined from an ESA study by the European Space Tribology Laboratory [36]is on the order of 1 to 10 N-m.

2.8 SUMMARY

Here are the maximum predicted levels of disturbance torque for all the phenomena described in this paper;

Table 2. Maximum Disturbance Torques

TORQUE	MAXIMUM VALUE (N-m)
Gravity Gradient	21.93
Aerodynamic	.119
Solar Radiation	.023
Earth Radiation	.052
Magnetic	.01
MRMS Z-Motion	202.47
Solar Panel Friction	10.0

3.0 ANALYSIS OF MOMENTUM BUILDUP: PITCH TORQUES ALONE

In order to predict the momentum response to disturbance torques of the entire vehicle, it is useful to first model the single axis response of the space station. Since the pitch axis will experience the largest aerodynamic torques, due to the offset of the center of pressure created by the OTV and OMV berths in the dual keel space station configuration, this is the axis that will be modeled.

Once modeled, the momentum response of the vehicle to these torques can be found by integrating them over time, and the peak momentum the disturbance torques will produce can be found from examining this function for momentum. This peak momentum will be the determining factor in the sizing of the momentum exchange devices that will be needed to deal with this disturbance momentum. Once the peak momentum is determined, it is then possible to predict the effect that various attitudes have upon the peak momentum value, the effect that uncertainties in attitude have upon the peak value, and the effect that uncertainties in the torque models have on the peak momentum value.

3.1 SIMPLE AERO/GRAVITY GRADIENT MODEL

The disturbance torques being considering in this section are;

1. Aerodynamic
2. Gravity Gradient
3. MRMS Motion

The total disturbance torque then becomes;

$$M_D = M_A + M_{GG} + M_{MRMS} \tag{83}$$

$$M_D = M_D(\theta, t) \tag{84}$$

The pitch torques can be modeled with differing levels of complexity, depending on whether effects such as the change in inertia of the space station with solar panel and MRMS motion are to be included. A set of simple torque models follows;

$$M_A = -1/2\ \rho_o v^2 C_D (A_{sp} r_{sp} + A_c r_c) \cos\theta\,(1 + 1/2\ \cos(nt)) \tag{85}$$

$$M_{GG} = 3n^2[(I_z - I_x)\sin\theta\cos\theta - I_{xz}] \tag{86}$$

$$M_{MRMS} = 2M_M r_{mz} v_{mz} n = 2M_M n v_{mz} (r_{mzo} + v_{mz} t) \tag{87}$$

(for z-motion of MRMS)

where;

θ = pitch angle
t = elapsed time in orbit from point of maximum atmospheric density
n = orbit rate = $2\pi/T$
ρ_o = average atmospheric density
v = magnitude of spacecraft velocity with respect to atmosphere
A_{sp} = projected area of the solar panels
A_c = projected area of the core
C_D = overall vehicle drag coefficient
r_c = core aerodynamic moment arm
r_{sp} = solar panel aerodynamic moment arm
I = vehicle inertia
m_{MRMS} = mass of MRMS
r_m = position of MRMS with respect to C.O.M.
v_m = velocity of MRMS with respect to C.O.M.

The assumptions made in formulating these simple equations for the disturbance torques on the space station are;

1. Solar Panels not rotating
2. Distance to C.O.P. constant over time
3. The drag coefficient doesn't change with attitude
4. The inertia of the vehicle doesn't change with solar panel and MRMS motion
5. There are no shadowing effects in the aerodynamic or radiation torques
6. The atmosperic density variation is a simple cosine model of the diurnal component of the variation

The total momentum built up over time is simply the integral of these torques over time.

$$H(\theta,t) = \int_0^t M_D(\theta,t)\, dt \qquad (88)$$

If we consider only the aerodynamic and gravity gradient torques, and then only the simple models for these torques, the expression for the momentum of the spacecraft as a function of time and attitude can be found.

$$M_A = K_1 \cos\theta (1 + 1/2 \cos(nt)) \tag{89}$$

$$M_{GG} = K_2 \sin\theta\cos\theta - K_3 \tag{90}$$

Where;

$$K_1 = -1/2\ \rho_o v^2 C_D (A_{sp} r_{sp} + A_c r_c) \tag{91}$$

$$K_2 = 3n^2 (I_z - I_x) \tag{92}$$

$$K_3 = 3n^2 I_{xz}$$

$$\begin{aligned} H(\theta,t) &= \int_0^t M_A + M_{GG}\, dt \\ &= \int_0^t [K_1 \cos\theta (1 + 1/2 \cos(nt)) + K_2 \sin\theta\cos\theta - K_3]dt \end{aligned} \tag{93}$$

$$H(\theta,t) = (K_1 \cos\theta)t + (K_1/2n \cos\theta)\sin(nt) + (K_2 \sin\theta\cos\theta)t - K_3 t \tag{94}$$

$$H(\theta,t) = (K_1 \cos\theta + K_2 \sin\theta\cos\theta - K_3)t + (K_1/2n \cos\theta)\sin(nt) \tag{95}$$

For this simple model, the disturbance momentum is just the superposition of a linear and a sinusoidal term.

The Average Torque Equilibrium Attitude (ATEA) is, for pitch alone, the angle at which if the spacecraft is fixed for a given time T, the net momentum buildup is zero.

$$H(\theta_A,T) = (K_1\cos\theta_A)T + (K_1/2n\cos\theta_A)\sin(nT) + (K_2\sin\theta_A\cos\theta_A)T - K_3T = 0 \quad (96)$$

$$H(\theta_A,T) = (K_1\cos\theta_A + K_2\sin\theta_A\cos\theta_A - K_3)T + (K_1/2n\cos\theta_A)\sin(nT) \quad (97)$$

If we choose the time T to be a multiple of the orbit period T, where $T=2\pi/n$, then the $\sin(nT)$ term is zero, and we are left with this condition to solve for θ_A;

$$K_1\cos\theta_A + K_2\sin\theta_A\cos\theta_A - K_3 = 0 \quad (98)$$

This is a transcendental equation, and as such cannot be solved explicitly for the ATEA, θ_A. But if the constants K_1, K_2, and K_3 are known, then an iterative solution for θ_A can be set up.

$$\theta_A = \sin^{-1}(1/K_2(K_3/\cos\theta_A - K_1)) \quad (99)$$

To find the peak momentum over the time period T, it is necessary to examine the extremums of the function $H(\theta,t)$ by taking the derivative of

$H(\theta,t)$ with respect to time and setting it equal to zero. Differentiating with respect to time yields the original torque expression.

$$dH/dt = [K_1\cos\theta(1 + 1/2\cos(nt_p)) + K_2\sin\theta\cos\theta - K_3]$$
$$= (K_1\cos\theta + K_2\sin\theta\cos\theta - K_3) + (K_1/2\cos\theta)\cos(nt_p) = 0 \quad (100)$$

$$\therefore t_p = 1/n \cos^{-1}\left(\frac{K_3 - K_1\cos\theta - K_2\sin\theta\cos\theta}{(K_1/2)\cos\theta}\right) = \text{time of peak momentum} \quad (101)$$

By substituting this expression for the time of peak momentum buildup on the space station into the expression for the momentum (95), the peak momentum buildup as a function of the attitude at which the spacecraft is held can be found.

$$H_p = (K_1\cos\theta + K_2\sin\theta\cos\theta - K_3)(1/n)\cos^{-1}\left(\frac{K_3 - K_1\cos\theta - K_2\sin\theta\cos\theta}{K_1/2\cos\theta}\right)$$
$$+ 1/n\sqrt{((K_1/2)\cos\theta)^2 - (K_3 - K_1\cos\theta - K_2\sin\theta\cos\theta)^2} \quad (102)$$

It is now possible to examine the effect of keeping the space station held at various attitudes on the value of the peak momentum accumulated over one orbit. The first attitude to be examined is the LVLH hold attitude. In this attitude, $\theta = 0$, and the equation for peak momentum reduces to;

$$H_p = (K_1 - K_3)(1/n)\cos^{-1}(2(K_3 - K_1)/K_1) + (1/2n)\sqrt{K_1^2 - 4(K_3 - K_1)^2} \quad (103)$$

This value exists only if $|K_3 - K_1| \leq K_1/2$ which means that the cosine terms in the momentum equation are not overpowered by the linear terms in such a way that there are no extremums of the function in the interval $0 \leq t \leq T$. Even if the value of H_p exists, it may still only be a local maximum or minimum, and intuitively, the maximum momentum buildup for one orbit should be at the end of the orbit, at $t = T$. At the end the momentum is;

$$\begin{aligned} H_p &= (K_1 - K_3)T + (K_1/2n)\sin(nT) \\ &= (K_1 - K_3)T \end{aligned} \quad (104)$$

If the space station is held in ATEA, then the peak momentum expression reduces to;

$$H_p = K_1/2n \cos\theta_A \quad (105)$$

To compare these two peak values, it is necessary to evaluate the constants numerically. The parameters for the dual keel space station are defined in Table 3 on page 68.

Table 3. Dual Keel Parameters, Solar Panels Fixed, No MRMS

A_{sp} = 1974.64 m^2
r_{sp} = +.3709 m
A_c = 261.17 m^2
r_c = =5.0672 m
I_x = 62105091 kg-m^2
I_z = 45995243 kg-m^2
I_{xz} = 5930594 kg-m^2
M_M = 10000.0 kg (w/payload)
M_c = 167869.2017 kg
M_{sp} = 5510.1999 kg
ρ_o = 1.5 X 10^{-12} kg/m^3
v = 7624 m/s
n = 1.1188 X 10^{-3} s^{-1}

For these values the ATEA pitch angle is;

θ_A = -23.6°

And the peak momenta are;

H_p(LVLH) = -124585.64 N-m-s

H_p(ATEA) = 35.28 N-m-s

For this simple model, the ATEA hold is much better that the LVLH hold. This is because the Dual Keel is an essentially aerodynamically

balanced design, so the dominant torques come from the gravity gradient. The ATEA is such that the gravity gradient torques are in equilibrium, so when the space station is moved away from ATEA and held in LVLH, a significant disturbance momentum is created that must be dealt with. That the difference is so large is only the case of this simple model, which is subject to the assumptions outlined earlier.

3.1.1 Simple Model with Solar Panel Rotation

If the solar panel motion is considered, the torques are of the same form as before, except that now the projected area of the solar panels to the incoming atmospheric particles is a function of time.

$$M_A = -1/2\ \rho_o v^2 C_D (A_{sp} r_{sp} + A_c r_c) \cos\theta (1 + 1/2 \cos(nt)) \quad (106)$$

$$M_{GG} = 3n^2[(I_z - I_x)\sin\theta\cos\theta - I_{xz}] \quad (107)$$

where

$$A_{sp} = A_{sp}\ |\cos(nt)| \quad (108)$$

So the torque becomes;

$$M_D = K_1\cos\theta\,(1 + 1/2\,\cos(nt))$$

$$+ K_1'\cos\theta\,(1 + 1/2\,\cos(nt)) \begin{cases} \cos(nt), & \text{for } 0 \le t \le \pi/2n \\ -\cos(nt), & \text{for } \pi/2n \le t \le 3\pi/2 \\ \cos(nt), & \text{for } 3\pi/2n \le t \le 2\pi/n \end{cases} \quad (109)$$

$$+ K_2\sin\theta\cos\theta - K_3$$

Where;

$$K_1 = -1/2\ \rho v^2 C_D A_c r_c \quad (110)$$

$$K_1' = -1/2\ \rho v^2 C_D A_{sp} r_{sp} \quad (111)$$

$$K_2 = 3n^2(I_z - I_x) \quad (112)$$

$$K_3 = 3n^2 I_{xz} \quad (113)$$

Integrating this expression for torque over time yields a new expression for the disturbance momentum that takes into account the rotation of the solar panels.

$$H(\theta, t) = K_1\cos\theta\,(t + 1/2n\,\sin(nt))$$

$$+ K_1'\cos\theta \begin{cases} (1/n\,\sin(nt) + t/4 + 1/8n\,\sin(2nt)) & 0 \le t \le \pi/2n \\ (2/n + \pi/4n - 1/n\,\sin(nt) - t/4 - 1/8n\,\sin(2nt)) & \pi/2n \le t \le 3\pi/2n \\ (4/n - \pi/2n + 1/n\,\sin(nt) + t/4 + 1/8n\,\sin(2nt)) & 3\pi/2n \le t \le 2\pi/n \end{cases}$$

$$+ (K_2\sin\theta\cos\theta - K_3)\,t \quad (114)$$

The assumption that the variation in spacecraft inertia due to the rotation of the solar panels can be ignored is valid for the pitch axis. The variation of the vehicle's inertia about this axis is zero since the rotation of the solar panels is constrained to be about this axis. However, the variation of the spacecraft's inertia about the other two axes due to solar panel motion can be significant, and since the pitch gravity gradient torque is dependent on these off axis inertias, the assumption must be examined more closely. The total vehicle inertia is;

$$I = I' + CJC^T - Kr_m^{\times}r_m^{\times} \tag{115}$$

The time varying portion of this inertia is the CJC^T term, which expands to,

$$CJC^T = \begin{bmatrix} J_1\cos^2(\Omega t) + J_3\sin^2(\Omega t) & 0 & (J_3 - J_1)\sin(\Omega t)\cos(\Omega t) \\ 0 & J_2 & 0 \\ (J_3 - J_1)\sin(\Omega t) & 0 & J_1\sin^2(\Omega t) + J_3\cos^2(\Omega t) \end{bmatrix} \tag{116}$$

The gravity gradient torque is a function of the I_x, I_z, and I_{xz} terms of the inertia matrix.

$$I_x = I_x' + J_1\cos^2(\Omega t) + J_3\sin^2(\Omega t) = I_x' + J_1 + (J_3 - J_1)\sin^2(\Omega t \tag{117}$$

$$I_z = I_z' + J_1\cos^2(\Omega t) + J_3\sin^2(\Omega t) = I_z' + J_1 + (J_3 - J_1)\cos^2(\Omega t \tag{118}$$

$$I_{xz} = I_{xz}' + (J_3 - J_1)\sin(\Omega t)\cos(\Omega t) \tag{119}$$

The inertias are all dependent on the difference between the J_3 and J_1 terms of the solar panel inertia. The closer these two values are, the less impact the solar panel motion has on the gravity gradient torque.

Some predicted values for solar panel inertia are;

$J_1 = 16545372.76\ N\text{-}m^2$

$J_3 = 1292047.280\ N\text{-}m^2$

$I_x' = 45559718.78\ N\text{-}m^2$

$I_z' = 30679373.76\ N\text{-}m^2$

$I_{xz}' = 5930594.86\ N\text{-}m^2$

$$\therefore \frac{J_3 - J_1}{J_1 + I_x'} = -.25 \tag{120}$$

$$\frac{J_3 - J_1}{J_1 + I_z'} = -.32 \tag{121}$$

and

$$\frac{J_3 - J_1}{I_{xz}'} = -2.57.32 \tag{122}$$

The ratios show that the time varying components of the inertias are significant in comparison to the inertia of the vehicle if the solar panels are considered as non-rotating.

3.2 COMPLEX TORQUE MODELS

A more complete modeling of the torques on the space station would take into account the inertia changes associated with the motion of the solar panels and MRMS, the resulting changes in the moment arms of the aerodynamic and radiation torques due to these mass shifts, and the torques due to the changing inertia of the space station as it is being held at a constant rate.

The motion of the solar panels produces no net torque about the vehicle y-axis, but it does cause the I_x, I_z, and I_{xz} vehicle inertias to be time varying, which affects the gravity gradient torque. Similarly, motion of the MRMS along directions parallel to the pitch axis produces no pitch torque, but does contribute to the changes in the gravity gradient torques. The motion of the MRMS parallel to the z-axis has the most pronounced effect on the spacecraft. It produces a sizable torque as well as both changing the vehicles inertia and changing the pitch moment arm of the aerodynamic torque by shifting the center of mass of the entire vehicle parallel to the z-axis. (Figure 15 on page 74)

The MRMS maneuvers are shown in Figure 16 on page 75.

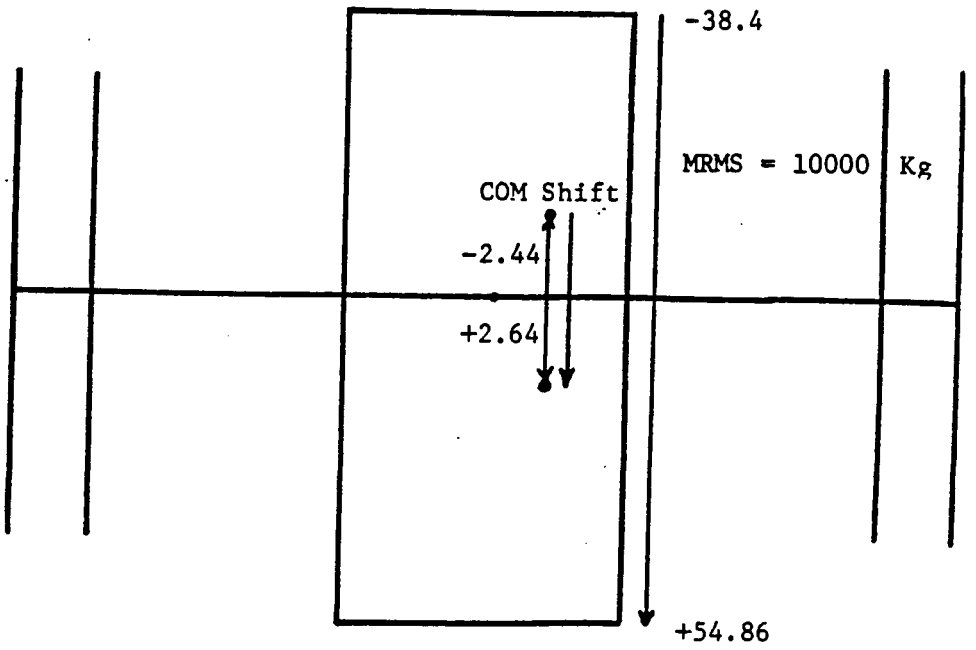

Figure 15. Shift of C.O.M. with MRMS motion

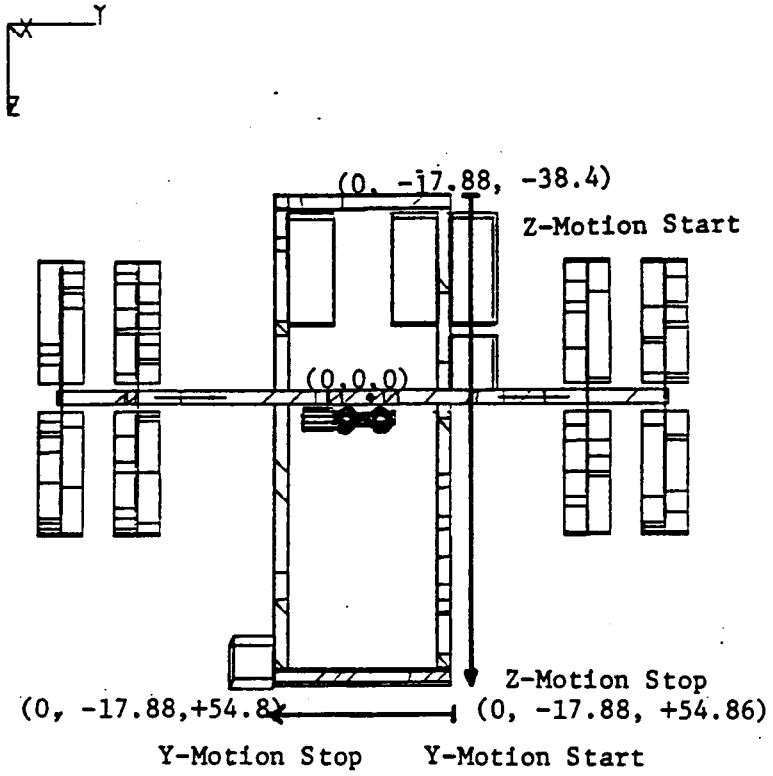

Figure 16. MRMS maneuvers

3.2.1 Complex Model Y-Motion of MRMS

The aerodynamic torque, for y-motion of the MRMS, is the same as for the case of no motion of the MRMS, except that the moment arms of the pitch torque are adjusted for whatever initial z position the MRMS has, which in this case is +54.86 m.

$$M_A = -1/2\ \rho_o v^2 C_D (A_c r_c + A_{sp} r_{sp})\ (1 + 1/2\ \cos(nt))\cos\theta \qquad (123)$$

where;

A_{sp} = frontal area of the solar panels

= $A_{sp}|\cos(nt)|$, due to solar panel rotation

The aero torque can be expressed as a function of time and the pitch angle.

$$M_A = K_1\cos\theta(1 + 1/2\cos(nt)) + K_1'\cos\theta(1 + 1/2\cos(nt)) \begin{cases} \cos(nt), & \text{for } 0 \le t \le \pi/2n \\ -\cos(nt), & \text{for } \pi/2n \le t \le 3\pi/2 \\ \cos(nt), & \text{for } 3\pi/2n \le t \le 2\pi/n \end{cases} \quad (124)$$

For simplicity, the parameters in the equation have been collected into the constants K_1 and K_1'

$$K_1 = -1/2\ \rho v^2 C_D A_c r_c \quad (125)$$

and

$$K_1' = -1/2\ \rho v^2 C_D A_{sp} r_{sp} \quad (126)$$

The pitch gravity gradient torque is a function of the I_x, I_z, and I_{xz} vehicle inertias.

$$M_{GG} = 3n^2[(I_z(t) - I_x(t))\sin\theta\cos\theta - I_{xz}(t)] \quad (127)$$

To determine the torque, the inertia must be found as a function of time, given the motion of the MRMS and the solar panels.

$$I = I' + CJC^T - Kr_T{}^x r_T{}^x \tag{128}$$

where;

$$K = \frac{M_M (M_{sp} + M_c)}{M_M + M_{sp} + M_c} \tag{129}$$

and

r_T = distance from core/solar panel center of mass to MRMS
J = solar panel inertia matrix = constant
C = transformation from solar panel to core coordinates
I' = core inertia matrix, plus the inertia due to the mass offset from solar panels = constant

$C = C(t)$ and $r_T = r_T(t)$

Again, the time varying portions of the inertia expression are;

$$CJC^T = \begin{bmatrix} J_1\cos^2(nt) + J_3\sin^2(nt) & 0 & (J_3 - J_1)\sin(nt)\cos(nt) \\ 0 & J_2 & 0 \\ (J_3 - J_1)\sin(nt)\cos(nt) & 0 & J_1\sin^2 + J_3\cos^2(nt) \end{bmatrix} \tag{130}$$

and

$$Kr_T{}^x r_T{}^x = K \begin{bmatrix} -(r_{Tz}{}^2 + r_{Ty}{}^2) & r_{Tx}r_{Ty} & r_{Tx}r_{Tz} \\ r_{Tx}r_{Ty} & -(r_{Tz}{}^2 + r_{Tx}{}^2) & r_{Ty}r_{Tz} \\ r_{Tx}r_{Tz} & r_{Ty}r_{Tz} & -(r_{Ty}{}^2 + r_{Tx}{}^2) \end{bmatrix} \tag{131}$$

For the y-motion of the MRMS; $r_{Tx} = 0$
$r_{Tz} = r_{Tzo} = \text{constant}$
$r_{Ty} = r_{Tyo} + v_{my}t$

This gives the time varying inertia components;

$$I_x(t) = I_x' + J_1\cos^2(nt) + J_3\sin^2(nt) + K(r_{Tz}^2 + r_{Ty}^2) \quad (132)$$
$$I_z(t) = I_z' + J_1\sin^2(nt) + J_3\cos^2(nt) + K(r_{Ty}^2) \quad (133)$$
$$I_{xz}(t) = I_{xz}' + (J_3 - J_1)\sin(nt)\cos(nt) \quad (134)$$

And the gravity gradient torque is;

$$M_{GG} = (K_2 - K_4 + K_3\cos(2nt))\sin\theta\cos\theta - K_5 - K_3/2\ \sin(2nt) \quad (135)$$

Again, for simplicity, the parameters have been collected into the constants K_2, K_3, K_4, and K_5, where the constants are defined as follows;

$$K_2 = 3n^2(I_z' - I_x') \quad (136)$$
$$K_3 = 3n^2(J_3 - J_1) \quad (137)$$
$$K_4 = 3n^2(Kr_{Tzo}^2) \quad (138)$$
$$K_5 = 3n^2(I_{xz}') \quad (139)$$

Adding the aerodynamic torque to the gravity gradient torque gives the total torque on the space station, for y-motion of the MRMS, as a function of time and pitch angle. Integrating that expression over time yields the disturbance momentum imparted to the spacecraft that will have to be dealt with by the CMG's.

$$H(\theta, t) = K_1 \cos\theta\,(t + 1/2n \sin(nt))$$

$$+ K_1' \cos\theta \begin{cases} (1/n \sin(nt) + t/4 + 1/8n \sin(2nt)) & 0 \le t \le \pi/2n \\ (2/n + \pi/4n - 1/n \sin(nt) - t/4 - 1/8n \sin(2nt)) & \pi/2n \le t \le 3\pi/2n \\ (4/n - \pi/2n + 1/n \sin(nt) + t/4 + 1/8n \sin(2nt)) & 3\pi/2n \le t \le 2\pi/n \end{cases}$$

$$+ ((K_2 - K_4)\,t + K_3/2n \sin(2nt))\sin\theta\cos\theta - K_5 t + K_3/4n \cos(2nt) - K_3/4n \tag{140}$$

This expression can be seen to reduce to the simpler expression for momentum that didn't take into account inertia changes from the internal motions, by setting the K_3 and K_4 constants to zero.

Now that we have this expression for the disturbance momentum, the questions that need to be answered are;

1. What is the ATEA (Average Torque Equilibrium Attitude) at which to fly the space station to cancel this momentum over a given time T?

2. What is the peak momentum expected for various attitudes?

3. What effects do uncertainties in the attitude and in the torque models have upon this peak momentum prediction?

The peak momentum is important as it will determine the sizing of the momentum exchange devices that will be used to compensate for this disturbance momentum.

The ATEA pitch angle can be found by employing its definition;

$$H(\theta_A, T) = 0 \quad , \quad T = 2\pi/n = \text{orbit period} \tag{141}$$

$$\therefore K_1\cos\theta_A(T) + K_1'\cos\theta_A(4/n) + (K_2 - K_4)T\sin\theta_A\cos\theta_A - K_5T = 0 \tag{142}$$

Solving this transcendental equation for θ_A can be accomplished iteratively by using this expression;

$$\theta_A = \sin^{-1}[1/(K_2 - K_4)\,((K_5/\cos\theta_A) - (K_1 + K_1'\,2/\pi))] \tag{143}$$

The time t=T was chosen because it simplifies the equation for θ_A, however any time could have been used, while multiples of T also give a simpler expression.

3.2.2 Complex Model Z-Motion of MRMS

For motion of the MRMS parallel to the z-axis, different expressions for the torque and momentum must be obtained. The variations of the

moment arms of the aerodynamic torque with a shifting center of mass, and the torque due to a changing I_y must be included along with the variation due to changing I_x, I_z, and I_{xz} inertias.

The aerodynamic torque for z-motion of the MRMS is;

$$M_A = (K_1 - K_1' t)\cos\theta\,(1 + 1/2\cos(nt))$$

$$\begin{cases} \div\ (K_2 - K_2' t)\cos\theta\,(1 + 1/2\cos(nt))\cos(nt) & \text{for } 0 \le t \le t_1 \\ (K_1 - K_1' t_1)\cos\theta\,(1 + 1/2\cos(nt)) & \\ +\ (K_2 - K_2' t_1)\cos\theta\,(1 + 1/2\cos(nt)) \begin{cases} \cos(nt), & \text{for } t_1 \le t \le \pi/2n \\ -\cos(nt), & \text{for } \pi/2n \le t \le 3\pi/2n \\ \cos(nt), & \text{for } 3\pi/2n \le t \le 2\pi/n \end{cases} & \text{for } t_1 \le t \le 2\pi/n \end{cases} \quad (144)$$

Where;

$$K_1 = -1/2\ \rho_o v^2 C_D A_c r_{co} \quad (145)$$

$$K_1' = -1/2\ \rho_o v^2 C_D A_c (M_M/M_c + M_{sp})\, v_{Mz} \quad (146)$$

$$K_2 = -1/2\ \rho_o v^2 C_D A_{sp} r_{spo} \quad (147)$$

$$K_2' = -1/2\ \rho_o v^2 C_D A_{sp} (M_M/M_c + M_{sp})\, v_{Mz} \quad (148)$$

and t_1 = time the MRMS motion stops

The gravity gradient torque for MRMS z-motion becomes;

$$M_{GG} = \begin{cases} (K_3 - K_4 t - K_5 t^2 + K_6 \cos(2nt))\sin\theta\cos\theta - K_7 - K_6/2 \sin(2nt) \\ \qquad\qquad \text{for } 0 \le t \le t_1 \\ (K_3 - K_4 t_1 - K_5 t_1^2 + K_6 \cos(2nt))\sin\theta\cos\theta - K_7 - K_6/2 \sin(2nt) \\ \qquad\qquad \text{for } t_1 \le t \le 2\pi/n \end{cases} \quad (149)$$

Where;

$$K_3 = 3n^2(I_z' - I_x' - Kr_{Tzo}^2) \quad (150)$$

$$K_4 = 3n^2(2Kr_{Tzo}v_{Mz}) \quad (151)$$

$$K_5 = 3n^2(Kv_{Mz}^2) \quad (152)$$

$$K_6 = 3n^2(J_3 - J_1) \quad (153)$$

$$K_7 = 3n^2(I_{xz}') \quad (154)$$

The torque from the changing I_y due to the MRMS motion is;

$$M_{MRMS} = 2M_M r_{mz} v_{mz} n = 2M_M n(r_{mzo} v_{mz} + v_{mz}^2 t) \quad (155)$$

(for z-motion of MRMS)

Integrating the sum of these three torques yields the expression for the disturbance momentum for the z-motion of the MRMS;

$$
H(\theta,\ t) = K_1\cos\theta\,(t + 1/2n\,\sin(nt))
$$

$$
\begin{cases}
+ K_2\cos\theta\,(1/n\,\sin(nt) + t/4 + 1/8n\,\sin(2nt)) \\
+ K_1'\cos\theta\,(t^2/2 + 1/2n^2\,\cos(nt) + t/2n\,\sin(nt) - 1/2n^2) \\
+ K_2'\cos\theta\,(t/n\,\sin(nt) + 1/n^2\,\cos(nt) + t/8n\,\sin(2nt) \\
\qquad + 1/16n^2\cos(2nt) + t^2/8 - 17/16n^2) \\
+ (K_3 t - K_4 t^2/2 - K_5 t^3/3 + K_6/2n\,\sin(2nt))\sin\theta\cos\theta \\
\qquad - K_7 t + K_6/4n\,\cos(2nt) - K_6/4n \\
+ 2M_M n\,(r_{mzo} v_{mz} t + v_{mz}^2/2\ t^2)
\end{cases}
$$

$$
\text{for } 0 \le t \le t_1
$$

$$
\begin{cases}
(K_1 - K_1' t_1)\cos\theta\,(t + 1/2n\,\sin(nt)) \\
+ Q_2 \\
+ ((K_3 - K_4 t_1 - K_5 t_1^2)\,t + K_6/2n\,\sin(2nt))\sin\theta\cos\theta \\
- K_7 t + K_6/4n\,\cos(2nt)\,(K_4 t_1^2/2 + 2/3\,K_5 t_1^3)\sin\theta\cos\theta - K_6/4n \\
+ 2M_M n\,(r_{mzo} v_{mz} t_1 + v_{mz}^2/2\ t_1^2) \\
+ (K_2 - K_2' t_1)\cos\theta \begin{cases} (1/n\,\sin(nt) + t/4 + 1/8n\,\sin(2nt)) \\ \qquad \text{for } t_1 \le t \le \pi/2n \\ (2/n + \pi/4n - 1/n\,\sin(nt) - t/4 - 1/8n\,\sin(2nt)) \\ \qquad \text{for } \pi/2n \le t \le 3\pi/2n \\ (4/n - \pi/2n + 1/n\,\sin(nt) + t/4 + 1/8n\,\sin(2nt)) \\ \qquad \text{for } 3\pi/2n \le t \le 2\pi/n \end{cases}
\end{cases}
$$

$$
\text{for } t_1 \le t \le 2\pi/n \qquad (156)
$$

where

$$
Q_2 = K_1'\cos\theta\,(t_1^2/2 - 1/2n^2\,\cos(nt_1) - 1/2n^2) \qquad (157)
$$

$$
+ K_2'\cos\theta\,(t_1^2/8 - 1/n^2\,\cos(nt_1) - 1/16n^2\,\cos(2nt_1) + 17/16n^2)
$$

And lastly, the ATEA angle for this maneuver can be found by an iterative solution of an equation of the form;

$$\theta_A = \sin^{-1}[1/C_4(C_5/\cos\theta_A - (C_1 + C_2 + C_3))] \quad (158)$$

where;

$$C_1 = (K_1 - K_1't_1)T \quad (159)$$

$$C_2 = (K_2 - K_2't_1)4/n \quad (160)$$

$$C_3 = Q_2/\cos\theta_A \quad (161)$$

$$C_4 = (K_3 - K_4t_1 - K_5t_1^2)T + (K_4t_1^2/2 + 2/3\ K_5t_1^3) \quad (162)$$

$$C_5 = -K_7T + 2M_Mn(r_{mzo}v_{mz}t_1 + v_{mz}^2/2\ t_1^2) \quad (163)$$

4.0 RESULTS FROM MODELS

In this section, the torques and momentum response from the simple model with solar panel rotation are presented in Figure 17 on page 86 to Figure 24 on page 93 .

The torques and momentum response from the complex model with no motion of the MRMS are presented in Figure 25 on page 94 to Figure 33 on page 102 .

The torques and momentum response from the complex model with Y-motion of the MRMS are presented in Figure 34 on page 103 to Figure 42 on page 111 .

And the torques and momentum response from the complex model with Z-motion of the MRMS are presented in Figure 43 on page 112 to Figure 51 on page 120.

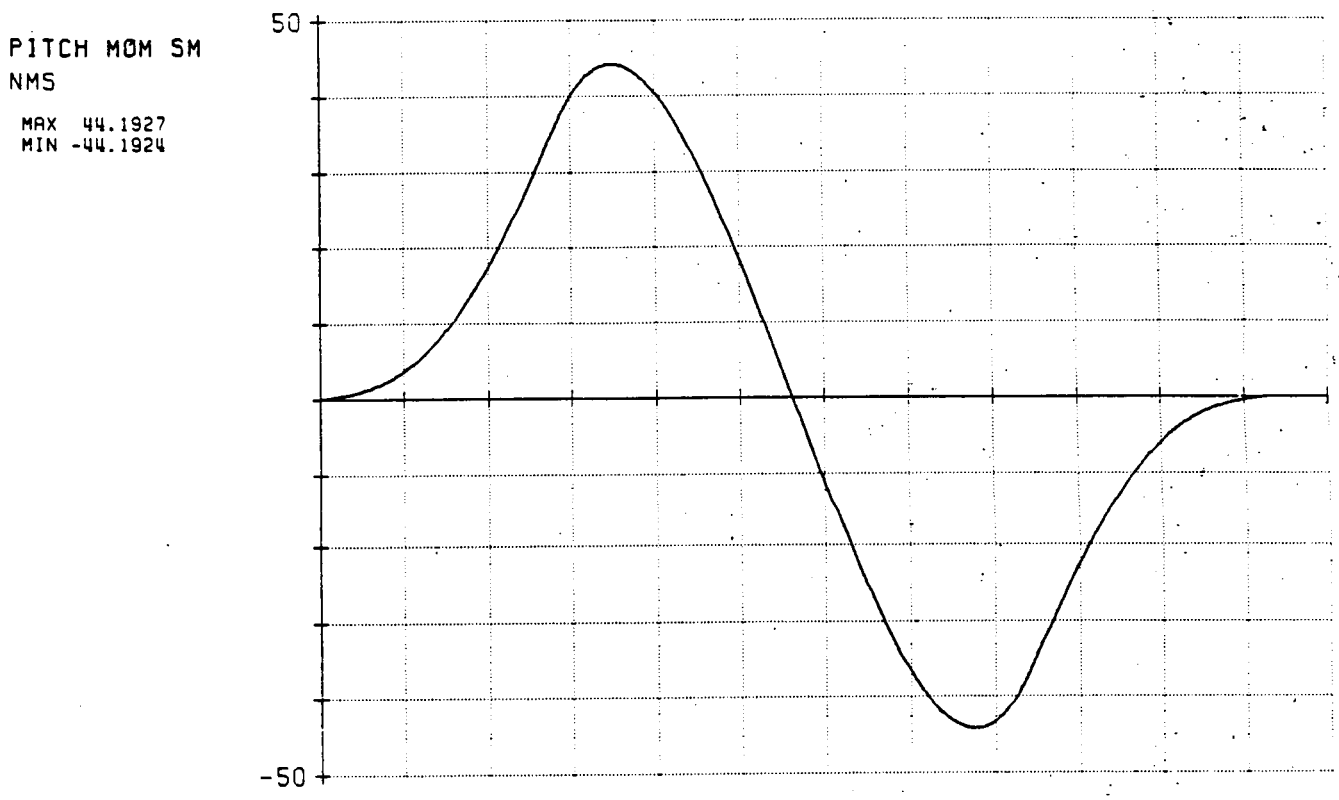

Figure 17. Momentum, Simple Model, ATEA hold

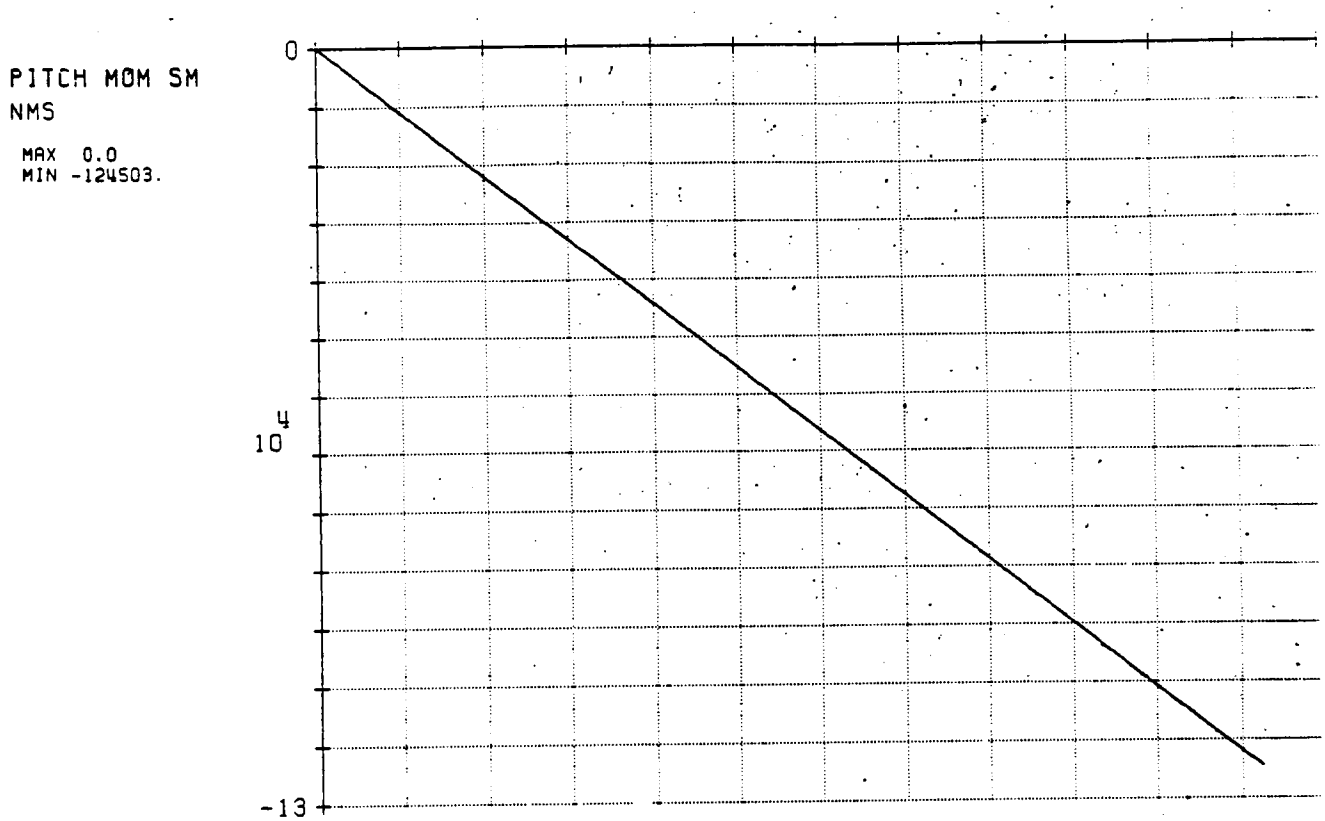

Figure 18. Momentum, Simple Model, LVLH hold

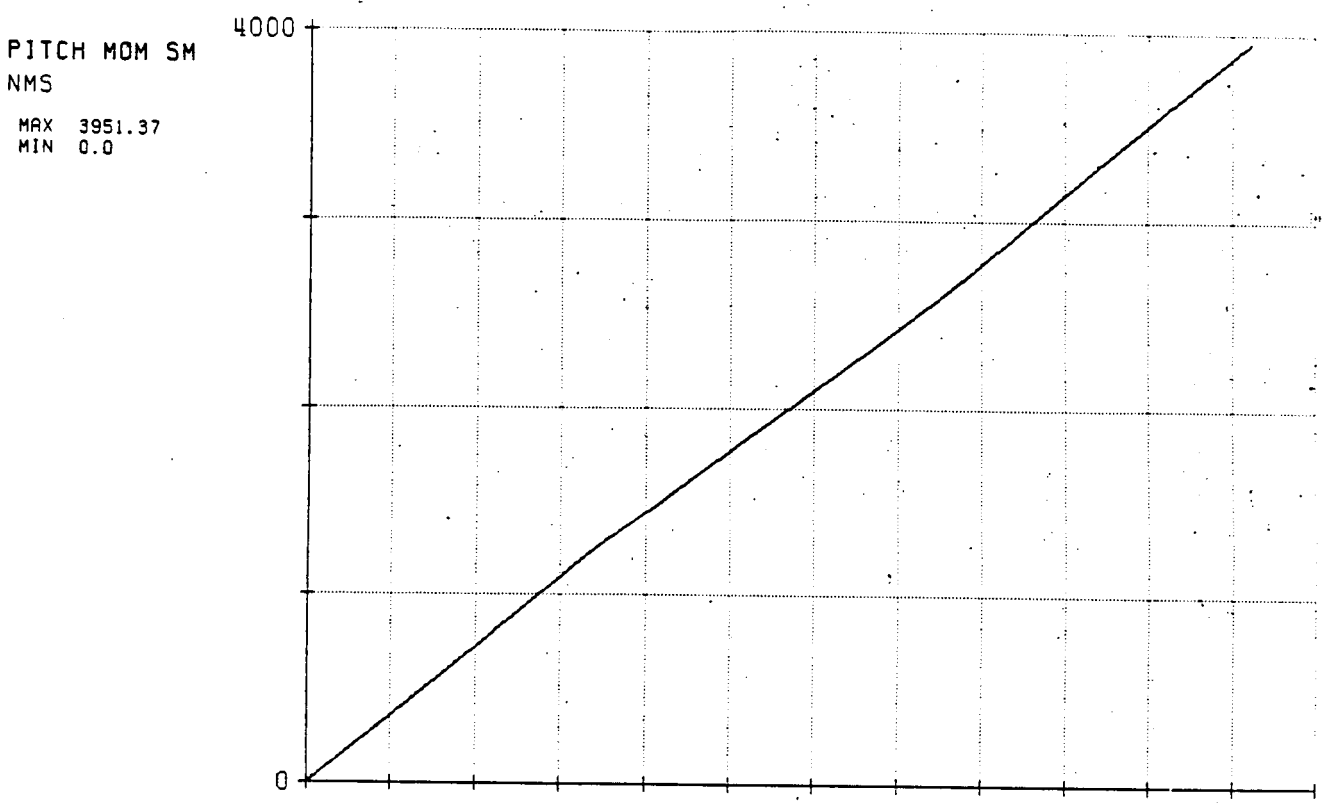

Figure 19. Momentum, Simple Model, ATEA - 1 deg hold

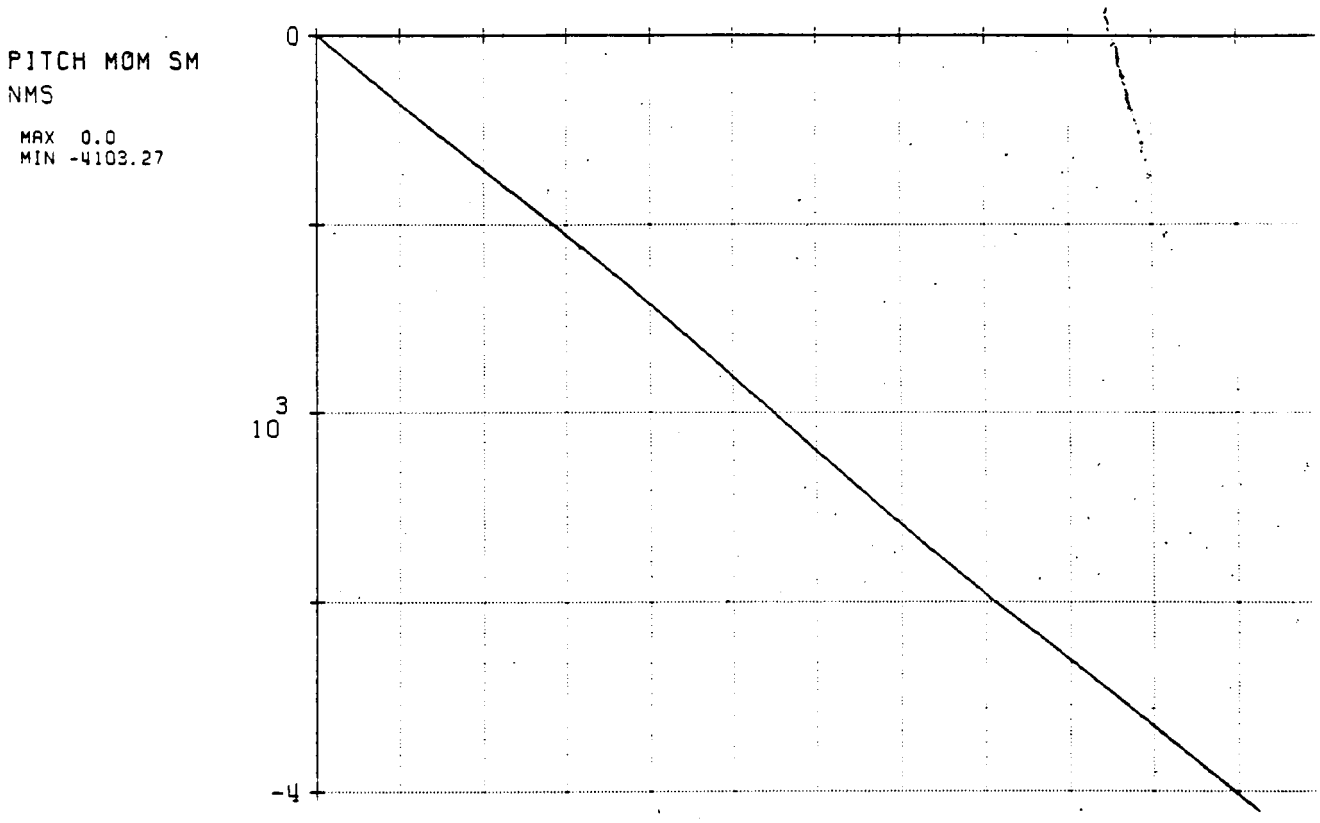

Figure 20. Momentum, Simple Model, ATEA + 1 deg hold

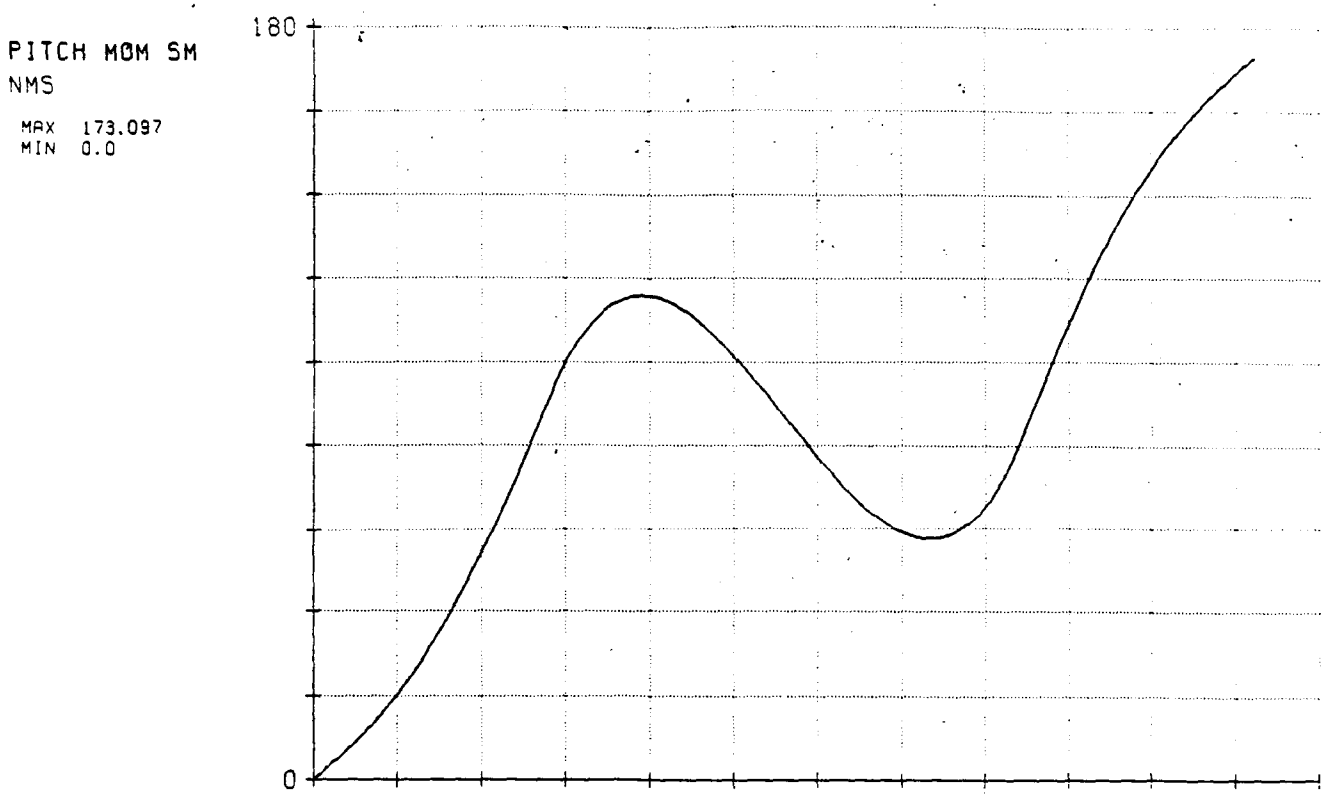

Figure 21. Momentum, Simple Model, ATEA hold, ρ + 50%

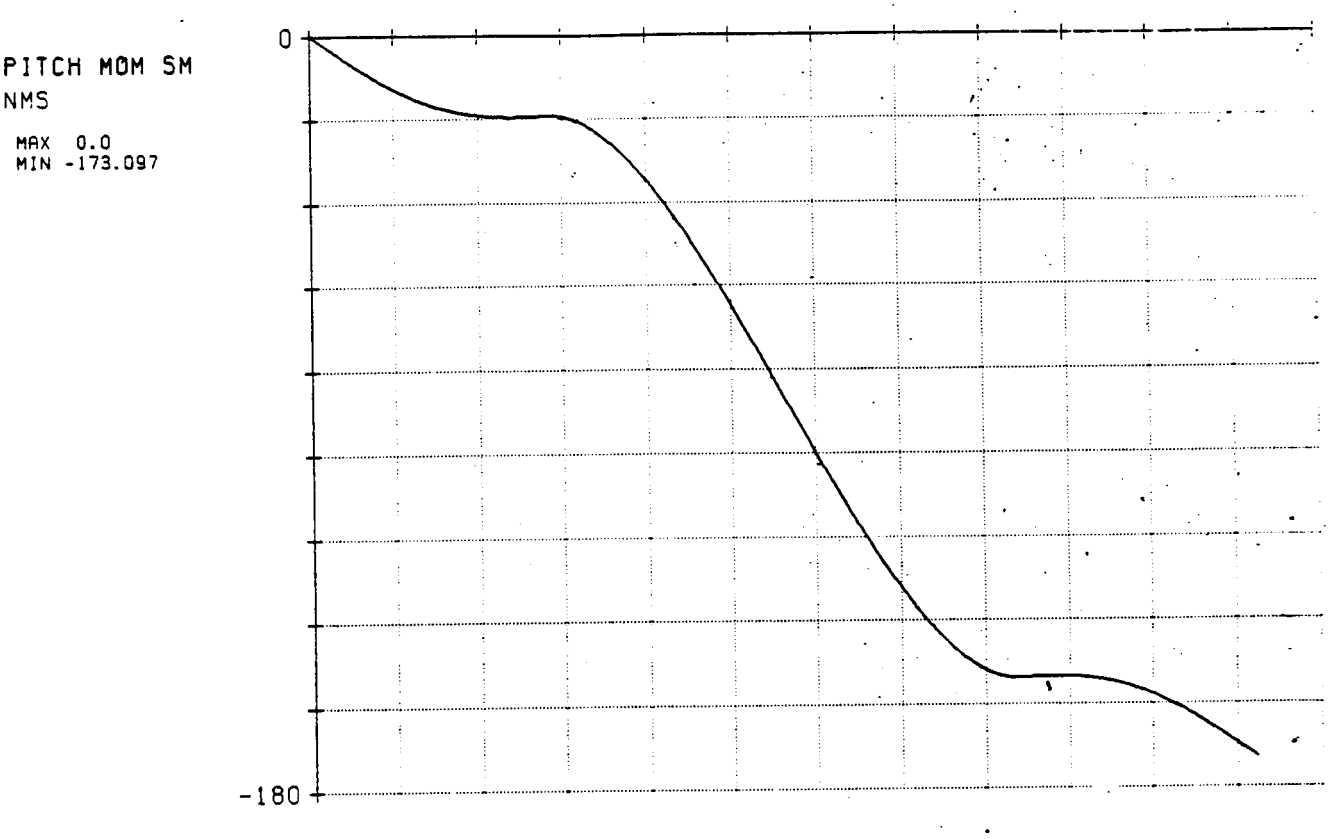

Figure 22. Momentum, Simple Model, ATEA hold, ρ - 50%

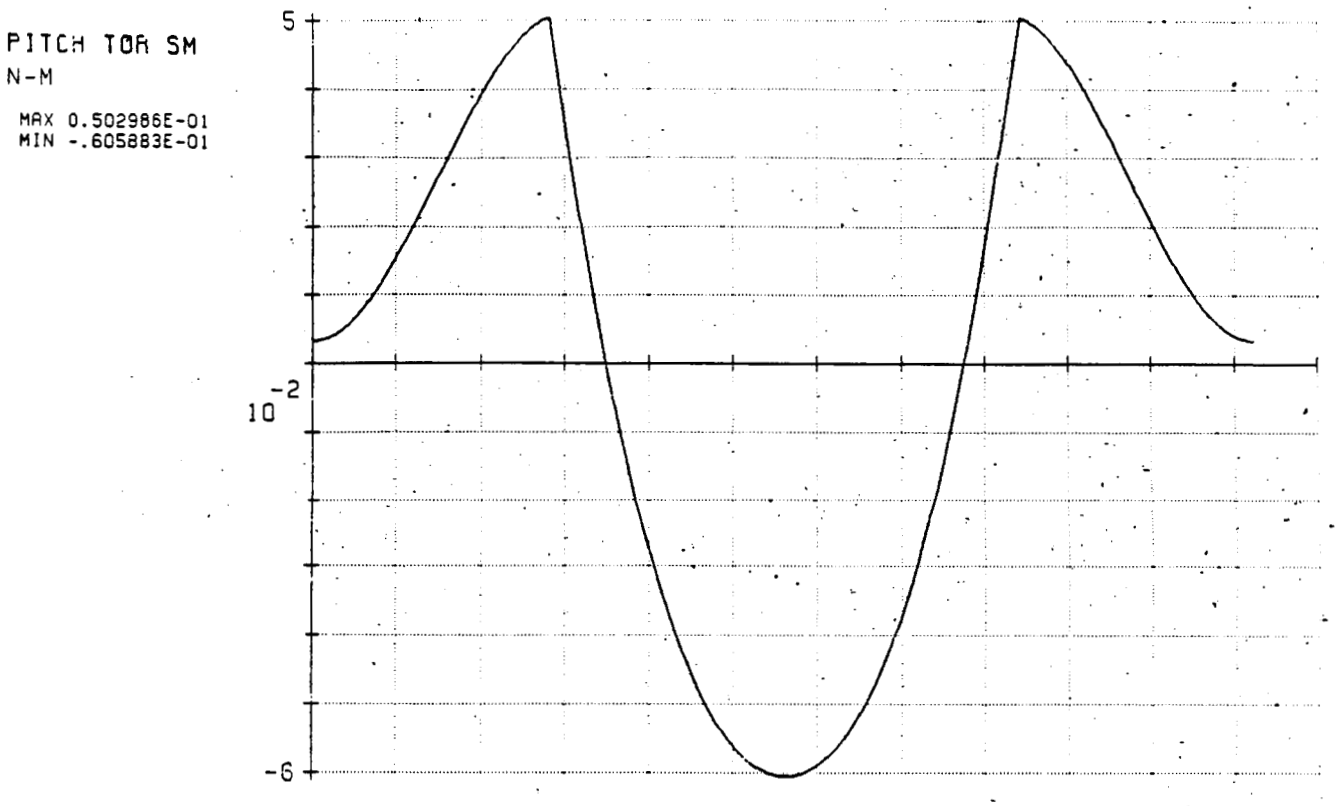

Figure 23. Torque, Simple Model, ATEA hold

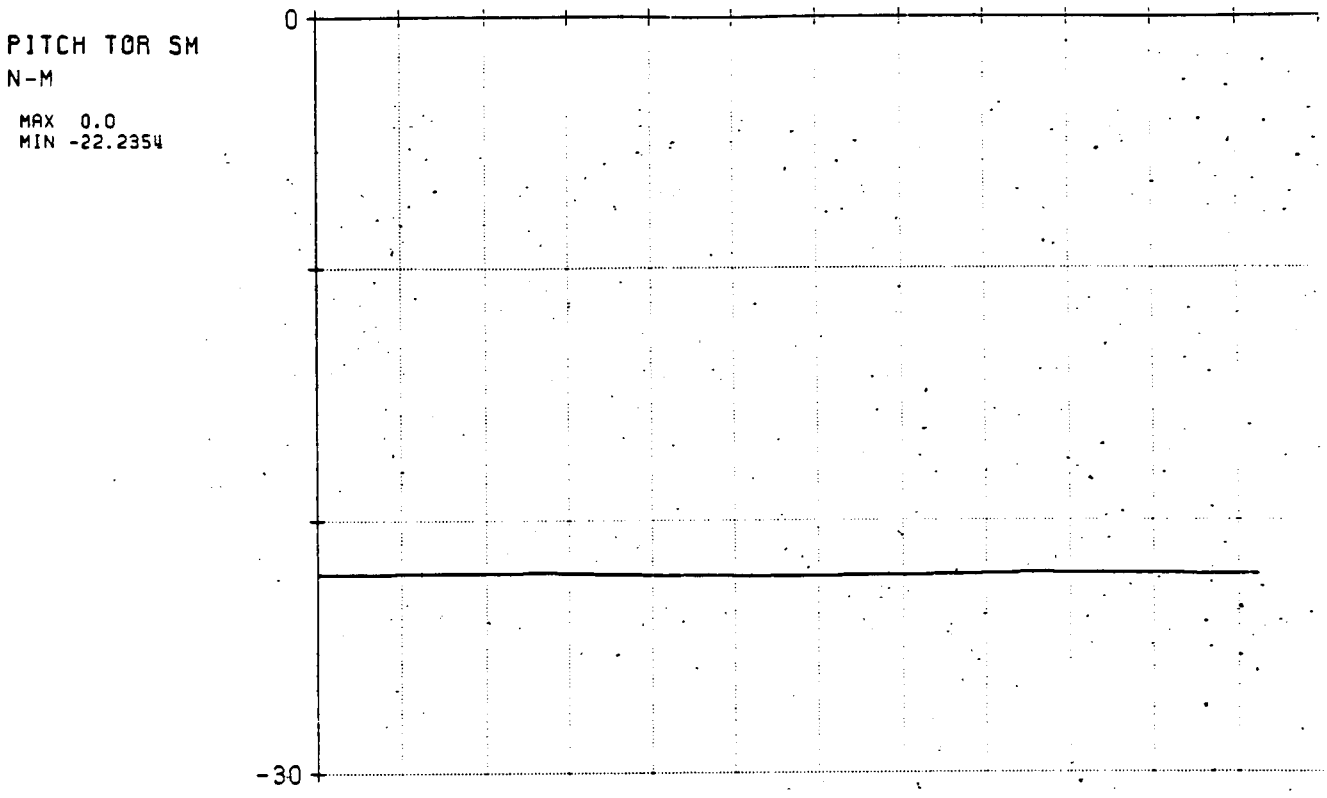

Figure 24. Torque, Simple Model, LVLH hold

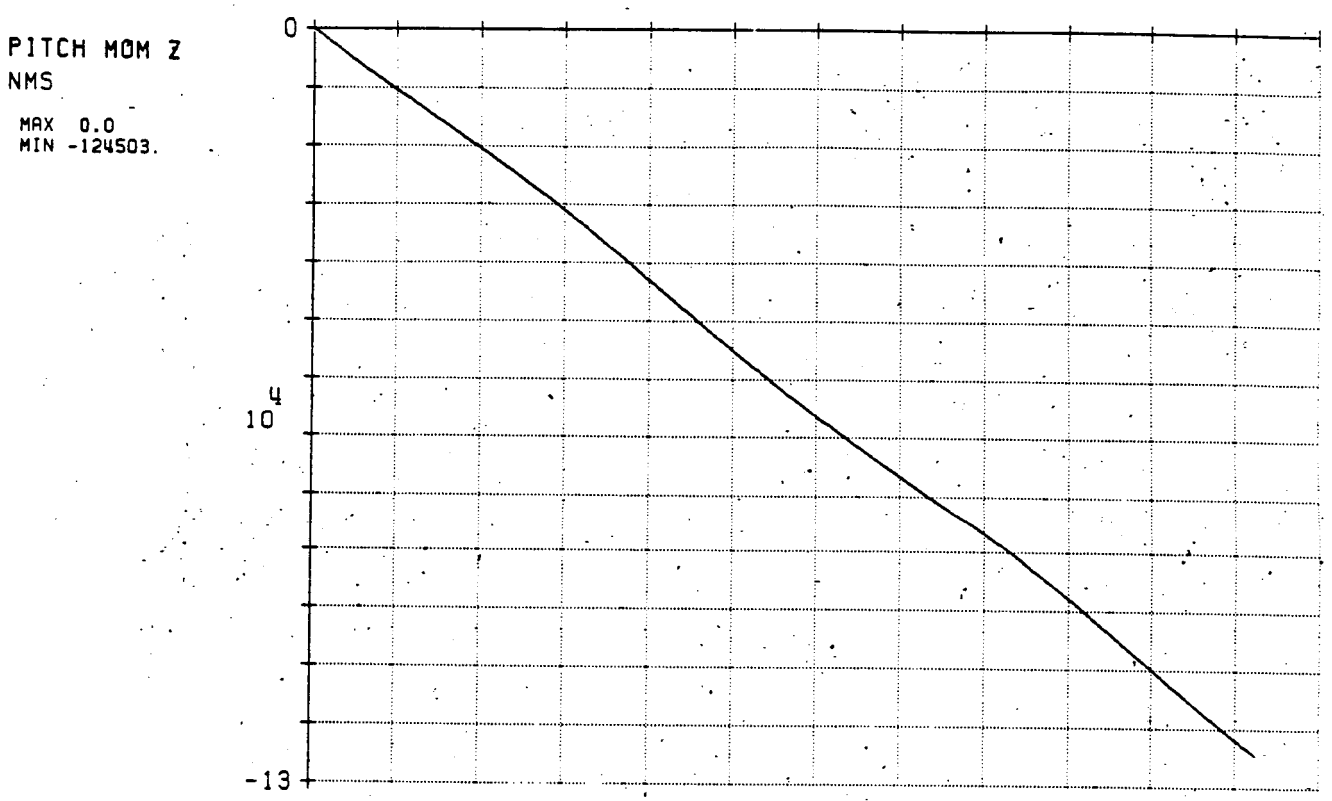

Figure 25. Momentum, No Motion MRMS, LVLH hold

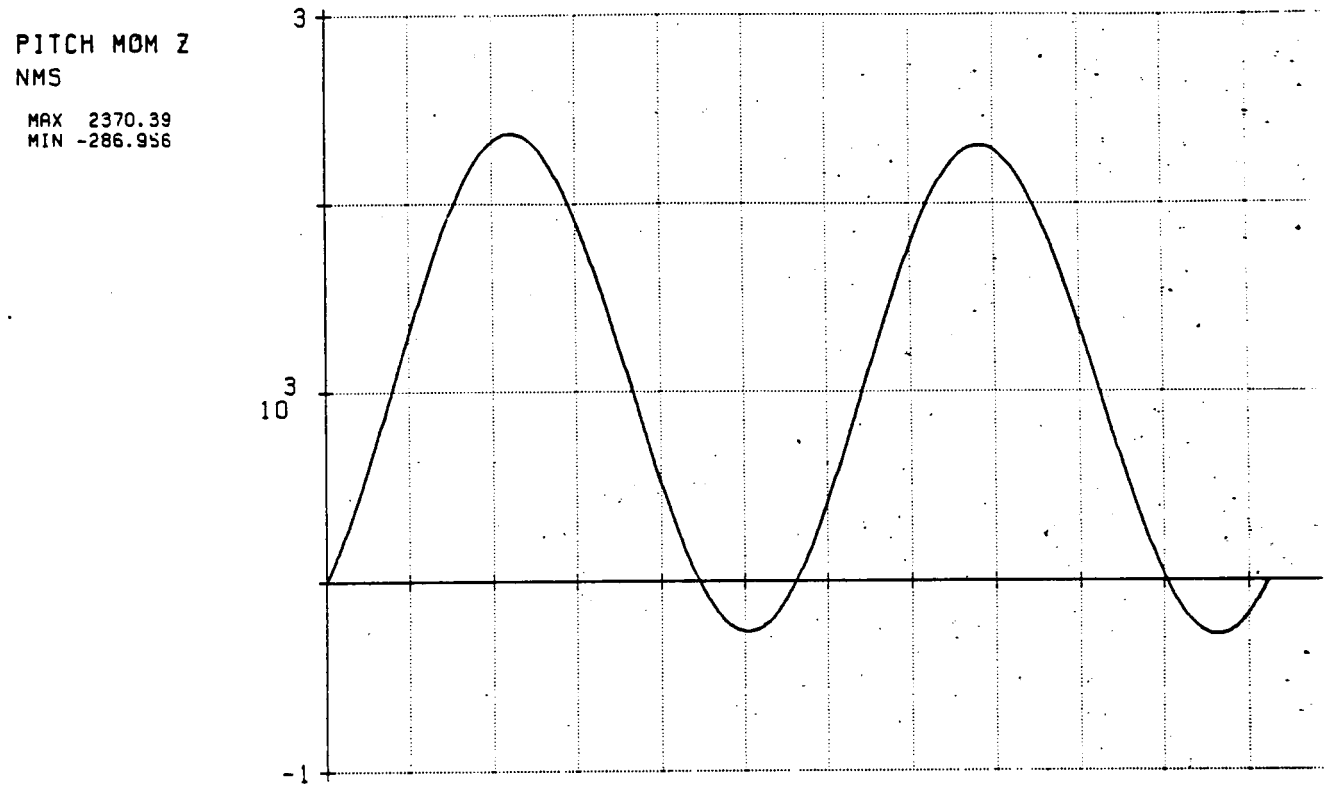

Figure 26. Momentum, No Motion MRMS, ATEA hold

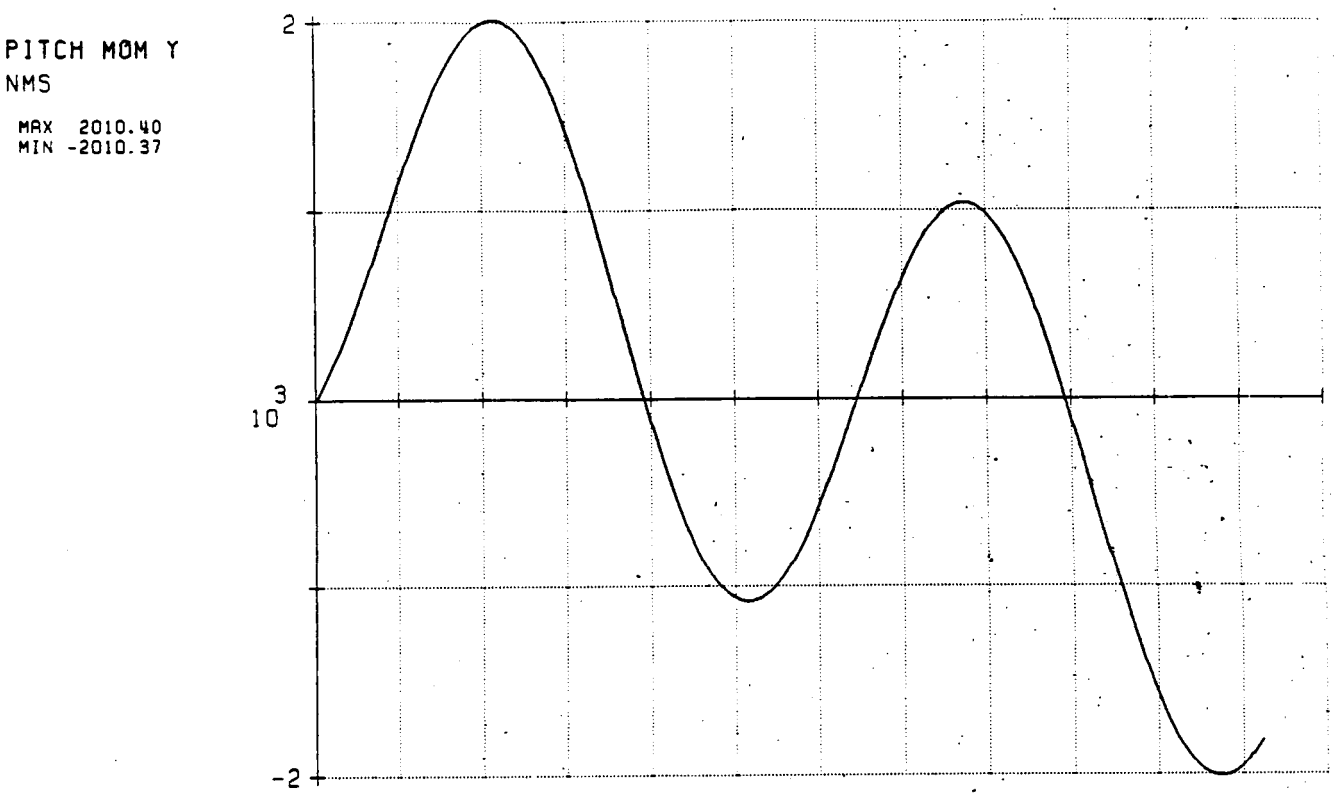

Figure 27. Momentum, No Motion MRMS, Min. Peak Momentum Attitude

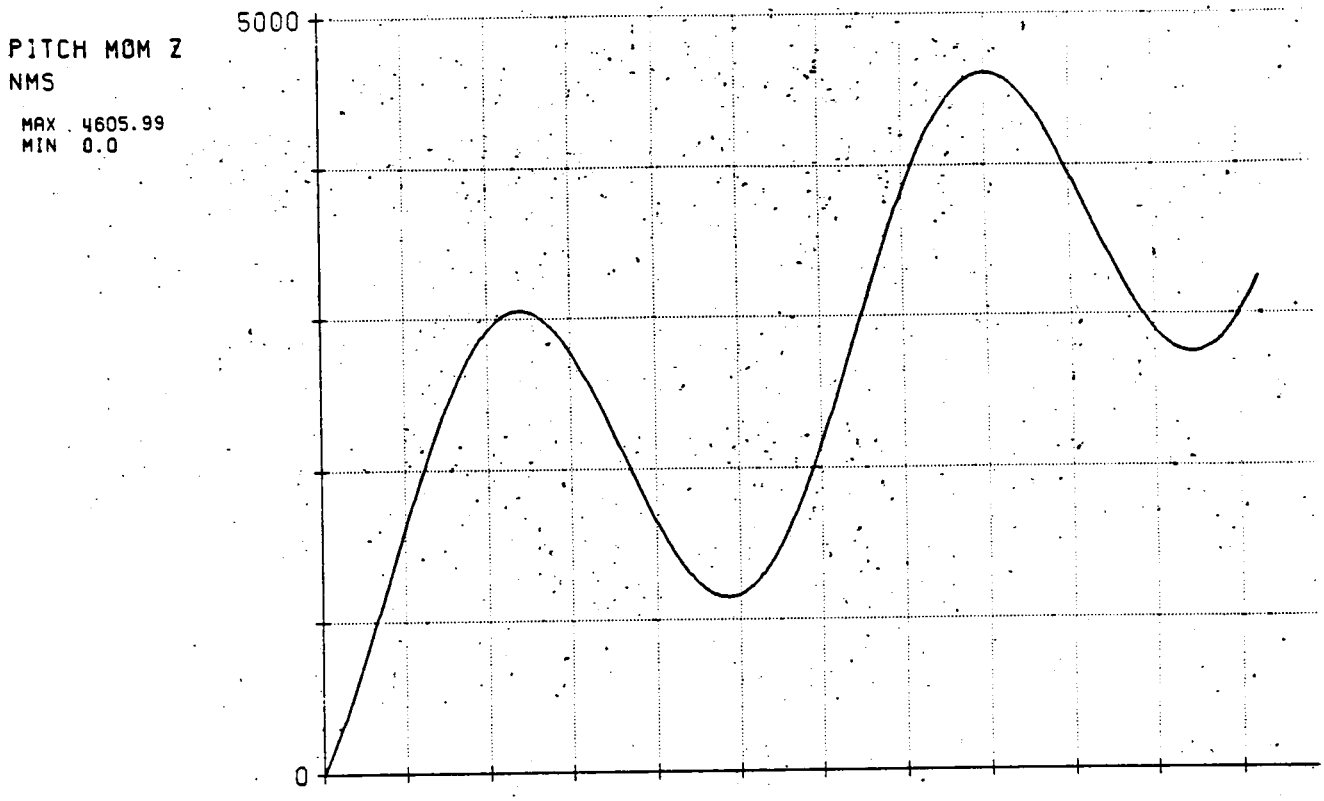

Figure 28. Momentum, No Motion MRMS, ATEA - 1 deg hold

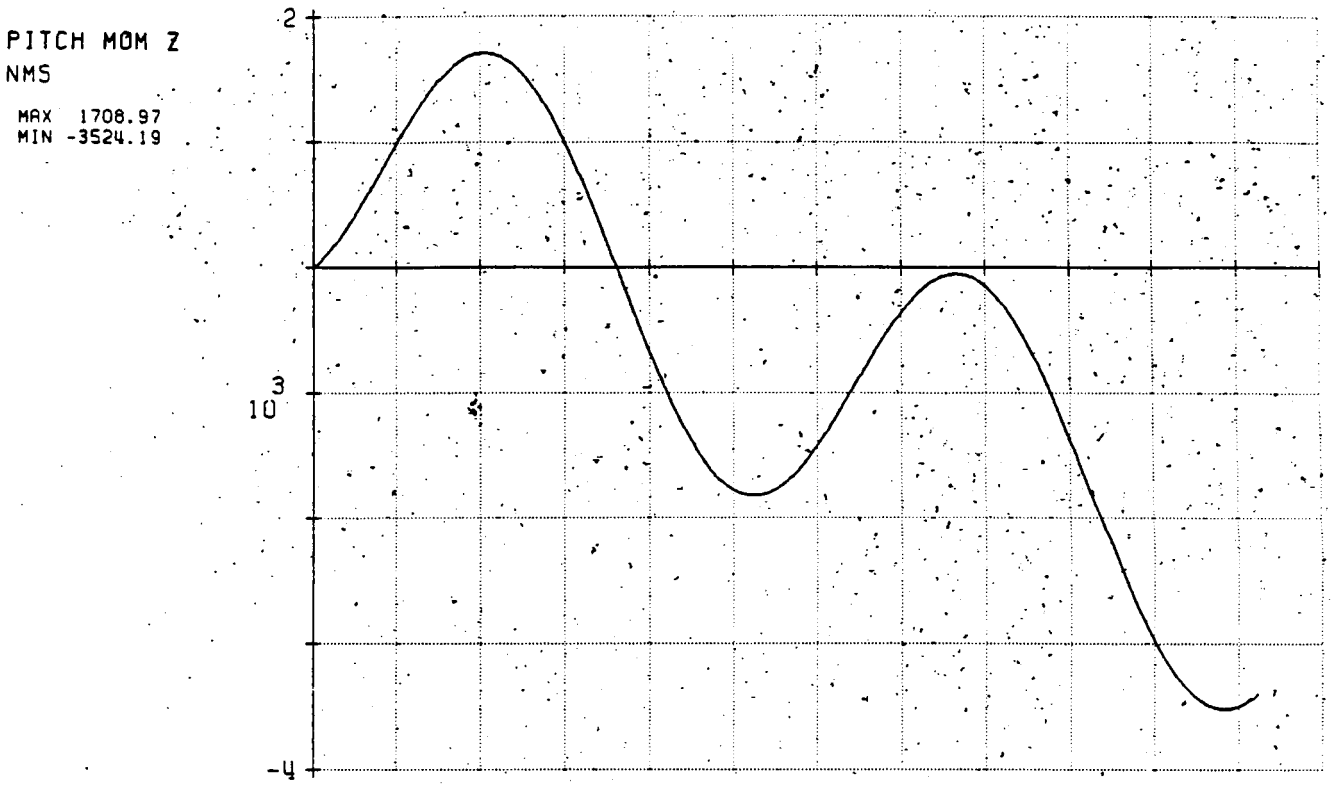

Figure 29. Momentum, No Motion MRMS, ATEA + 1 deg hold

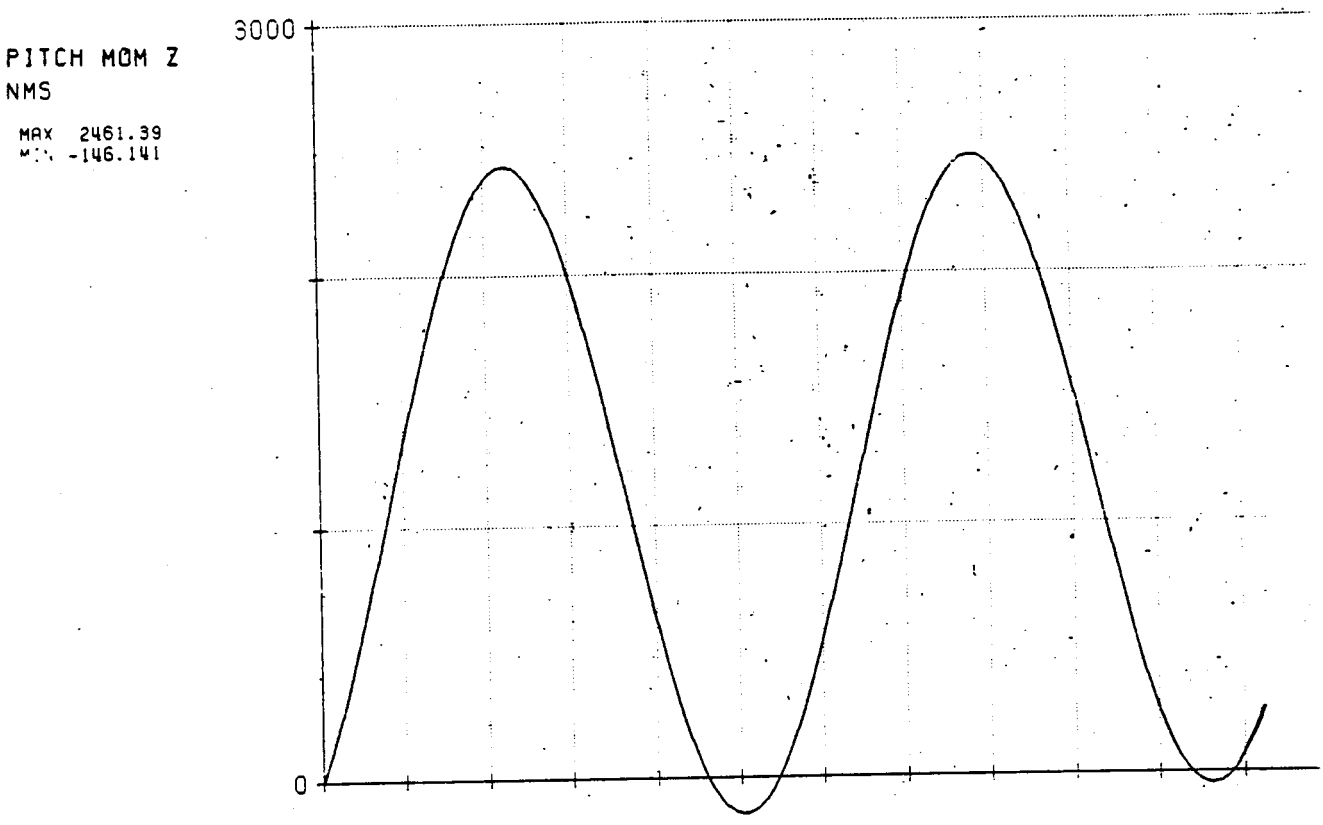

Figure 30. Momentum, No Motion MRMS, ATEA hold, ρ + 50%

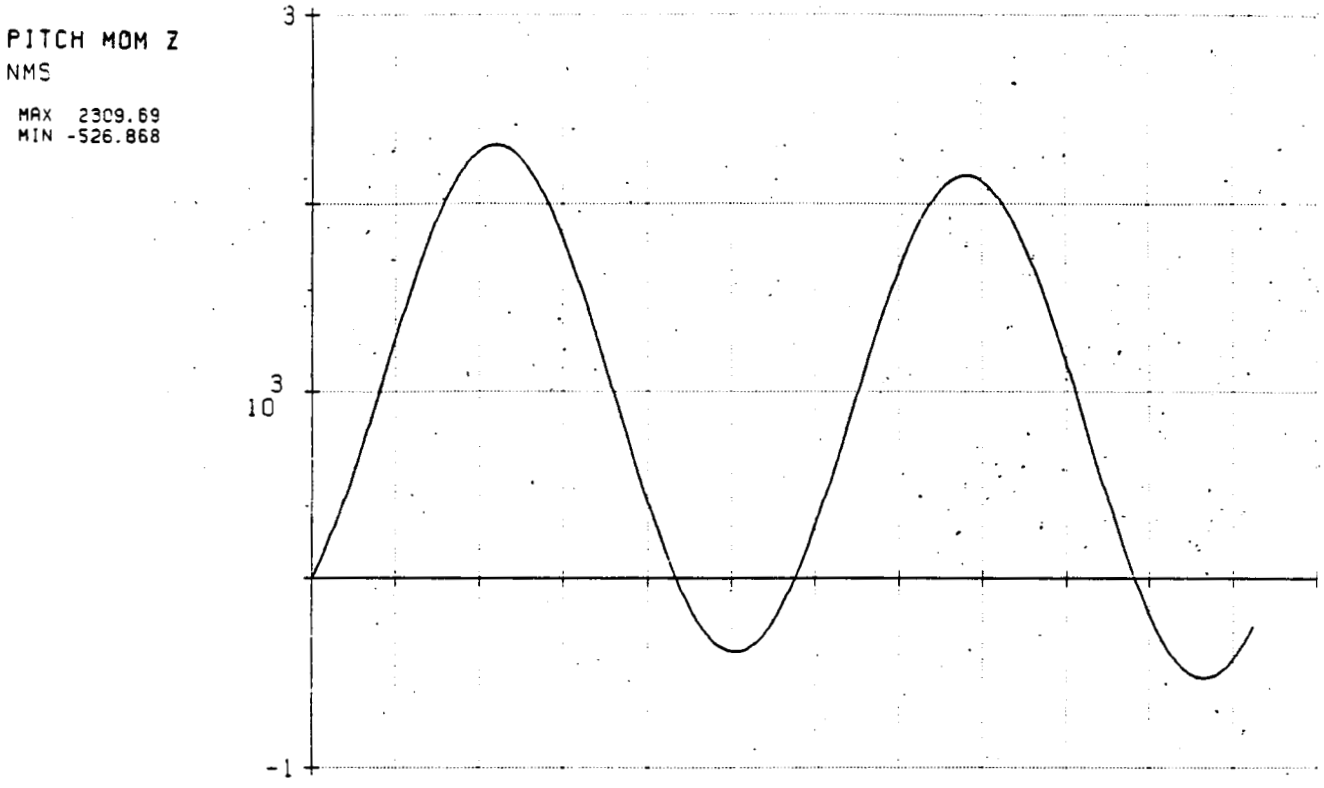

Figure 31. Momentum, No Motion MRMS, ATEA hold, ρ - 50%

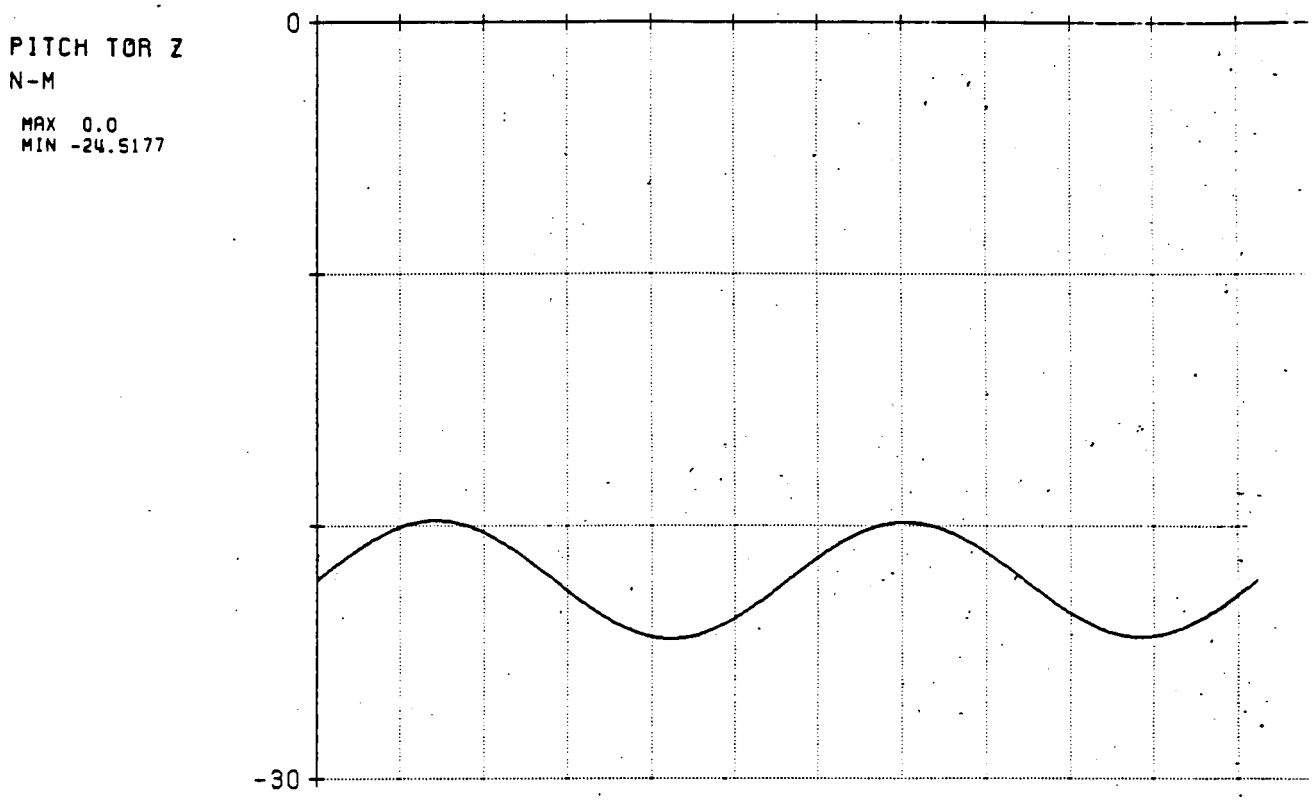

Figure 32. Torque, No Motion MRMS, LVLH hold

C-2

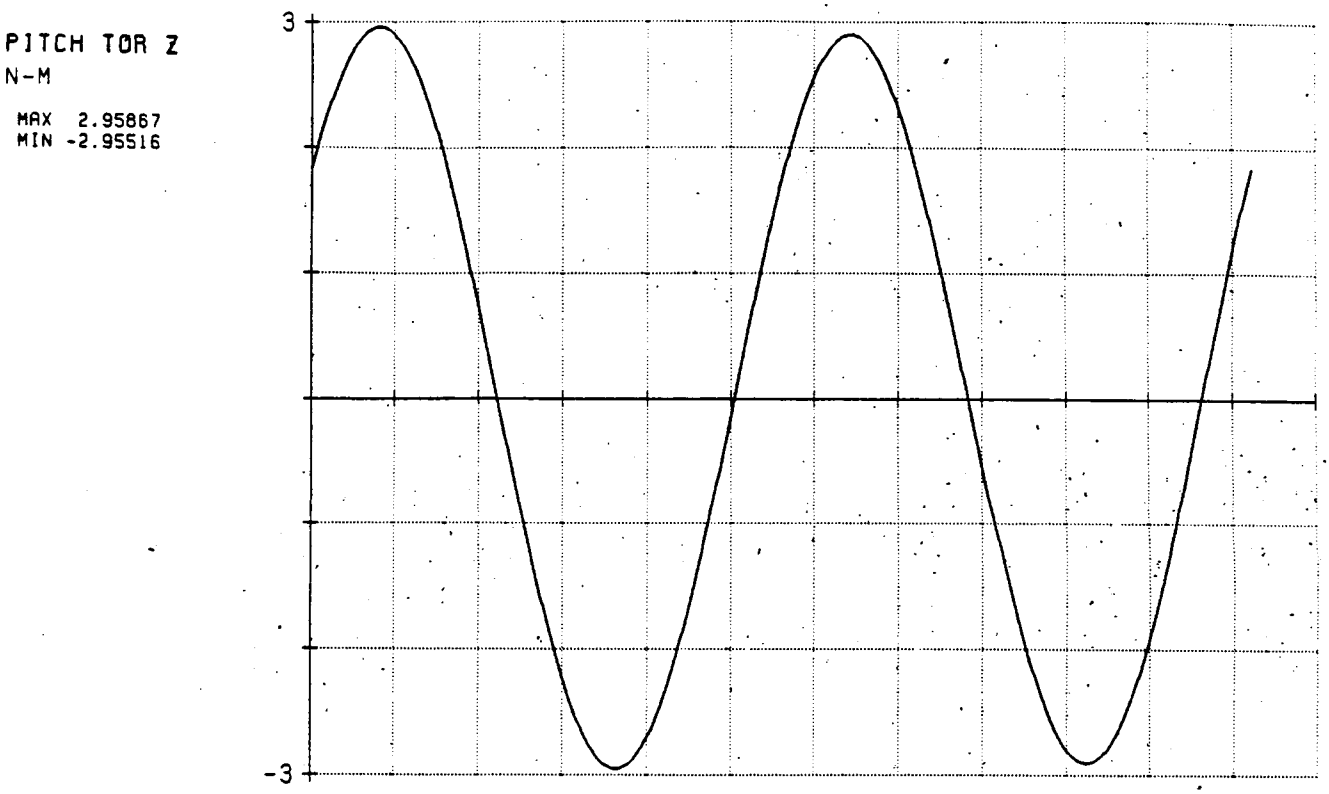

Figure 33. Torque, No Motion MRMS, ATEA hold

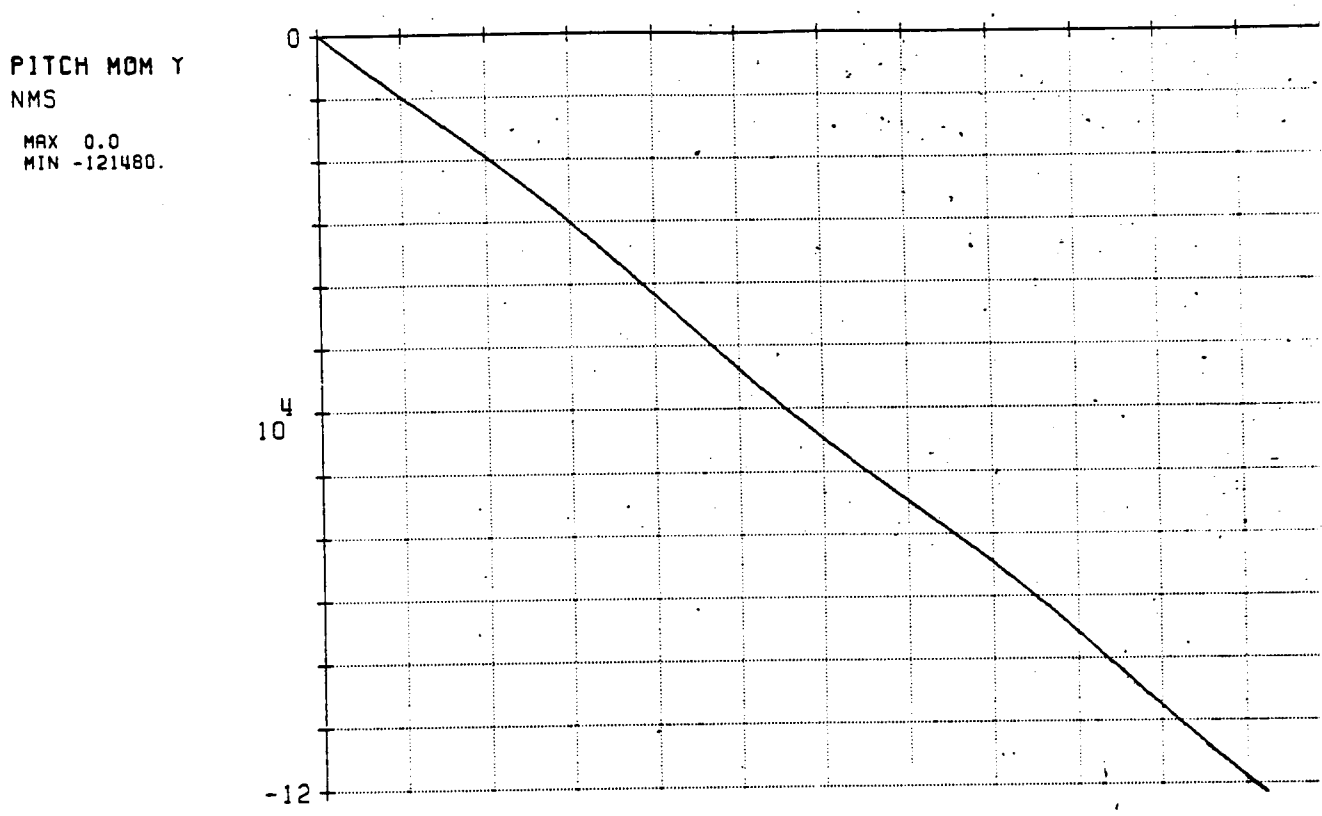

Figure 34. Momentum, Y-Motion MRMS, LVLH hold

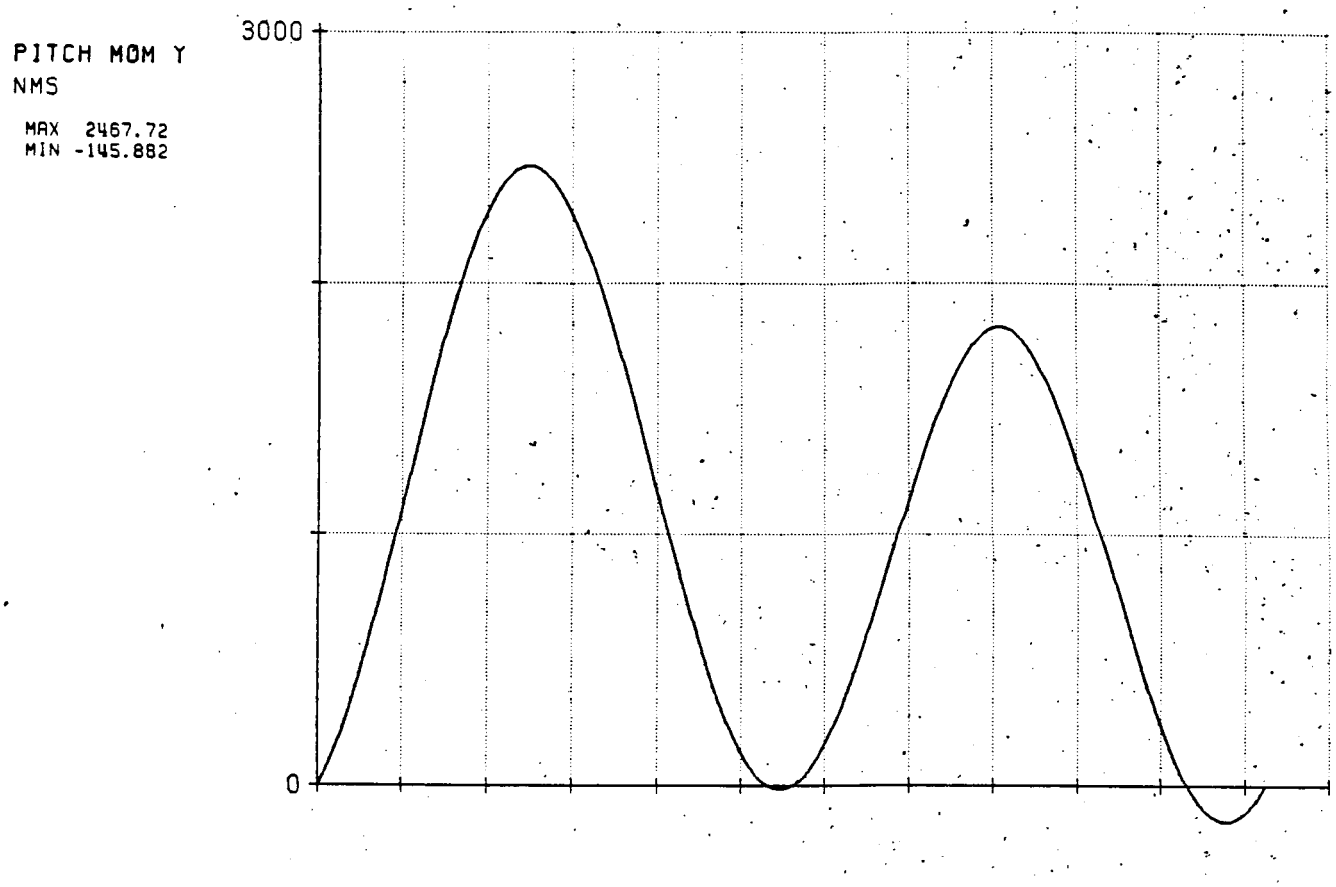

Figure 35. Momentum, Y-Motion MRMS, ATEA hold

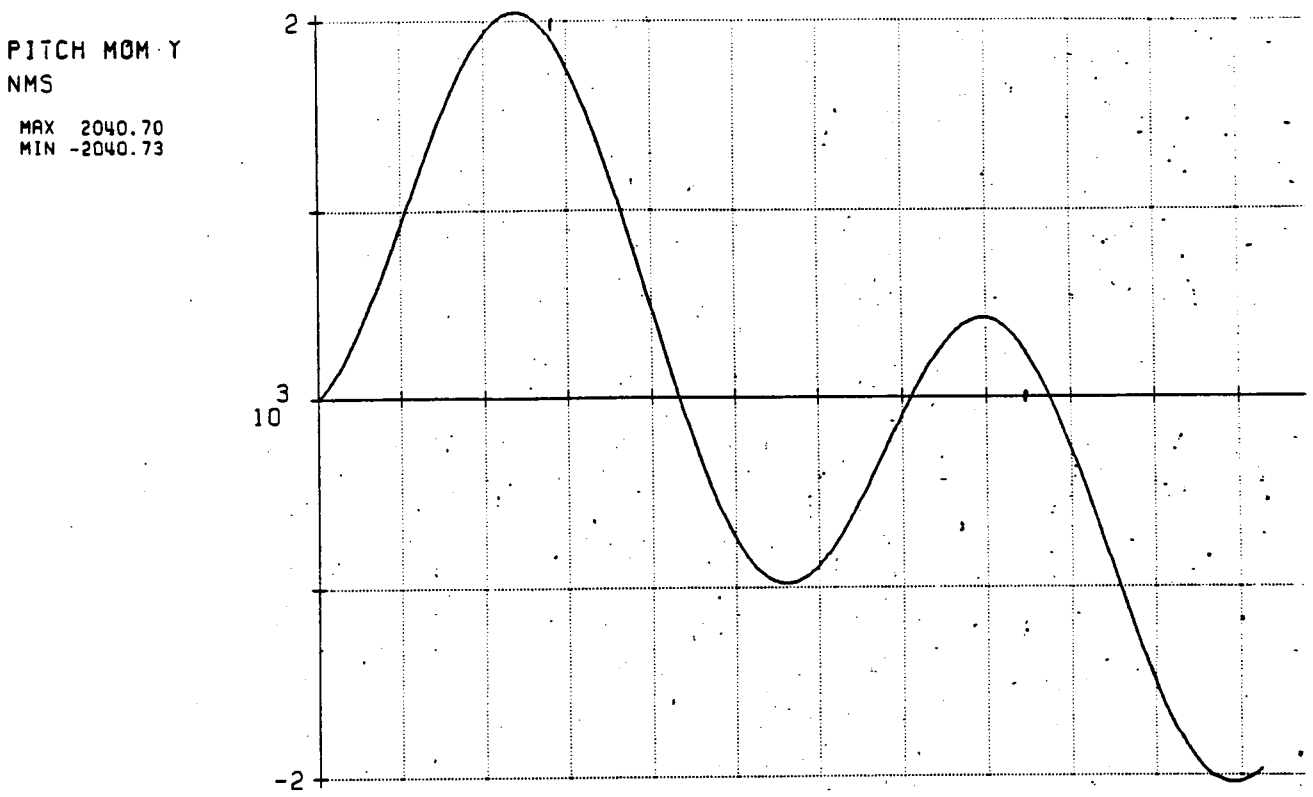

Figure 36. Momentum, Y-Motion MRMS, Min. Peak Momentum Attitude

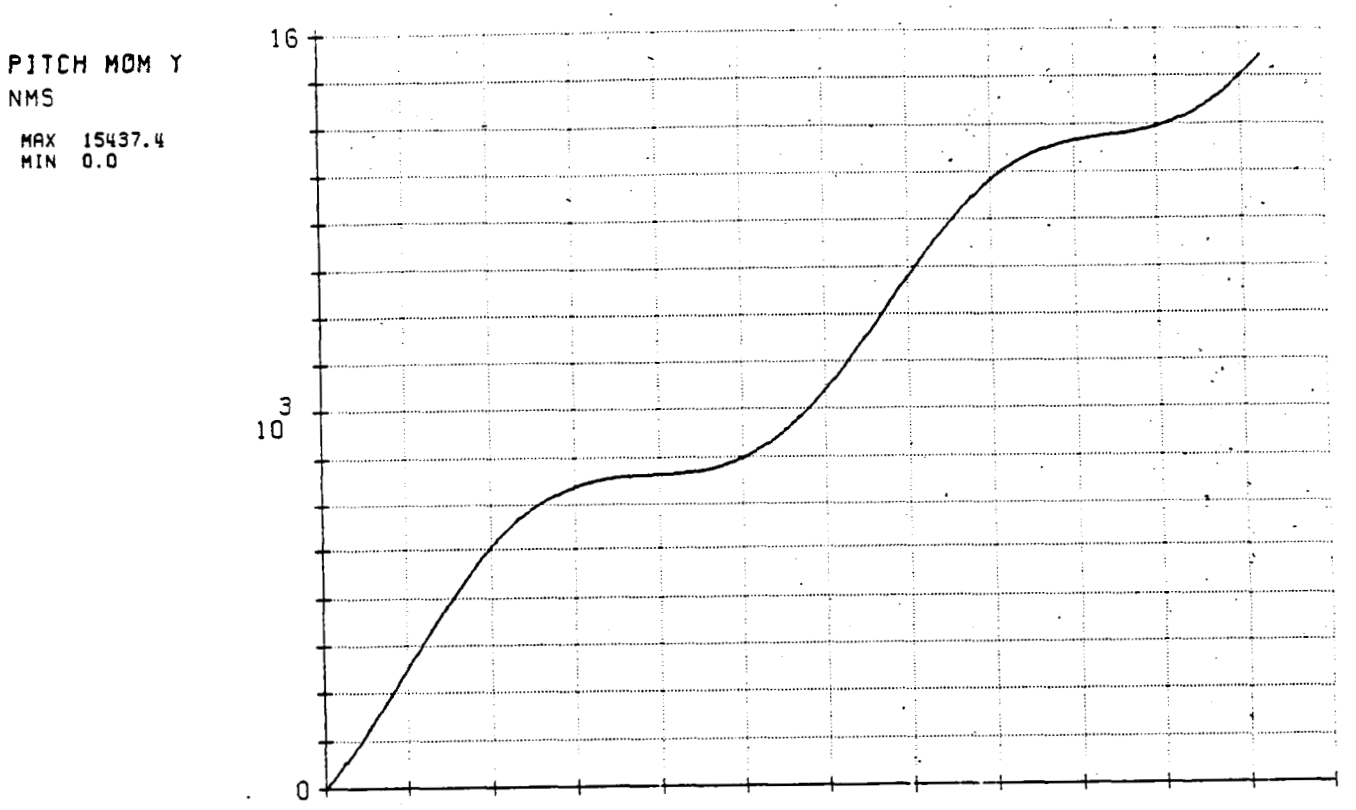

Figure 37. Momentum, Y-Motion MRMS, ATEA - 1 deg hold

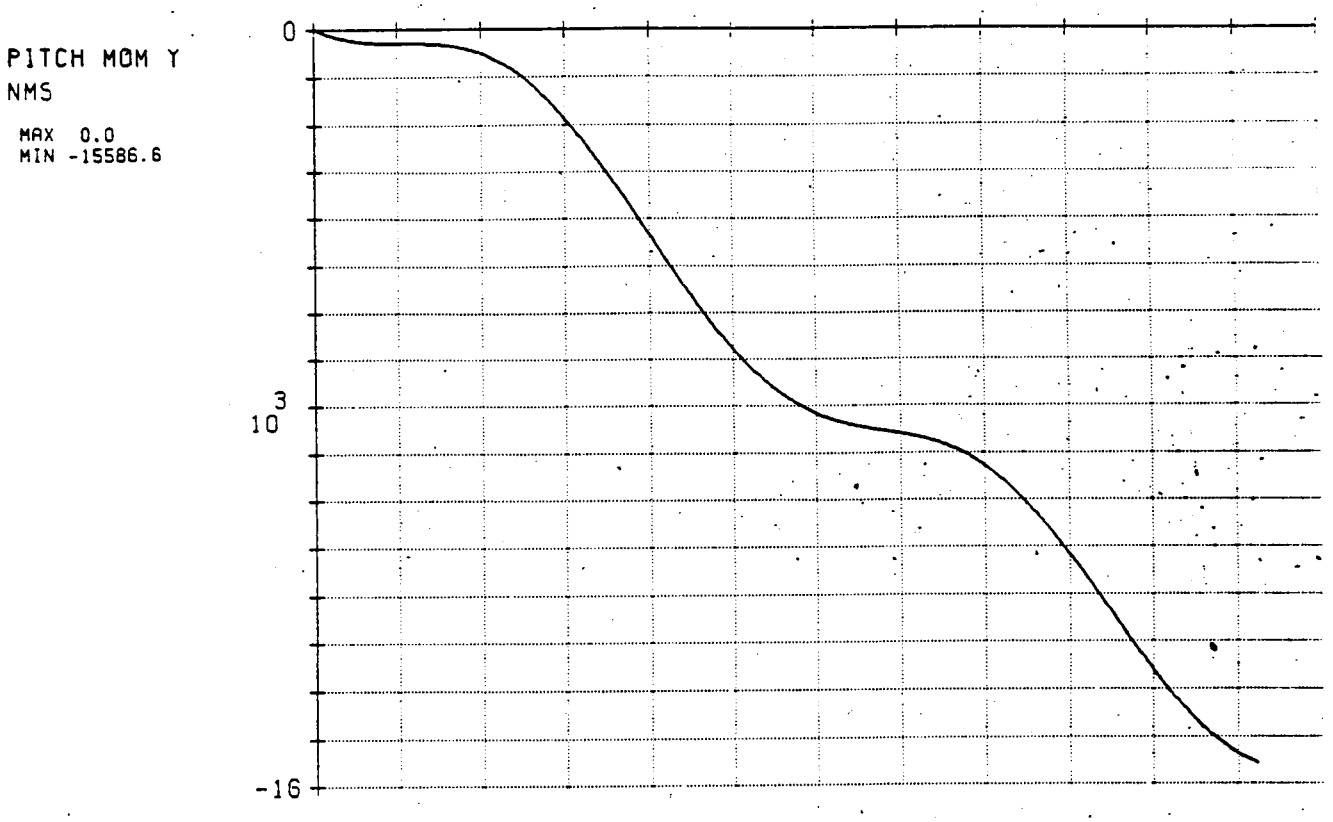

Figure 38. Momentum, Y-Motion MRMS, ATEA + 1 deg hold

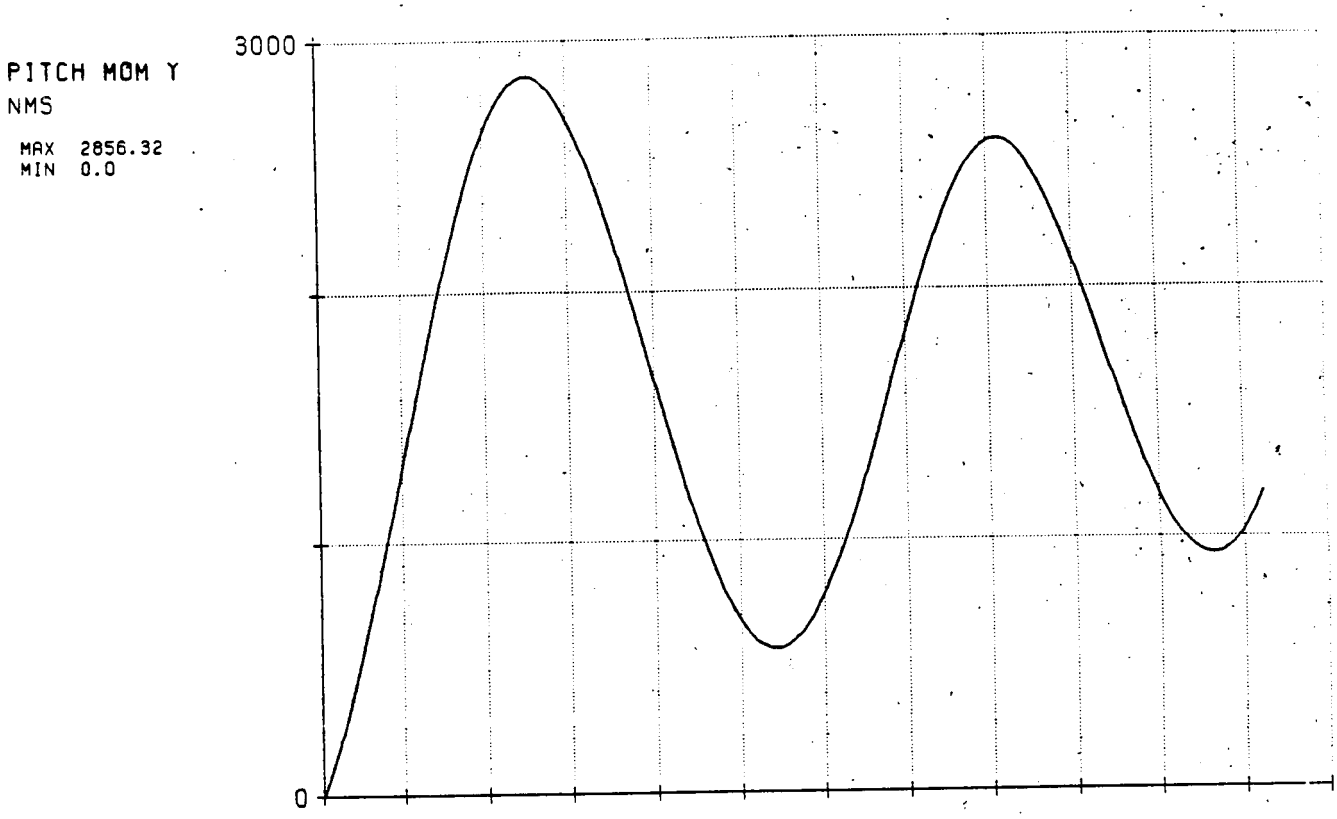

Figure 39. Momentum, Y-Motion MRMS, ATEA hold, ρ + 50%

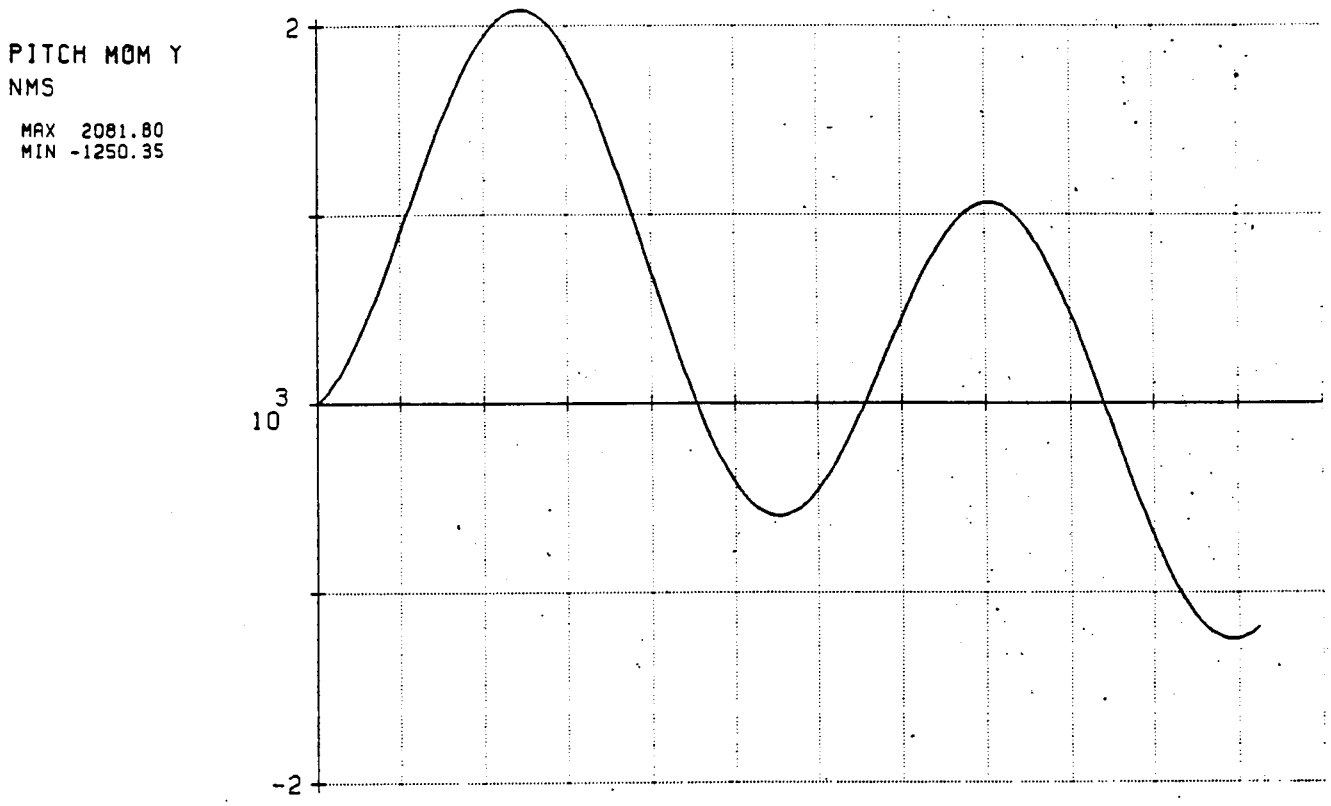

Figure 40. Momentum, Y-Motion MRMS, ATEA hold, ρ - 50%

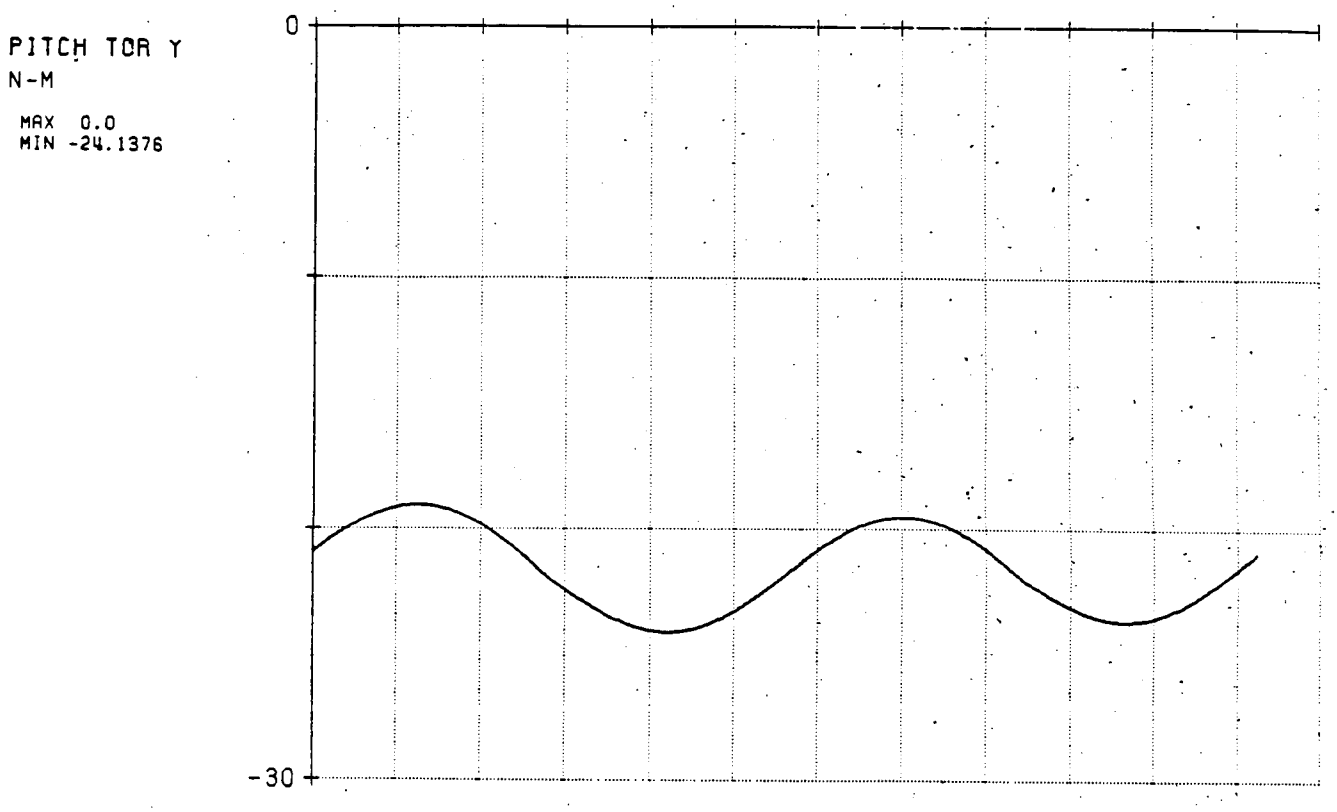

Figure 41. Torque, Y-Motion MRMS, LVLH hold

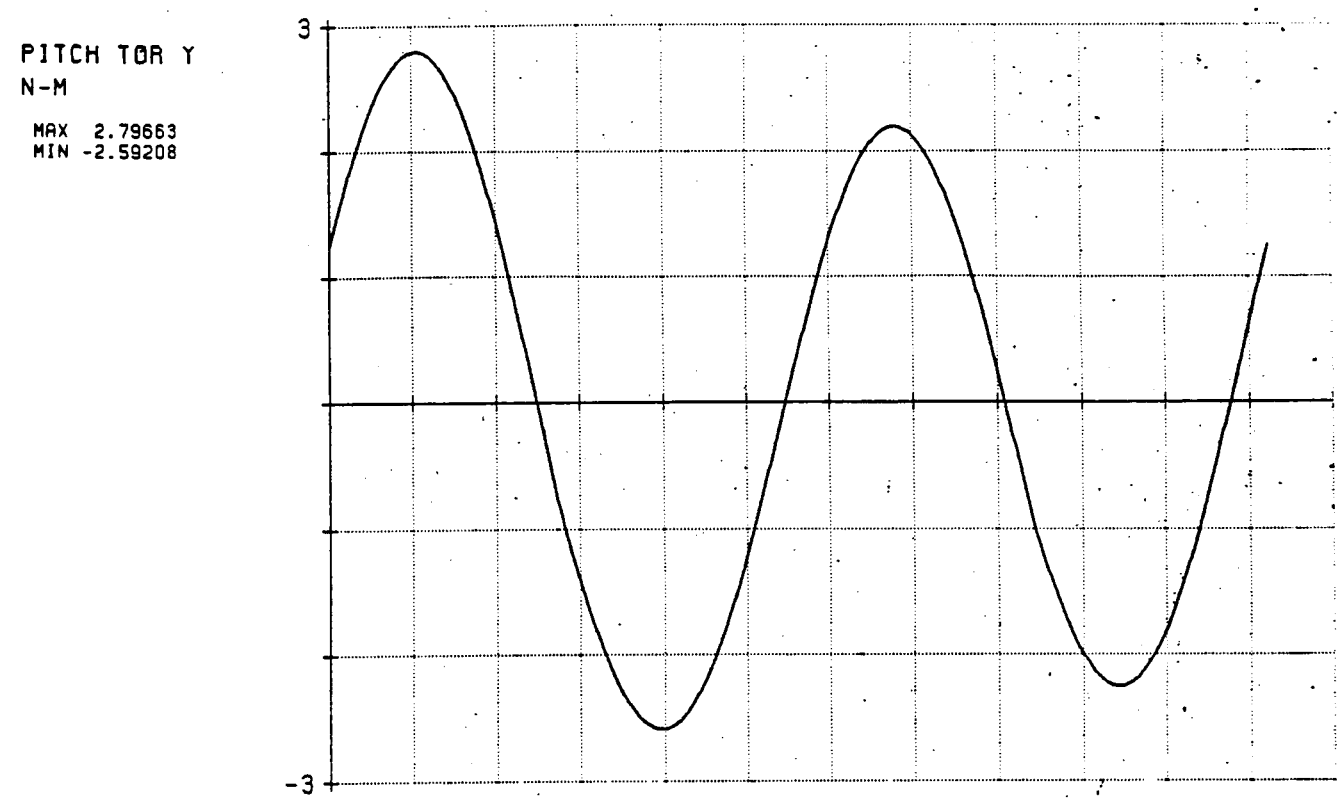

Figure 42. Torque, Y-Motion MRMS, ATEA hold

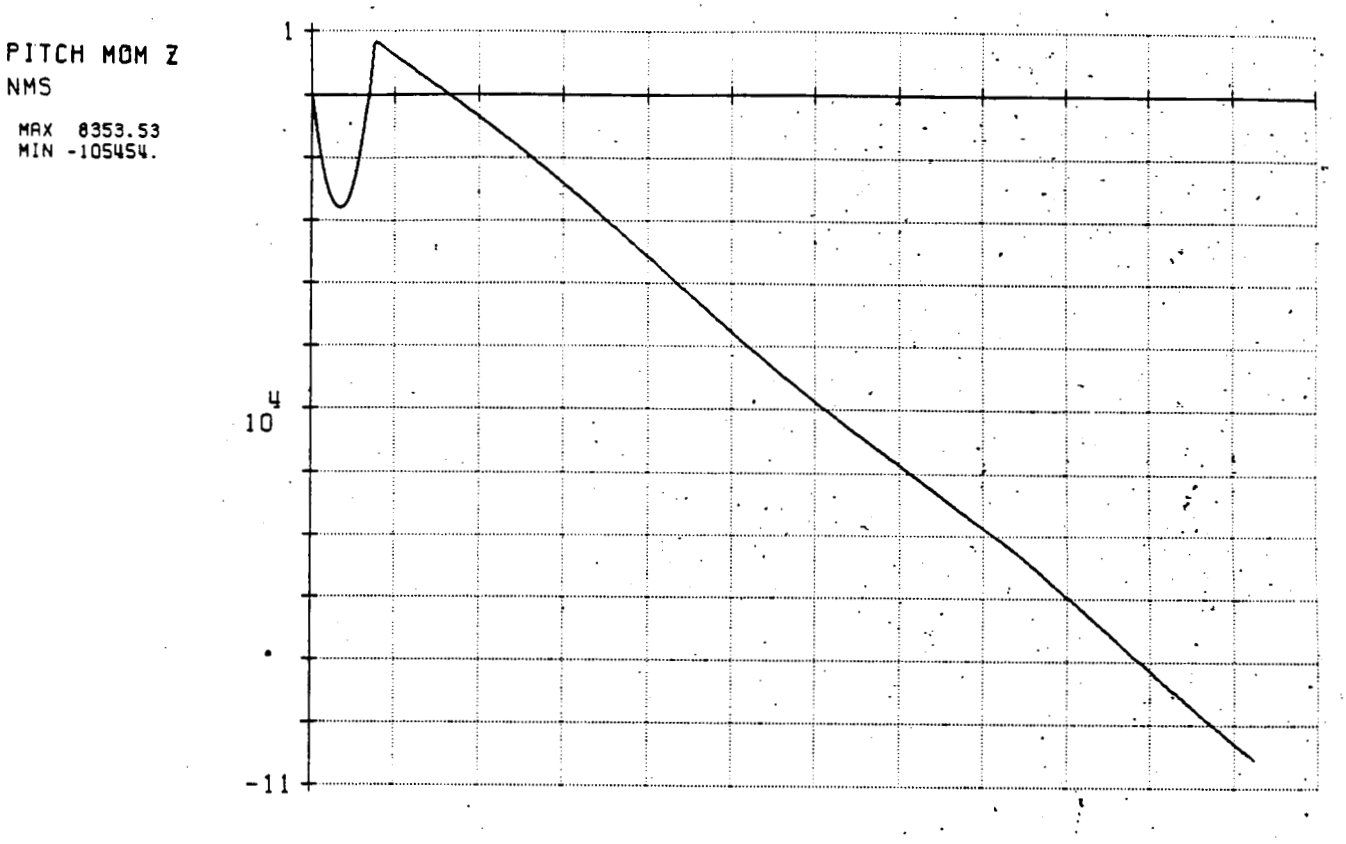

Figure 43. Momentum, Z-Motion MRMS, LVLH hold

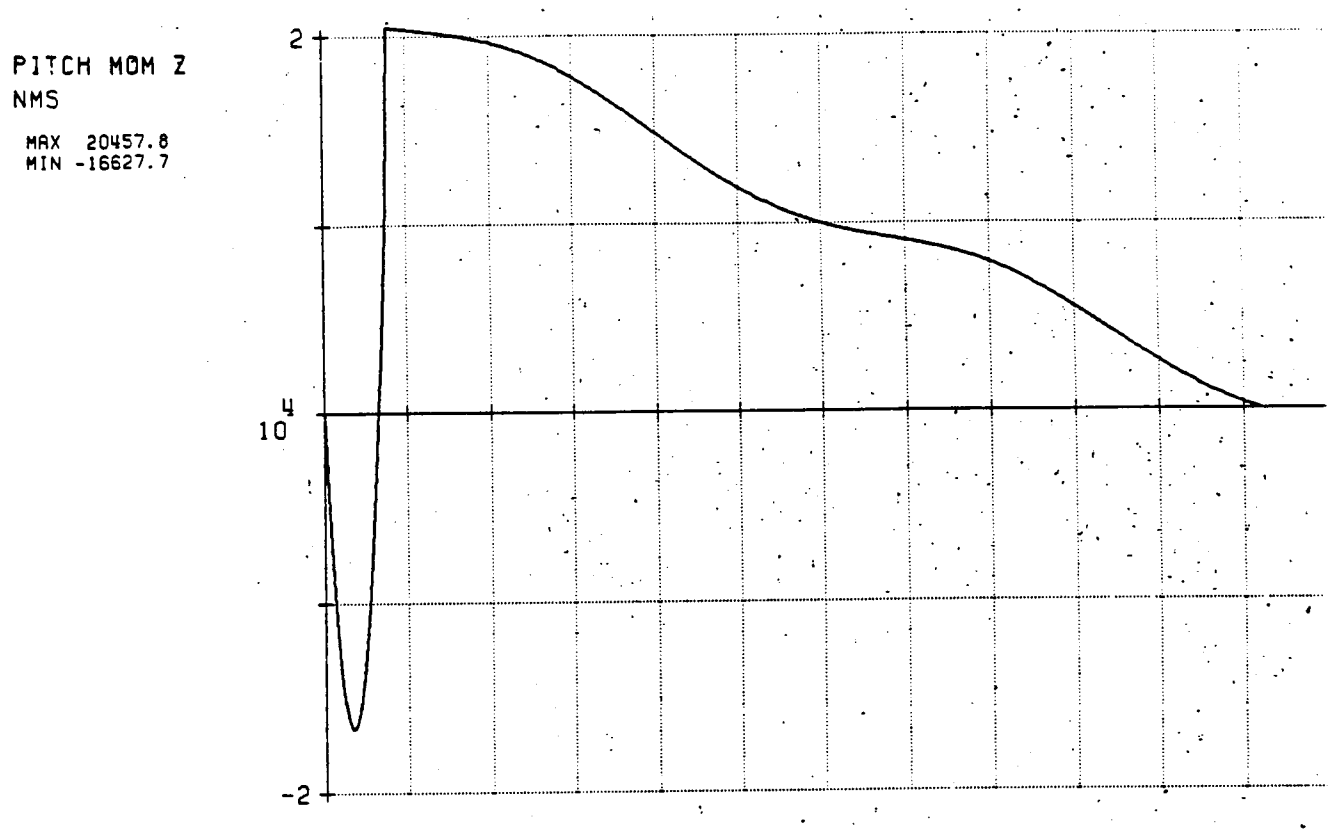

Figure 44. Momentum, Z-Motion MRMS, ATEA hold

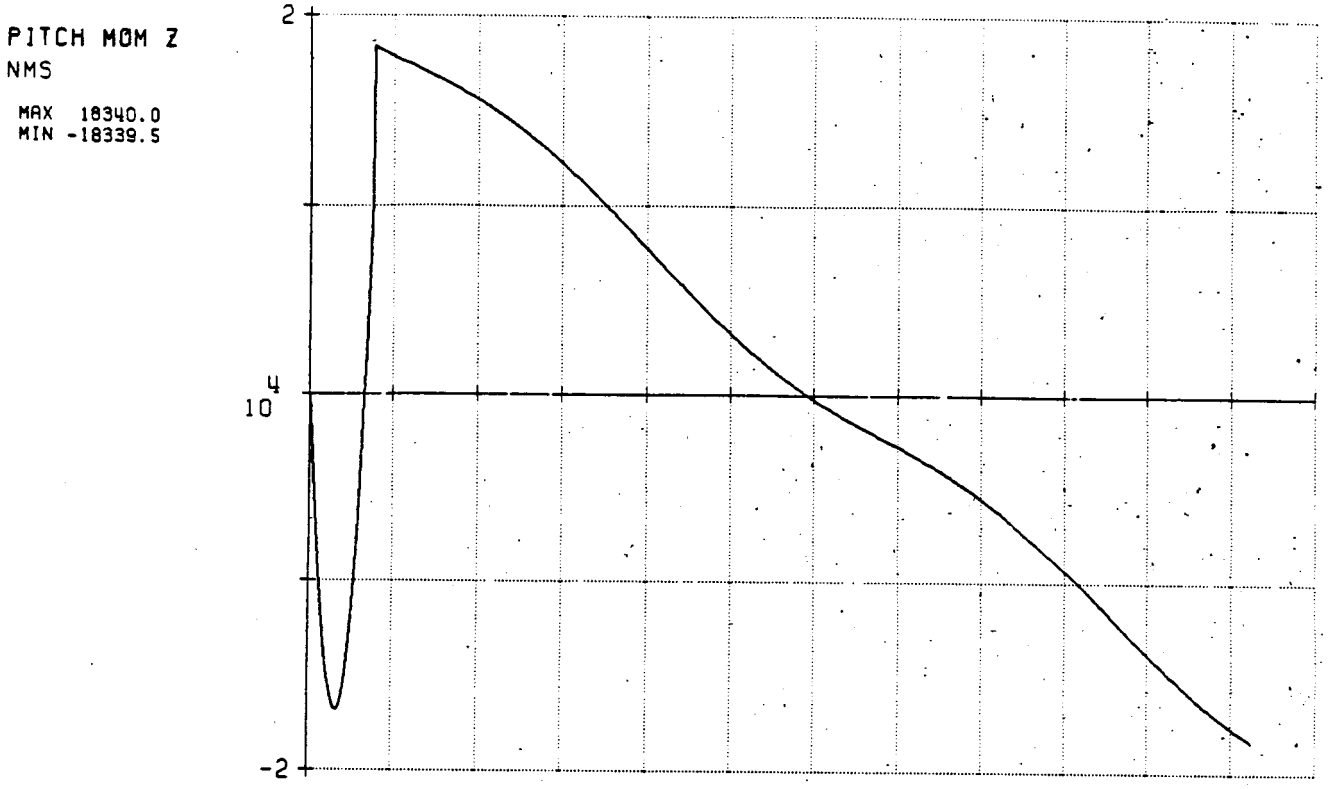

Figure 45. Momentum, Z-Motion MRMS, Min. Peak Momentum Attitude

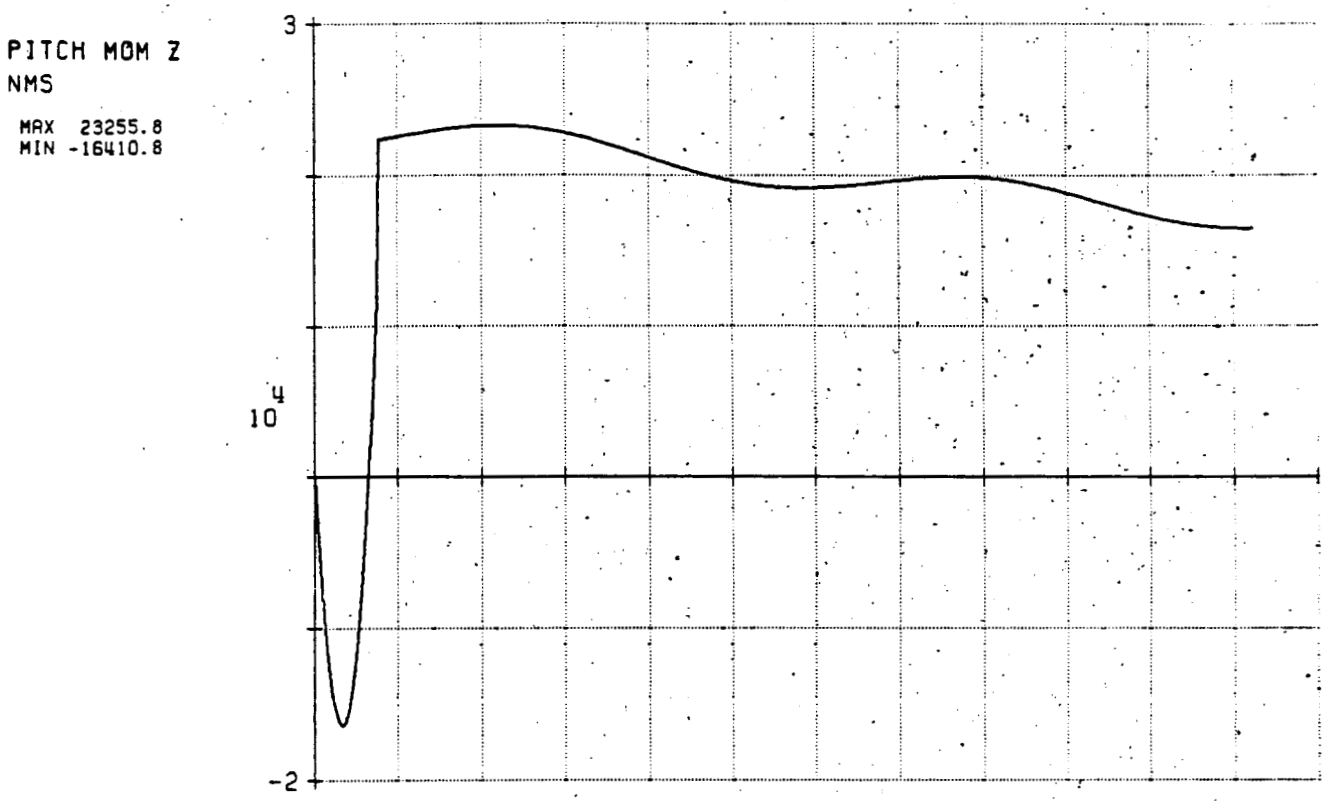

Figure 46. Momentum, Z-Motion MRMS, ATEA - 1 deg hold

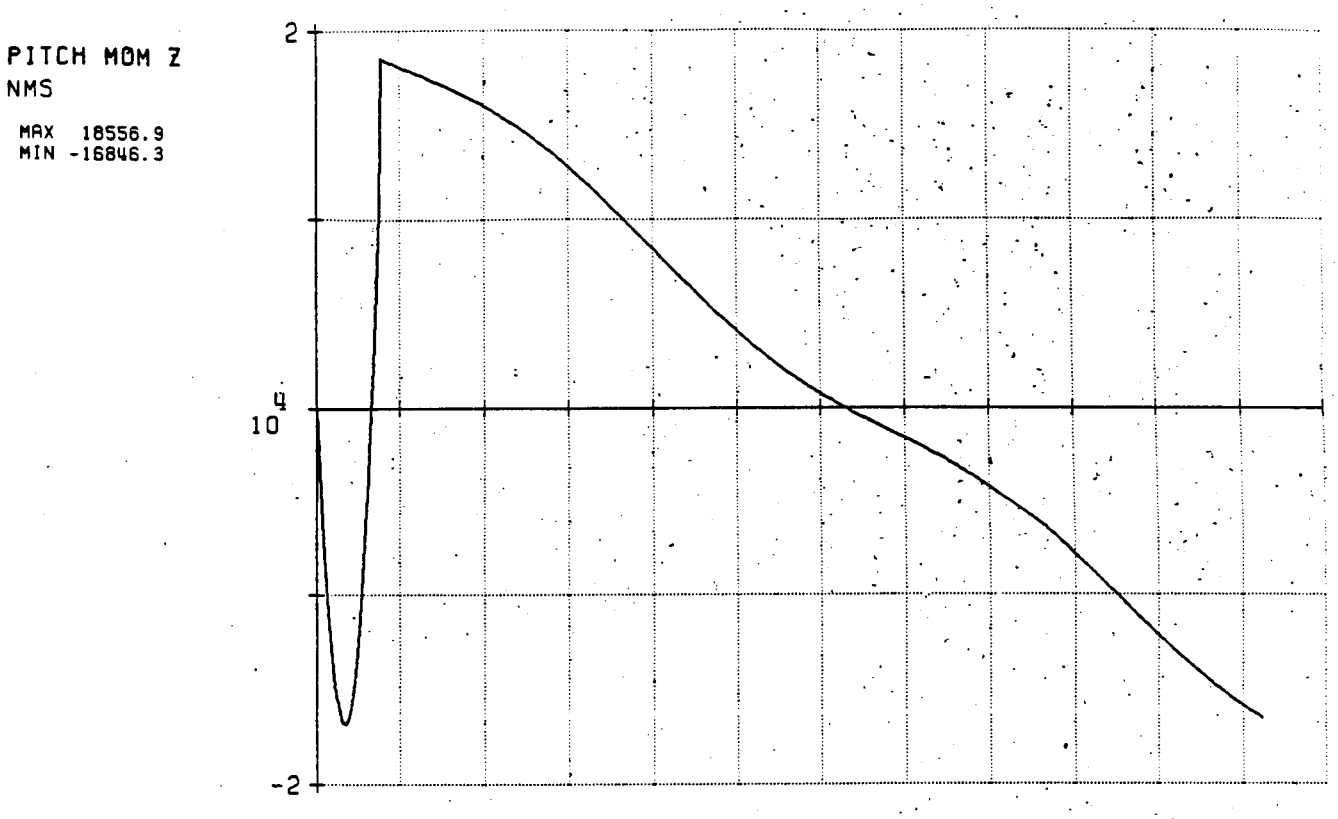

Figure 47. Momentum, Z-Motion MRMS, ATEA + 1 deg hold

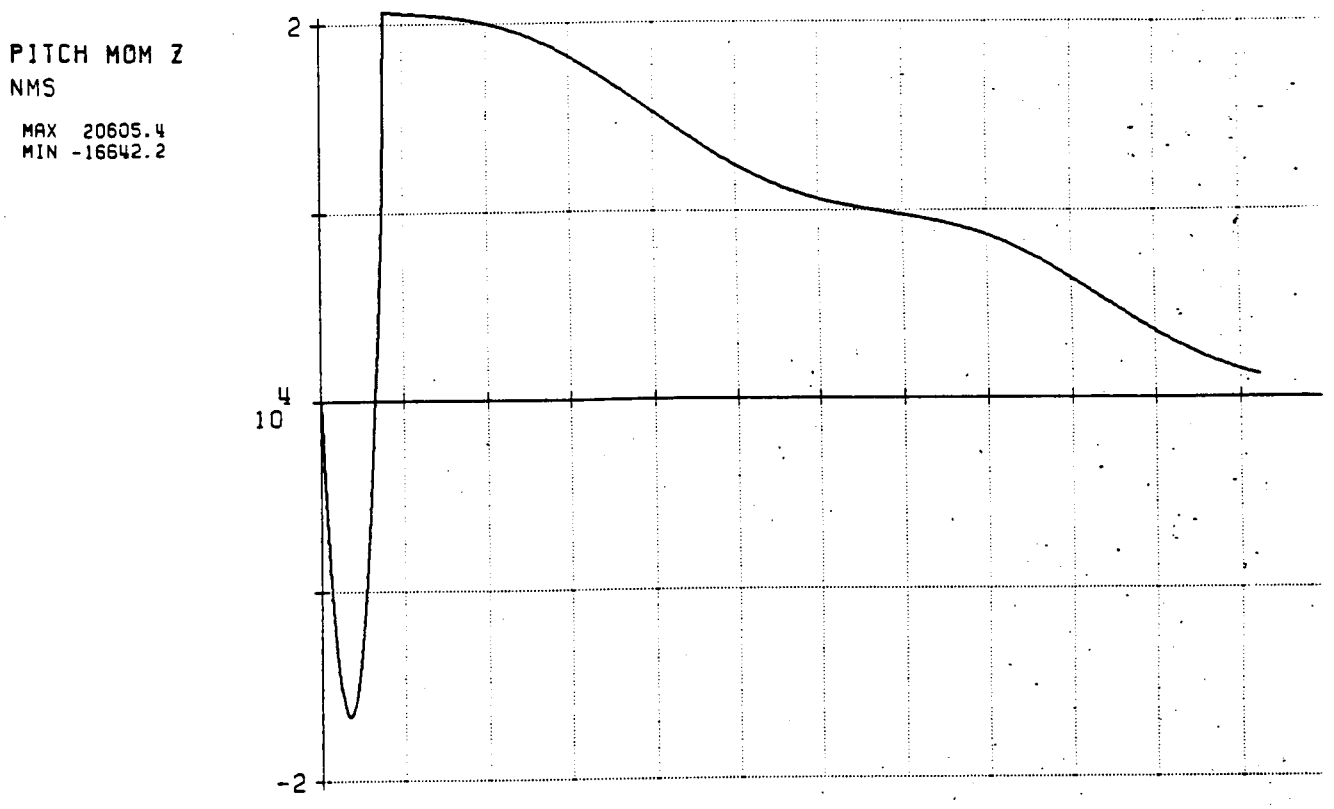

Figure 48. Momentum, Z-Motion MRMS, ATEA hold, ρ + 50%

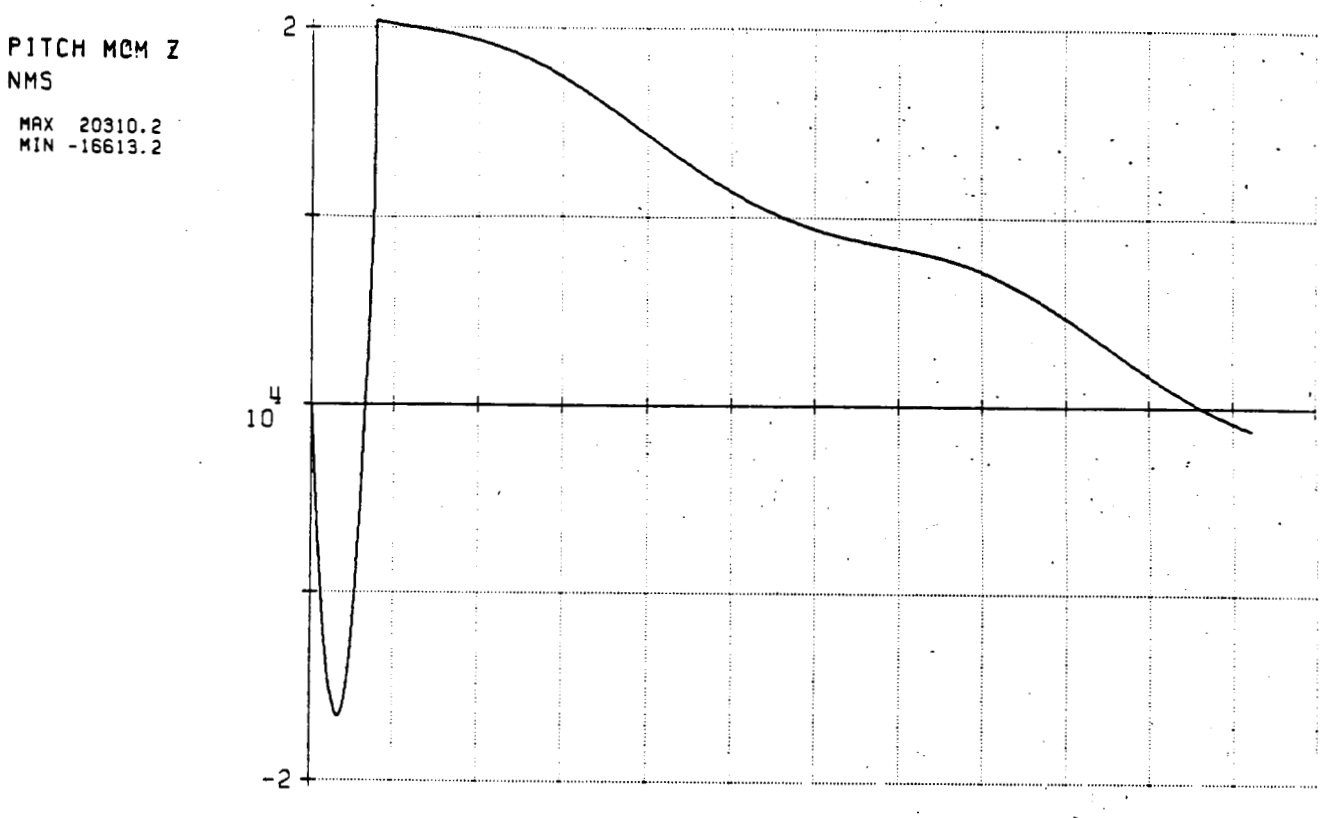

Figure 49. Momentum, Z-Motion MRMS, ATEA hold, ρ - 50%

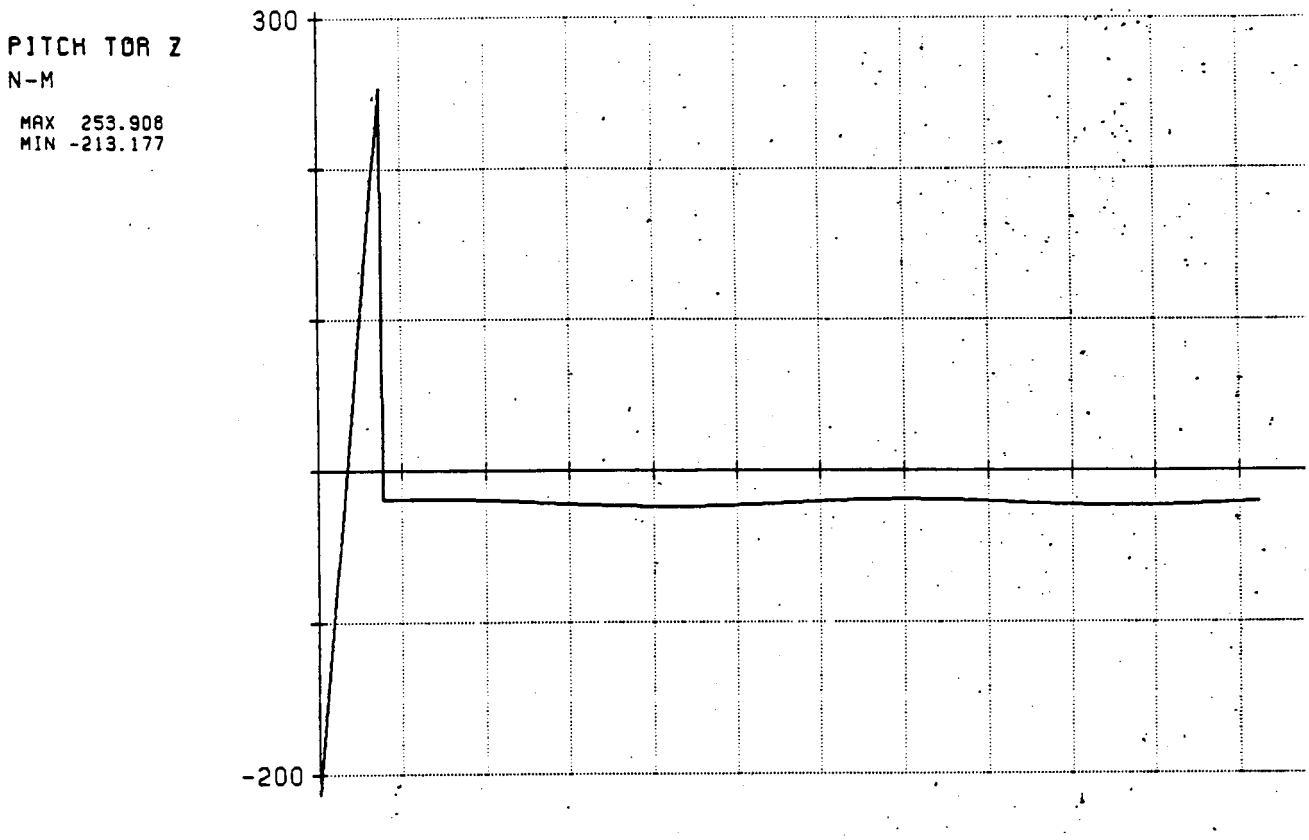

Figure 50. Torque, Z-Motion MRMS, LVLH hold

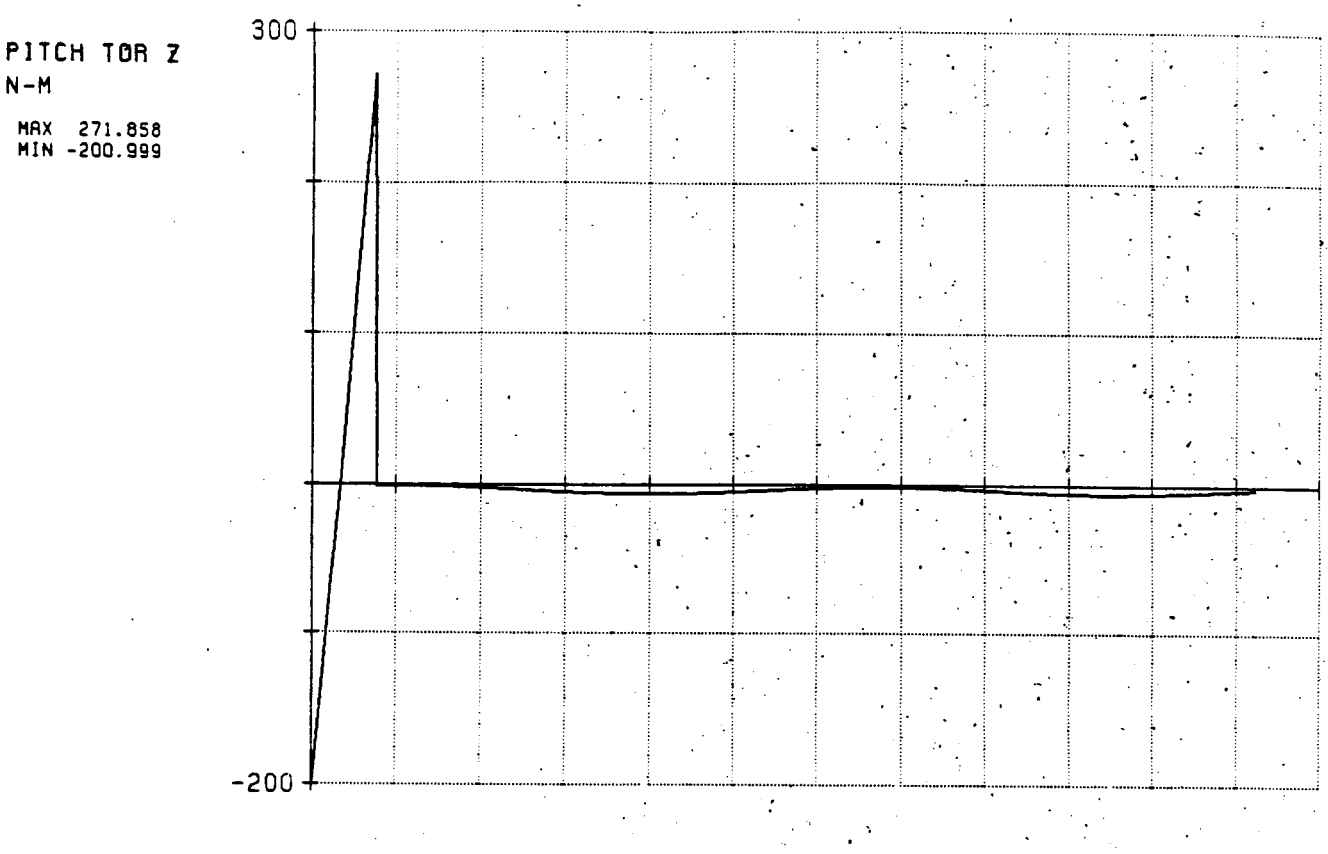

Figure 51. Torque, Z-Motion MRMS, ATEA hold

5.0 DISCUSSION OF RESULTS

5.1 ATTITUDE AND PEAK MOMENTUM

The peak disturbance momentum varies significantly with the attitude at which the space station is held. (Table 4 on page 123) For all the models, and all possible motions of the MRMS, it can be seen that it is significantly better to hold the spacecraft fixed at the ATEA angle than to hold the vehicle axes aligned with the LVLH frame. The factor of four reduction observed for the simple model in [5] is now a factor of fifty reduction in the peak disturbance momentum due to the more aerodynamically balanced design of the dual keel space station design when compared to the previous power tower design.

Comparing the peak momentum observed with the simple model and that observed with the complex model with no MRMS motion shows the importance of including the effects of the motion of the solar panels on the inertia of the space station in the analysis. This leads to an increase in the expected peak momentum on the order of a factor of fifty.

The better performance at the ATEA attitude can also be attributed to the fact that the vehicle axes of the dual keel design are not the principal axes of the space station. A large xz product of inertia exists when the vehicle axes are aligned with the LVLH frame which produces a large pitch gravity gradient torque.

The most important result of examining the effect of attitude on the peak disturbance momentum is the discovery that, except for the simple torque model, the ATEA attitude does not produce the minimum peak disturbance momentum on the space station. The ATEA angle is close to the attitude which produces the minimum peak momentum (Table 5 on page 124), but the actual angle that produces the minimum peak momentum is less than the ATEA angle by up to one degree. The reason for this is that while the ATEA attitude guarantees that the disturbance momentum will be zero at the end of the time interval T, it does not guarantee that the median disturbance momentum will be zero during that interval. The angle which makes the median disturbance momentum zero is that which produces the minimum peak momentum.

Fixing the space station's attitude at the angle which minimizes the peak disturbance momentum does not necessarily give zero momentum at the end of the time interval. Whatever momentum is left must be dealt with on the next time interval, so this minimum peak momentum attitude may not be the best attitude. And as can be seen is Table 4 on page 123,

the reduction in peak momentum from the ATEA hold case is only 10-20% for all the models.

Table 4. Peak Momentum vs. Attitude Specification

CASE	Peak Momentum (N-m-s)	% Difference From Nominal
Simple model, ATEA hold	44.1927	———
Simple model, LVLH hold	-124503.0	+281627.53%
No MRMS motion, ATEA hold	2370.39	———
No MRMS motion, Minimum Peak Momentum Attitude	2010.40	-15.2%
No MRMS motion, LVLH hold	-124503.0	+5152.43%
Y motion MRMS, ATEA hold	2467.73	———
Y motion MRMS, Minimum Peak Momentum Attitude	2040.70	-17.3%
Y motion MRMS, LVLH hold	-121480.0	+4822.74%
Z motion MRMS, ATEA hold	20445.0	———
Z motion MRMS, Minimum Peak Momentum Attitude	18430.0	-10.3%
Z motion MRMS, LVLH hold	-105469.0	+415.87%

Table 5.

Attitude	Pitch Angle
Simple Model ATEA hold	-23.57820760 deg
No MRMS motion ATEA	-26.27417614 deg
No MRMS motion min. peak momentum attitude	-25.73385 deg
Y-motion MRMS ATEA	-7.64112094 deg
Y-motion MRMS min. peak momentum attitude	-7.51450 deg
Z-motion MRMS ATEA	-6.28786112 deg
Z-motion MRMS min. peak momentum attitude	-5.18090 deg

5.2 MRMS MANEUVER AND PEAK MOMENTUM

The motion of the MRMS increases the peak disturbance momentum in general. Motion parallel to the y-axis of the space station produces a slight increase in the peak momentum, while motion parallel to the z-axis and for the full length of the space station increases the peak momentum by an order of magnitude. (Table 6 on page 126)

It also can be seen that, for z motion of the MRMS, the peak momentum is dependent on the speed at which the MRMS moves. Faster speeds decrease the peak momentum slightly. Taking advantage of this has its

limits in that the MRMS will have some maximum speed at which it can move. Also, the analysis of the momentum buildup shown here does not take into account the starting and stopping torques of the MRMS, which become more significant as its operating speed is increased.

Also, if the MRMS z motion is less than the entire length of the vehicle, then the peak disturbance momentum resulting from the motion is greatly reduced. If the distance traveled is only 20 meters instead of 90 meters, the peak momentum can be reduced by a factor of 10, as seen in Table 6 on page 126.

Because the motion of the MRMS parallel to the z axis produces such a large peak momentum, it might be more efficient to treat it as an isolated disturbance and deal with it individually, rather than include it in any prediction scheme where an optimal attitude is being chosen.

Table 6. Peak Momentum vs. MRMS Maneuver

CASE	Peak Momentum (N-m-s)	% Difference From Nominal
No MRMS motion, ATEA hold	2370.39	————
Y motion MRMS, ATEA hold	2467.73	+4.1% (over no motion)
Z motion MRMS, ATEA hold	20445.0	+762.5% (over no motion)
Z motion, Faster, Vm=.5 m/s	18791.2	-8.09%
Z motion, Slower, Vm=.125 m/s	23664.7	+15.75%
Z motion, Shorter distance	2913.45	-85.75%
Z motion, Shorter, Slower	2939.27	-85.62%
Z motion, Stop at C.O.M.	-12728.5	-37.74%

5.3 ATTITUDE UNCERTAINTY AND PEAK MOMENTUM

Another question that must be answered after the most desirable attitude is determined is how closely can this attitude be followed. A reasonable estimate of the accuracy of the control of the space station is that it will be able to hold an attitude to within +1 deg or -1 deg error. The resulting effect on the peak momentum of being that far off from the ATEA angle is shown in Table 7 on page 128.

It can be seen that the attitude uncertainty has a substantial effect on the peak momentum in the no MRMS motion case, and a very large effect on the peak momentum in the Y motion case, but the Z motion case is relatively insensitive to errors in attitude.

The effect on the Y motion peak momentum of an error in attitude is important because with a relatively small error the peak momentum value is raised to nearly that of the Z motion case. This is probably due to the large aerodynamic moment arm that is produced when the MRMS is stationed at the lower keel, as it is in the y axis manuever.

There is no longer an advantage of a lower peak momentum when dealing with the y axis maneuver versus the z axis maneuver due to this error in the attitude.

Table 7. Peak Momentum vs. Uncertainty in Attitude

CASE	Peak Momentum (N-m-s)	% Difference From Nominal
No MRMS motion, ATEA hold (pitch angle = -26.274176 deg)	2370.39	———
No MRMS motion, ATEA + 1 deg	-3524.19	+48.68%
No MRMS motion, ATEA - 1 deg	4605.99	+94.31%
Y motion MRMS, ATEA hold (pitch angle = -7.6411209 deg)	2467.73	———
Y motion MRMS, ATEA + 1 deg	-15586.6	+531.62%
Y motion MRMS, ATEA - 1 deg	15437.4	+525.57%
Z motion MRMS, ATEA hold (pitch angle = -6.2878611 deg)	20445.0	———
Z motion MRMS, ATEA + 1 deg	18544.1	-9.3%
Z motion MRMS, ATEA - 1 deg	23244.7	+13.69%

5.4 AERODYNAMIC MODEL UNCERTAINTY AND PEAK MOMENTUM

The real uncertainty in all of these momentum models is the aerodynamic torque and momentum contribution. As already noted, the atmospheric density and the vehicle drag coefficient are unpredictable in the short term due to effects such as solar activity and shadowing of one part of the space station by another. The effect of errors in different aerodynamic parameters in the model is shown in Table 8 on page 129, Table 9 on page 130, and Table 10 on page 131

Variations from the predicted values of the aerodynamic parameters have little effect on the no motion MRMS and z motion MRMS peak disturbance momentum values. The effect on the y motion case is greater, with a 50% variation in the atmospheric density producing a 25% increase in the peak momentum value. In general, the contribution to the peak momentum is small so variations in the aerodynamic model have little effect. The y motion case is affected the most because for that case the moment arms of the core and solar panels are the largest.

Table 8. Peak Momentum vs. Uncertainty in Aerodynamic Parameters

CASE No MRMS Motion	Peak Momentum (N-m-s)	% Difference From Nominal
Actual density = pred. density (Pred. density = 1.5X10E-12)	2370.39	———
Act. den. = Pred. den. - 50%	2309.69	-2.56%
Act. den. = Pred. den. + 50%	2461.39	+3.84%
Act. drag = Pred. drag - 20% (Pred. drag coefficient = 2.7)	2345.93	-1.03%
Act. drag = Pred. drag + 20%	2394.84	+1.03%
Act. SParea=Pred. SParea - 25% (Pred. S.P. area = 1974.64)	2393.43	+.97%
Act. SParea=Pred. SParea + 25%	2347.35	-.97%
Act. Carea = Pred. Carea - 25% (Pred. CORE area = 261.17)	2316.92	-2.26%
Act. Carea = Pred. Carea + 25%	2427.72	-2.42%

Table 9. Peak Momentum vs. Uncertainty in Aerodynamic Parameters

CASE Y Motion MRMS	Peak Momentum (N-m-s)	% Difference From Nominal
Actual density = Pred. density (Pred. density = 1.5X10E-12)	2467.73	————
Act. den. = Pred. den. - 50%	1889.96	-23.41%
Act. den. = Pred. den. + 50%	3051.58	+23.66%
Act. drag = Pred. drag - 20% (Pred. drag coefficient = 2.7)	2235.77	-9.40%
Act. drag = Pred. drag + 20%	2700.62	+9.44%
Act. SParea=Pred. SParea - 25% (Pred. S.P. area = 1974.64)	2280.85	-7.57%
Act. SParea=Pred. SParea + 25%	2654.83	+7.58%
Act. Carea = Pred. Carea - 25% (Pred. CORE area = 261.17)	2364.57	-4.18%
Act. Carea = Pred. Carea + 25%	2571.59	+4.21%

Table 10. Peak Momentum vs. Uncertainty in Aerodynamic Parameters

CASE Z Motion MRMS	Peak Momentum (N-m-s)	% Difference From Nominal
Actual density = Pred. density (Pred. density = 1.5X10E-12)	20445.0	————
Act. den. = Pred. den. - 50%	20223.7	-1.08%
Act. den. = Pred. den. + 50%	20666.4	+1.08%
Act. drag = Pred. drag - 20% (Pred. drag coefficient = 2.7)	20356.5	-.43%
Act. drag = Pred. drag + 20%	20533.6	+.43%
Act. SParea=Pred. SParea - 25% (Pred. S.P. area = 1974.64)	20441.7	-.02%
Act. SParea=Pred. SParea + 25%	20448.3	+.02%
Act. Carea = Pred. Carea - 25% (Pred. CORE area = 261.17)	20337.6	-.53%
Act. Carea = Pred. Carea + 25%	20552.4	+.53%

5.5 MASS PROPERTIES UNCERTAINTIES AND PEAK MOMENTUM

In Table 11 on page 133, Table 12 on page 134 , and Table 13 on page 135 the effects of uncertainties in the values of the masses and inertias of the space station upon the peak value of the disturbance momentum are shown. In each case the spacecraft was held in the ATEA attitude.

It can be seen that the Z motion case is relatively insensitive to changes in either the inertia components or the masses of the different elements. None of the cases responds with a significant change in peak momentum to a change in the core or solar panel mass, but both the no motion and y motion case peak momentum values are increased significantly by an 10% uncertainty in the inertia components of the core and solar panels.

Another interesting effect that can be seen in the graphs of the momentum response of the space station to errors in the inertia values of the models, is that the ATEA angle is not affected by changes in the inertia values of the solar panels. This is because their cyclic motion produces a net zero momentum and so doesn't require any compensation for in the ATEA.

Table 11. Peak Momentum vs. Uncertainty in Mass and Inertia

CASE No MRMS Motion	Peak Momentum (N-m-s)	% Difference From Nominal
Actual Mass SP = Pred. Mass SP (Pred. Mass SP = 5510.1999 kg)	2370.39	———
Act.MassSP = Pred.MassSP - 10%	2365.51	-.21%
Act.MassSP = Pred.MassSp + 10%	2375.24	+.20%
Act. MassC = Pred. MassC - 10% (Pred. Mass Core=167869.2 kg)	2375.78	+.23%
Act. MassC = Pred. MassC + 10%	2365.95	-.19%
Act. IZP = Pred. IZP - 10% (Pred. IZP = 30679373.76kg-m2)	25681.3	+983.42%
Act. IZP = Pred. IZP + 5%	-12840.7	+441.71%
Act. IZP = Pred. IZP + 10%	-25578.3	+979.08%
Act. IXP = Pred. IXP - 5% (Pred. IXP = 45559718.78kg-m2)	-19068.7	+804.45%
Act. IXP = Pred. IXP + 10%	38137.4	+1508.91%
Act. IXZP = Pred. IXZP - 10% (Pred. IXZP = 5930594.86kg-m2)	12506.9	+427.63%
Act. IXZP = Pred. IXZP + 10%	12507.0	+427.63%
Act. J1 = Pred. J1 - 10% (Pred. J1 = 16545372.76 kg-m2)	-855.16	-63.92%
Act. J1 = Pred. J1 + 10%	5531.05	+133.34%
Act. J3 = Pred. J3 - 10% (Pred. J1 = 15315869.66 kg-m2)	5296.18	+123.43%
Act. J3 = Pred. J3 + 10%	-620.27	-73.83%

Table 12. Peak Momentum vs. Uncertainty in Mass and Inertia

CASE Y Motion MRMS	Peak Momentum (N-m-s)	% Difference From Nominal
Actual Mass M = Pred. Mass M (Pred. Mass MRMS = 10000 kg)	2467.73	———
Act.Mass M = Pred.Mass M - 10%	-7904.86	+220.33%
Act.Mass M = Pred.Mass M + 10%	7819.11	+216.85%
Act.MassSP = Pred.MassSP - 10% (Pred. Mass SP = 5510.1999 kg)	2473.18	+.22%
Act.MassSP = Pred.MassSP + 10%	2462.31	-.22%
Act. MassC = Pred. MassC - 10% (Pred. Mass Core=167869.2 kg)	2460.52	-.29%
Act. MassC = Pred. MassC + 10%	2365.95	+.27%
Act. IZP = Pred. IZP - 10% (Pred. IZP = 30679373.76kg-m2)	8526.52	+245.52%
Act. IZP = Pred. IZP + 10%	-8526.53	+245.52%
Act. IXP = Pred. IXP - 10% (Pred. IXP = 45559718.78kg-m2)	-12662.1	+413.11%
Act. IXP = Pred. IXP + 10%	12662.1	+413.11%
Act. IXZP = Pred. IXZP - 10% (Pred. IXZP = 5930594.86kg-m2)	12506.9	+406.82%
Act. IXZP = Pred. IXZP + 10%	12507.0	+406.82%
Act. J1 = Pred. J1 - 10% (Pred. J1 = 16545372.76 kg-m2)	-1042.87	-57.74%
Act. J1 = Pred. J1 + 10%	5288.25	+114.30%
Act. J3 = Pred. J3 - 10% (Pred. J1 = 15315869.66 kg-m2)	5078.50	+105.80%
Act. J3 = Pred. J3 + 10%	-844.10	-65.79%

Table 13. Peak Momentum vs. Uncertainty in Mass and Inertia

CASE Z Motion MRMS	Peak Momentum (N-m-s)	% Difference From Nominal
Actual Mass M = Pred. Mass M (Pred. Mass MRMS = 10000 kg)	20445.0	———
Act.Mass M = Pred.Mass M - 10%	18047.0	-11.73%
Act.Mass M = Pred.Mass M + 10%	22845.2	+11.74%
Act.MassSP = Pred.MassSP - 10% (Pred. Mass SP = 5510.1999 kg)	20468.5	+.11%
Act.MassSP = Pred.MassSP + 10%	20421.7	-.11%
Act. MassC = Pred. MassC - 10% (Pred. Mass Core=167869.2 kg)	20211.5	-1.14%
Act. MassC = Pred. MassC + 10%	20640.5	+.96%
Act. IZP = Pred. IZP - 10% (Pred. IZP = 30679373.76kg-m2)	20988.7	+2.66%
Act. IZP = Pred. IZP + 10%	19966.1	-2.34%
Act. IXP = Pred. IXP - 10% (Pred. IXP = 45559718.78kg-m2)	19733.7	-3.48%
Act. IXP = Pred. IXP + 10%	21496.4	+5.14%
Act. IXZP = Pred. IXZP - 10% (Pred. IXZP = 5930594.86kg-m2)	21844.1	+6.84%
Act. IXZP = Pred. IXZP + 10%	19594.5	-4.16%
Act. J1 = Pred. J1 - 10% (Pred. J1 = 16545372.76 kg-m2)	19740.2	-3.45%
Act. J1 = Pred. J1 + 10%	22104.4	+8.12%
Act. J3 = Pred. J3 - 10% (Pred. J1 = 15315869.66 kg-m2)	21924.6	+7.24%
Act. J3 = Pred. J3 + 10%	19792.6	-3.19%

5.6 CONCLUSION

In all these cases, the Z motion of the MRMS has produced the largest values of peak momentum for ATEA hold. If the effect of the MRMS motion is to be included in the predictive momentum management scheme, then the values of peak momentum for the Z motion case will be the values used to size the momentum exchange devices necessary to compensate for the disturbances. It can be seen that the values of peak momentum for the Z motion of the MRMS are relatively insensitive to errors in the models or measurements that went into predicting what attitude is best for decreasing the peak momentum value. Because of this insensitivity it appears that the predictive scheme will work even with the inaccuracies in the models and uncertainties in the measurements. But this is at the cost of accepting the highest expected momentum values, and being required to carry momentum exchange devices sized accordingly. If MRMS motion were compensated for independent of the predictive momentum management system, then the peak momentum value could be reduced by a factor of five, to that of the expected peak disturbance momentum for the no MRMS motion case with a 1 deg attitude uncertainty.

Also, the results show that the goal of minimizing peak momentum is not necessarily the best goal since it leaves a large disturbance momentum at the end of the predicting time interval. And while the ATEA

angle doesn't produce the minimum peak disturbance momentum, it does come relatively close, as well as leaving zero disturbance momentum at the end time.

5.7 RECOMMENDATIONS FOR FUTURE WORK

The minimum peak momentum attitude must be defined explicitly and a compromise between the ATEA attitude and the minimum peak momentum attitude be found.

Also the effect of expanding the time scale of the prediction of torques should be examined. How does it affect the uncertainty in the environment and how does it affect the peak momentum and ATEA calculation?

APPENDIX A. EQUATIONS OF MOTION

The model of the space station from which the models in the momentum analysis were derived is one which consists of three interconnected rigid bodies. These bodies are the core of the space station (habitability, logistics and laboratory modules as well as the supporting truss structure), the rotating solar panels, and the mobile remote manipulation system (MRMS). As well as being rigid, each component in the composite structure is assumed to have a constant inertia and mass, in its own frame. The MRMS is assumed to be a point mass so its inertia is negligible.

This model was chosen because it will allow the for the examination of the effects of two important internal disturbance torques on the attitude motion of the space station; the friction torque between the rotating solar panels and the core, and the inertia change torques due to the motion of the MRMS, as well as the effects of external torques such as the gravity gradient and aerodynamic torques.

To start the derivation of the equations of motion of the three-body space station, first define the angular momentum of the composite spacecraft, which is the momentum of each component about its own center of

mass, plus the moment of the linear momentum of each component about the composite center of mass. Bodies 1, 2, and 3, are the core, solar panels, and MRMS, respectively;

$$H_o = A[I_1\omega + I_2(\omega+\Omega) + I_3\omega + m_1(r_1 \times dr_1/dt) + m_2(r_2 \times dr_2/dt) + m_3(r_3 \times dr_3/dt) \quad (164)$$

where r_1, r_2, and r_3 are the vector positions of the three bodies with respect to the vehicle center of mass, in an inertial frame.

Since the solar panel center of mass remains fixed with respect to the center of mass of the core, these two bodies can be combined into one, with the core/solar panels now being body 1 and the MRMS now being body 2;

$$H_o = A[(I + CJC^T)\omega + CJ\Omega + m_1 r_1^{\times}(\omega^{\times} r_1 + dr_1/dt) + m_2 r_2^{\times}(\omega^{\times} r_2 + dr_2/dt)] \quad (165)$$

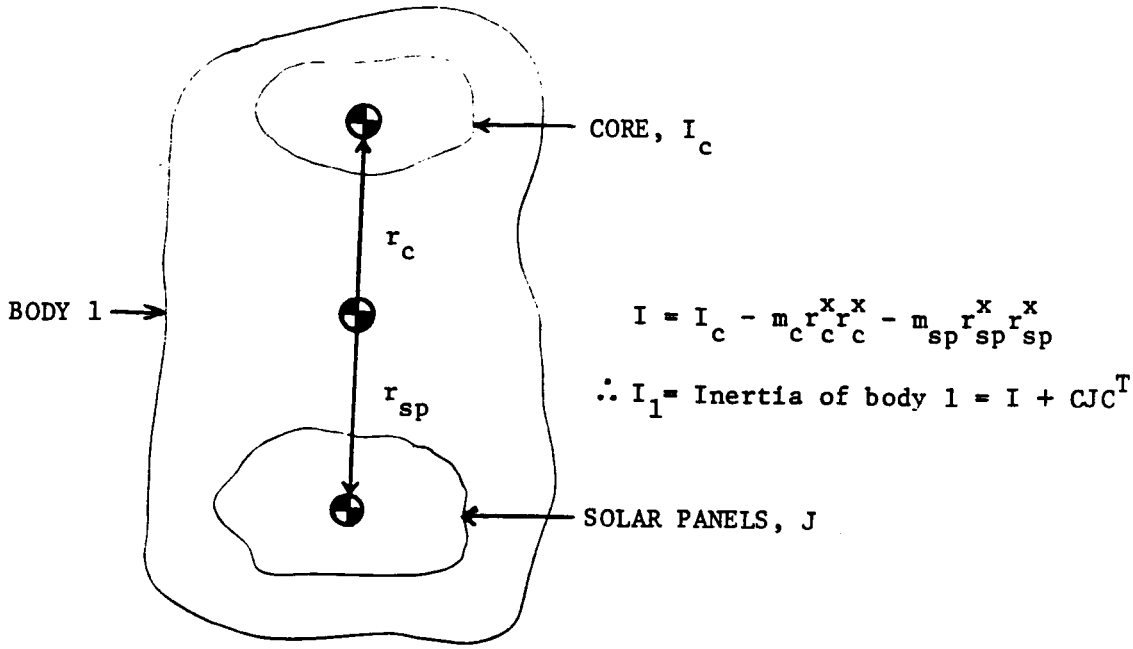

Figure 52. The definition of I and "two" bodies

where;

I = inertia of the core structure about its own c.o.m., plus the inertia due to the mass offset of the core and solar panels from their combined center of mass

J = inertia of the solar arrays about their own c.o.m and in their own frame

ω = angular velocity of the entire space station, in the body frame

Ω = angular velocity of the solar arrays with respect to the core expressed in the solar panel frame.

C = transformation matrix from solar panel frame to the core frame

A = transformation matrix from core frame to the inertial frame

m_1 = mass of core and solar panels combined

m_2 = mass of the MRMS

r_1 = vector from total space station c.o.m. to the c.o.m. of the core and solar panels combined

r_2 = vector from total space station c.o.m. to the MRMS (and r_1, r_2 are now in the body frame)

The notation $(\ )^{\times}$ refers to the skew symmetric matrix that is constructed from a column matrix. When multiplied by another vector The skew symmetric matrix gives the matrix equivalent of a vector cross product.

Since the centers of mass of the MRMS, core/solar panels, and the total vehicle remain colinear, the whole system can be represented by one vector from the core/solar panel center of mass to the MRMS.

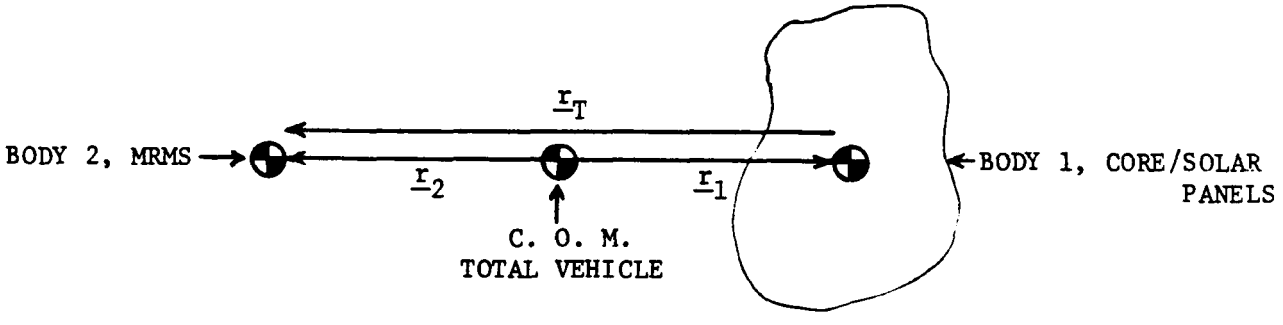

$$\underline{r}_t = \underline{r}_2 - \underline{r}_1$$

Figure 53. The definition of r_T in terms of r_1 and r_2

$$r_1 = \frac{m_2 r_T}{(m_1+m_2)} \qquad r_2 = \frac{m_1 r_T}{(m_1+m_2)} \tag{166}$$

Using these definitions for r_1 and r_2, the momentum equation becomes,

$$H_B = [(I + CJC^T - Kr_T{}^x r_T{}^x)\omega + CJ\Omega + Kr_T{}^x dr_T/dt] \tag{167}$$

where

r_T = vector from the c.o.m. of the combined core and solar panels to the MRMS

$K = m_1 m_2/(m_1 + m_2)$ ('reduced mass' of system)

Differentiating the angular momentum with respect to time in the core frame yields an expression for the torque on the vehicle in the core frame.

$$\begin{aligned} M = {} & I''d\omega/dt + \omega^x I''\omega + \omega^x CJ\Omega + C(\Omega^x J - J\Omega^x)C^T\omega + CJd\Omega/dt \\ & + K(\omega^x r_T{}^x dr_T/dt + r_T{}^x \omega^x dr_T/dt \\ & + dr_T/dt{}^x \omega^x r_T + r_T{}^x d^2 r_T/dt^2) \end{aligned} \tag{168}$$

where;

$I'' = I + CJC^T - Kr_T{}^x r_T{}^x$ (inertia of total vehicle)

In differentiating this equations, the following matrix identities were used;

$$dA/dt = \omega^{x}A \tag{169}$$

$$dC/dt = \Omega^{x}C \tag{170}$$

In order to solve this equations for the angular velocity of the space station, expressions are needed for the time rate of change of the solar panel rate, $d\Omega/dt$, and the time rate of change of the MRMS velocity, d^2r_T/dt^2. These expressions are obtained by writing the equations of motion of the solar panels and the MRMS separately. The equations of motion for the solar panels alone are;

$$H_o = ACJ(\Omega + C^{T}\omega) \tag{171}$$

$$M_F = dH_o/dt \tag{172}$$

$$M_F = \omega^{x}CJ\Omega + \omega^{x}CJC^{T}\omega + CJd\Omega/dt + CJC^{T}d\omega/dt + (\Omega^{x}J - J\Omega^{x})C^{T}\omega \tag{173}$$

$$\therefore d\Omega/dt = J^{-1}C^{T}[M_F - \omega^{x}CJ\Omega - C(\Omega^{x}J - J\Omega^{x})C^{T}\omega - \omega^{x}CJC^{T}\omega - CJC^{T}d\omega/dt] \tag{174}$$

where M_F is the disturbance torque plus the frictional torque exerted on the solar panels at the hinge between the solar panels and the core of the space station. The equations of motion for the MRMS alone are;

$$s_T = Ar_T \tag{175}$$

$$ds_T/dt = A\omega^{\times}r_T + Adr_T/dt \tag{176}$$

$$d^2s_T/dt^2 = A\omega^{\times}\omega^{\times}r_T + A(d\omega/dt)^{\times}r_T + 2A\omega^{\times}dr_T/dt + Ad^2r_T/dt^2 = F_o \tag{177}$$

where F_o = MRMS inertial acceleration

and s_T = MRMS inertial position vector

$$F_m = dv_T/dt + 2\omega^{\times}v_T + (d\omega/dt)^{\times}r_T + \omega^{\times}\omega^{\times}r_T \tag{178}$$

where F_m is the acceleration of the MRMS in the body frame.

$$\therefore d^2r_T/dt^2 = dv_T/dt = F_m - 2\omega^{\times}dr_T/dt - (d\omega/dt)^{\times}r_T - \omega^{\times}\omega^{\times}r_T \tag{179}$$

The three derived equations of motion, for the MRMS, solar panels and for the total vehicle, all assume that there are no constraints on the relative motion between the components of the space station. In fact, the motions of the MRMS and the solar panels are very constrained. The solar panels can rotate only about the Y axis of the vehicle, and so must have zero position, rate and acceleration about the other two axes.

The MRMS is constrained by the essentially planar configuration of the dual keel space station to move along a direction that is parallel to the either the y or z axis of the space station. The position and velocity of the MRMS for a given portion of this motion are effectively

scalars. The rate and angle of the solar panel displacement are also scalars because the rotation of the solar panels is always about the Y axis of the space station.

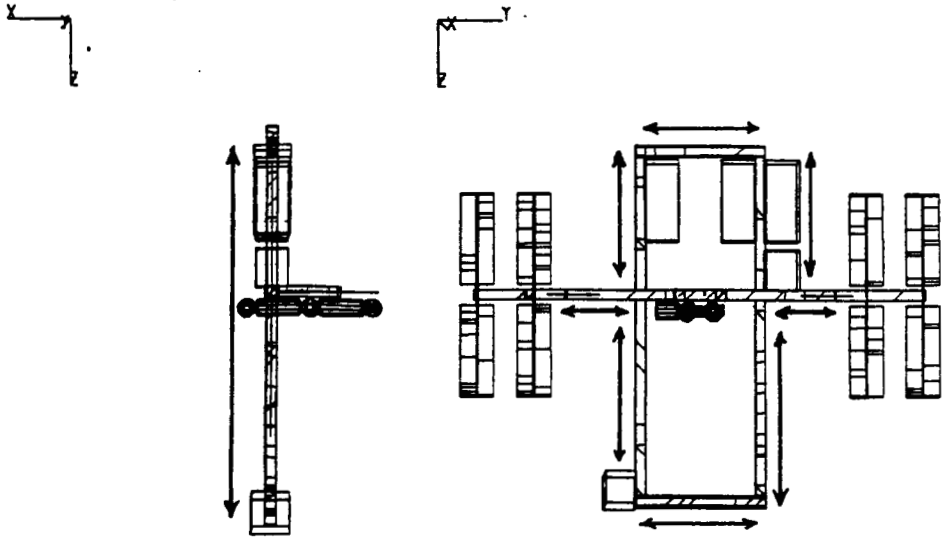

Figure 54. Constraints on MRMS motion

If the system state vector is defined to be a combination of the angular rate of the entire space station, ω, the state of the solar panels; Ω, θ, and the state of the MRMS; r_T, v_T, then a coupled set of state equations can be derived by solving the previous three sets of equations of motion, eqn's (168) (174) (179) , for the rate of change of the state. The equations of motion of the MRMS and solar panels with the constraints on their motion added are needed.

For motion of the MRMS parallel to the vehicle Y-axis, the equations of motion for the MRMS become;

$$d^2r_T/dt^2 = \begin{bmatrix} 0 \\ (F_m)_y - (2\omega^x dr_T/dt)_y - ((d\omega/dt)^x r_T)_y - (\omega^x\omega^x r_T)_y \\ 0 \end{bmatrix} \quad (180)$$

And for motion of the MRMS parallel to the vehicle Z-axis, the equations of motion become;

$$d^2r_T/dt^2 = \begin{bmatrix} 0 \\ 0 \\ (F_m)_z - (2\omega^x dr_T/dt)_z - ((d\omega/dt)^x r_T)_z - (\omega^x\omega^x r_T)_z \end{bmatrix} \quad (181)$$

For the rotation of the solar panels about the Y axis of the vehicle alone, the equations of motion become;

$$d\Omega/dt = J^{-1}C^T \begin{bmatrix} 0 \\ (M_F)_y - (\omega^x CJ\Omega)_y - (C(\Omega^x J - J\Omega^x)C^T\omega)_y - (\omega^x CJC^T\omega)_y - (CJC^T d\omega/dt)_y \\ 0 \end{bmatrix} \quad (182)$$

The notation $()_y$ and $()_z$ refers to the y and z component of the column matrix that results from each expression, respectively. By substituting these equations for the motion of the solar panels and the MRMS into the equations of motion for the entire space station, (168) the equations of motion for the core of the vehicle, including the constraints on the MRMS and solar panel motion can be derived. There are two sets of these equations, one for motion of the MRMS parallel to the Z-axis and one for motion parallel to the Y-axis. They are, respectively;

(Y-motion of MRMS)

$$
\begin{aligned}
M = &\begin{bmatrix} (I''d\omega/dt)_x + (\omega^x I''\omega)_x + (\omega^x CJ\Omega)_x + (C(\Omega^x J - J\Omega^x)C^T\omega)_x \\ (I''d\omega/dt)_y + (\omega^x I''\omega)_y + (\omega^x CJ\Omega)_y + (C(\Omega^x J - J\Omega^x)C^T\omega)_y \\ (I''d\omega/dt)_z + (\omega^x I''\omega)_z + (\omega^x CJ\Omega)_z + (C(\Omega^x J - J\Omega^x)C^T\omega)_z \end{bmatrix} \\
&+ \begin{bmatrix} 0 \\ (M_F)_y - (\omega^x CJ\Omega)_y - (C(\Omega^x J - J\Omega^x)C^T\omega)_y - (\omega^x CJC^T\omega)_y - (CJC^T d\omega/dt)_y \\ 0 \end{bmatrix} \\
&+ K\begin{bmatrix} (\omega^x r_T{}^x dr_T/dt)_x \\ (\omega^x r_T{}^x dr_T/dt)_y \\ (\omega^x r_T{}^x dr_T/dt)_z \end{bmatrix} + K\begin{bmatrix} (r_T{}^x \omega^x dr_T/dt)_x \\ (r_T{}^x \omega^x dr_T/dt)_y \\ (r_T{}^x \omega^x dr_T/dt)_z \end{bmatrix} + K\begin{bmatrix} (dr_T/dt{}^x \omega^x r_T)_x \\ (dr_T/dt{}^x \omega^x r_T)_y \\ (dr_T/dt{}^x \omega^x r_T)_z \end{bmatrix} \\
&+ Kr_T{}^x \begin{bmatrix} 0 \\ (F_m)_y - (2\omega^x dr_T/dt)_y - ((d\omega/dt)^x r_T)_y - (\omega^x \omega^x r_T)_y \\ 0 \end{bmatrix}
\end{aligned} \tag{183}
$$

(Z-motion of MRMS)

$$
\begin{aligned}
M = &\begin{bmatrix} (I''d\omega/dt)_x + (\omega^x I''\omega)_x + (\omega^x CJ\Omega)_x + (C(\Omega^x J - J\Omega^x)C^T\omega)_x \\ (I''d\omega/dt)_y + (\omega^x I''\omega)_y + (\omega^x CJ\Omega)_y + (C(\Omega^x J - J\Omega^x)C^T\omega)_y \\ (I''d\omega/dt)_z + (\omega^x I''\omega)_z + (\omega^x CJ\Omega)_z + (C(\Omega^x J - J\Omega^x)C^T\omega)_z \end{bmatrix} \\
&+ \begin{bmatrix} 0 \\ (M_F)_y - (\omega^x CJ\Omega)_y - (C(\Omega^x J - J\Omega^x)C^T\omega)_y - (\omega^x CJC^T\omega)_y - (CJC^T d\omega/dt)_y \\ 0 \end{bmatrix} \\
&+ K\begin{bmatrix} (\omega^x r_T{}^x dr_T/dt)_x \\ (\omega^x r_T{}^x dr_T/dt)_y \\ (\omega^x r_T{}^x dr_T/dt)_z \end{bmatrix} + K\begin{bmatrix} (r_T{}^x \omega^x dr_T/dt)_x \\ (r_T{}^x \omega^x dr_T/dt)_y \\ (r_T{}^x \omega^x dr_T/dt)_z \end{bmatrix} + K\begin{bmatrix} (dr_T/dt{}^x \omega^x r_T)_x \\ (dr_T/dt{}^x \omega^x r_T)_y \\ (dr_T/dt{}^x \omega^x r_T)_z \end{bmatrix} \\
&+ Kr_T{}^x \begin{bmatrix} 0 \\ 0 \\ (F_m)_z - (2\omega^x dr_T/dt)_z - ((d\omega/dt)^x r_T)_z - (\omega^x \omega^x r_T)_z \end{bmatrix}
\end{aligned} \tag{184}
$$

These equations can now be solved for $d\omega/dt$, in terms of a new 'inertia' matrix, I''', and a new 'moment' vector, M'.

$$\underbrace{\begin{bmatrix} (I_{11}'' - Kr_2^2) & (I_{12}'' + Kr_2r_1) & I_{13}'' \\ (I_{12}'' + Kr_1r_2) & (I_{22}'' - J_2 - Kr_1^2) & I_{23}'' \\ I_{13}'' & I_{23}'' & I_{33}'' \end{bmatrix}}_{I''' \text{ (Z motion of MRMS)}} \begin{bmatrix} d\omega_1/dt \\ d\omega_2/dt \\ d\omega_2/dt \end{bmatrix} = \begin{bmatrix} M_1' \\ M_2' \\ M_3' \end{bmatrix} \quad (185)$$

where 1,2,3 = x,y,z

$$\underbrace{\begin{bmatrix} (I_{11}'' - Kr_3^2) & I_{12}'' & (I_{13}'' + Kr_3r_1) \\ I_{12}'' & (I_{22}'' - J_2) & I_{23}'' \\ (I_{13}'' + Kr_1r_3) & I_{23}'' & (I_{33}'' - Kr_1^2) \end{bmatrix}}_{I''' \text{ (Y motion of MRMS)}} \begin{bmatrix} d\omega_1/dt \\ d\omega_2/dt \\ d\omega_2/dt \end{bmatrix} = \begin{bmatrix} M_1' \\ M_2' \\ M_3' \end{bmatrix} \quad (186)$$

The state equations for Y motion of the MRMS are;

$$\begin{aligned} d\omega/dt &= I'''M' \\ d\Omega/dt &= J^{-1}C^T[(M_F)_y - (\omega^x CJ\Omega)_y - (C(\Omega^x J - J\Omega^x)C^T\omega)_y - (\omega^x CJC^T\omega)_y - (CJC^T d\omega/dt)_y] \\ d\theta/dt &= \Omega \\ dv_T/dt &= [(F_m)_y - (2\omega^x dr_T/dt)_y - ((d\omega/dt)^x r_T)_y - (\omega^x\omega^x r_T)_y] \\ dr_T/dt &= v_T \end{aligned} \quad (187)$$

The state equations for Z motion of the MRMS are;

$$
\begin{aligned}
d\omega/dt &= I'''M' \\
d\Omega/dt &= J^{-1}C^{T}[(M_F)_y - (\omega^{x}CJ\Omega)_y - (C(\Omega^{x}J - J\Omega^{x})C^{T}\omega)_y - (\omega^{x}CJC^{T}\omega)_y - (CJC^{T}d\omega/dt)_y] \\
d\theta/dt &= \Omega \qquad (188) \\
dv_T/dt &= [(F_m)_z - (2\omega^{x}dr_T/dt)_z - ((d\omega/dt)^{x}r_T)_z - (\omega^{x}\omega^{x}r_T)_z] \\
dr_T/dt &= v_T
\end{aligned}
$$

These state equations are coupled and nonlinear, and also have time varying coefficients. They have been left in the full nonlinear form as a linearization would have put constraints upon the magnitudes of the rates and attitudes for which the equations are valid. A linearization is usually employed when the goal is a stability analysis of the system. In this case we are assuming that whatever control system is employed will be able to deal with any passive instability of the space station. The equations are in a form which is suitable for numerical integration in order to determine the time history of the state; ω, Ω, θ, v_T, r_T. Once this is known, the momentum buildup on the space station due to the modeled disturbance torques may be found.

LIST OF REFERENCES

1. Paluszek, M.A., "A Weather Satellite and Pilot Buoy for the Space Station", Space Station Memo No. 85-20, 10/29/85.

2. Fredo, R.M., "A Numerical Procedure for Calculating the Aerodynamic Coefficients for Complex Spacecraft Configurations in Free-Molecular Flow", Pennsylvania State University, Master of Science Thesis, August,1980.

3. Gabaldo, M.L.A., "Drag Modelling for and Orbital Navigator", Master of Science Thesis, May 1982, CSDL Report #T-780.

4. "Workshop on Satellite Drag", NOAA Space Environment Lab., March 18-19,1982, Boulder,Colo., Pub.#82-253113.

5. Paluszek, M.A., "Aerodynamic Effectors for Attitude Control", Space Station Memo No. 85-13, 4/27/85.

6. Kaplan, M.H., "Attitude Dynamics and Euler's Eqns.", Modern Spacecraft Dynamics and Control, John Wiley and Sons, New York, 1976.

7. Paluszek, M.A., "Space Station Passive Stability and Aerodynamic Balancing", Space Station Memo No. 85-14, 6/3/85.

8. Hughes, P.C., "Chapter 8 Spacecraft Torques", Spacecraft Attitude Dynamics, John Wiley and Sons, New York, 1986.

9. Wertz, J.R.,et. al., "Chapters 4,5,and 17", Spacecraft Attitude Determination and Control, Astrophysics and Space Science Library, Volume 73.

10. Barlier, F., Boudon, Y., Falin, J.F., Futally, R., Villain, J.P., Walch, J.J., Mainguy, A.M., Bordet, J.P., "Preliminary Results Obtained from the Low-g Accelerometer CACTUS", COSPAR meeting, 1978.

11. Falin, J.L., Kockarts, G., Barlier, F., "Densities from the CACTUS Accelerometer as an External Test of the Validity of Thermospheric Models", Advanced Space Research, Vol. 1, 1981, pp.221-225.

12. Hopkins, M., Hahn, E., "Autonomous Momentum Management for the CDG Planar Space Station", AIAA 23rd Aerospace Sciences Meeting, Jan. 14-17, 1985, AIAA Report #85-0031.

13. Jacchia, L.G., "Empirical Models of the Thermosphere and Requirements for Improvements", Advances in Space Research, Vol. 1,1981, Smithsonian Astrophysical Observatory, Cambridge, Mass.

14. Malchow, H., "Atmospheric Density and Space Station Attitude Control", Presentation, CSDL.

15. Hattis, P., "An Optimal Pitch Axis Momentum Management Concept for Space Station CMGs", Space Station Memo No. 85-7, 3/4/85.

16. Wang, S.J., Ih, C.C., Lin, Y., Mettler, E., "Space Station Dynamic Modeling, Disturbance Accomodation, and Adaptive Control", Workshop on Identification and Control of Flexible Space Structures, June 4-6, 1984, San Diego, Ca.

17. Hattis, P., Kirchwey, K., Malchow, H., "Baseline Space Station GN&C Design", Space Station Memo No. 85-5, 2/26/85.

18. Paluszek, M., "A Crew Disturbance Model for the Space Station Simulator", Space Station Memo No. 84-2, 2/10/84.

19. Hahn, E., "Autonomous Momentum Management for Space Station", NASA Contractor Report #171256, Allied Bendix Corporation, 10/15/84.

20. Dowd, D.L., Tapley, B.D., "Density Models for the Upper Atmosphere", Celestial Mechanics, Vol. 20, 1979, pp.271-295.

21. Weidner, D.K., Hasseltine, C.L., Smith, R.E., "Models of Earth's Atmosphere (120 to 1000 km)", NASA SP-8021, May,1969.

22. Menees, G.P., Park, C., Wilson, J.F., Brown, K.G., "Determination of Atmospheric Density Using a Space Launched Projectile", AIAA 23rd Aerospace Sciences Meeting, Jan. 14-17, 1985, AIAA Report #85-0327.

23. Mettler, E., Milman, M.H., Rodriguez, G., Tolivar, A.F., "Space Station On-Orbit Identification and Performance Monitor", AIAA 23rd Aerospace Sciences Meeting, Jan. 14-17, 1985, AIAA Report #85-0357.

24. Vaughan, W.W., DeVries, L.L., et. al., The Earth's Atmosphere, American Institute of Aeronautics and Astronautics, New York, 1972.

25. Eyles, D., Paluszek, M., Vaughan, R., User's Guide to the Space Station Simulator, Rev. 1, Charles Stark Draper Laboratory, Report #1673, 6/4/85.

26. "Spacecraft Radiation Torques", NASA Space Vehicle Design Criteria Series, Guidance & Control, NASA SP-8027, Oct. 1969.

27. Solar Cell Array Design Handbook, Jet Propulsion Laboratory, California Institute of Technology, JPL SP 43-38, Vol. 1, Oct. 1976.

28. "Spacecraft Aerodynamic Torques", NASA Space Vehicle Design Criteria Series, Guidance & Control, NASA SP-8058, Jan. 1971.

29. Lord, R. G., "Tangential Momentum Accommodation Coefficients of Rare Gases on Polycrystalline Metal Surfaces", Progress in Astronautics and Aeronautics, Vol. 51: Part 1, 10th International Symposium on Rarefied Gas Dynamics, AIAA, 1976.

30. Thomas, L. B., Lord, R. G., "Comparative Measurements of Tangential Momentum and Thermal Accommodations on Polished and on Roughened

Steel Spheres", Progress in Astronautics and Aeronautics, 8th International Symposium on Rarefied Gas Dynamics, AIAA, 1972.

31. Seidl, M., Steinheil, E., "Measurement of Momentum Accomodation Coefficients on Surfaces Characterized By Auger Spectroscopy, SIMS, and LEED", Progress in Astronautics and Aeronautics, 9th International Symposium on Rarefied Gas Dynamics, AIAA, 1974.

32. Lampis, M., "Some Applications of a Model for Gas-Surface Interaction", Progress in Astronautics and Aeronautics, 8th International Symposium on Rarefied Gas Dynamics, AIAA, 1972.

33. Muller, W. J. C., "Parametric Representation of Beam Accomodation Coefficients", Progress in Astronautics and Aeronautics, 9th International Symposium on Rarefied Gas Dynamics, AIAA, 1974.

34. Evlanov, E. N., Lebedev, Yu. V., Leonas, V. B., "On the Possible Method of Gas-Satellite Surface Interaction Studies", Progress in Astronautics and Aeronautics, 9th International Symposium on Rarefied Gas Dynamics, AIAA, 1974.

35. Jones, H. M., Roger, N., "The Design and Developement of a Constant-Speed Solar Array Drive", 19th Aerospace Mechanisms Symposium, NASA CP 2371, May 1-3, 1985.

36. Anderson, J. C., Roberts, E. W., "Satellite Slip Ring Performance - A Summary of the European Space Tribology Laboratory (ESTL) Work, 1974-1981", National Centre of Tribology, Risley (England), N83-21355.

37. Van Leeuwen, A., Rosen, E., Carrier, L., "The Global Positioning System and Its Application in Spacecraft Navigation", Global Positioning System, The Institute of Navigation, Washington, D.C., 1980.